# A comparative study of protoheme and heme d catalases: Role of the heme and the heme pocket in catalysis and ligand binding

By:

Mary C. Maj
(BSc. (Hons), Brock University)

A thesis submitted to the Department of Biological Sciences in Partial Fulfillment of the Requirements for the Degree of Master of Science

July 1996
Brock University,
St. Catharines, Ontario,
Canada

## Abstract

Catalase dismutes $H_2O_2$ to $O_2$ and $H_2O$. In successive two-electron reactions $H_2O_2$ induces both oxidation and reduction at the heme group. In the first step the protoheme prosthetic group of beef liver catalase forms compound I, in which the heme has been oxidized from $Fe^{3+}$ to $Fe^{4+}$=O and a porphyrin radical has been created. Compound II is formed by the one-electron reduction of comp I. It retains $Fe^{4+}$=O but lacks the porphyrin radical and is catalytically inert. Molecular structures are available for *Escherichia coli* Hydroperoxidase II, *Micrococcus lysodeiktus*, *Penicillium vitale* and beef liver enzymes, which contain different hemes and heme pockets.

In the present work, the pockets and substrate access channels of protoheme (beef liver & *Micrococcus*) and heme d (HPII of *E. coli* and *Penicillium*) catalases have been analysed using Quanta™ and CharmM™ molecular modeling packages on the Silicon Graphics Iris Indigo 2 computer. Experimental studies have been carried out with two catalases, HPII (and its mutants) and beef liver. Fluoride and formate are inhibitors of both enzymes, and their binding is modulated by the heme and by distal residues N201 & H128. Both HPII and beef liver enzymes form compound I with $H_2O_2$ or peracetate. The

# A comparative study of protoheme and heme d catalases: Role of the heme and the heme pocket in catalysis and ligand binding

By:

Mary C. Maj
(BSc. (Hons), Brock University)

A thesis submitted to the Department of Biological Sciences in Partial Fulfillment of the Requirements for the Degree of Master of Science

July 1996
Brock University,
St. Catharines, Ontario,
Canada

## Abstract

Catalase dismutes $H_2O_2$ to $O_2$ and $H_2O$. In successive two-electron reactions $H_2O_2$ induces both oxidation and reduction at the heme group. In the first step the protoheme prosthetic group of beef liver catalase forms compound I, in which the heme has been oxidized from $Fe^{3+}$ to $Fe^{4+}$=O and a porphyrin radical has been created. Compound II is formed by the one-electron reduction of comp I. It retains $Fe^{4+}$=O but lacks the porphyrin radical and is catalytically inert. Molecular structures are available for *Escherichia coli* Hydroperoxidase II, *Micrococcus lysodeiktus*, *Penicillium vitale* and beef liver enzymes, which contain different hemes and heme pockets.

In the present work, the pockets and substrate access channels of protoheme (beef liver & *Micrococcus*) and heme d (HPII of *E. coli* and *Penicillium*) catalases have been analysed using Quanta™ and CharmM™ molecular modeling packages on the Silicon Graphics Iris Indigo 2 computer. Experimental studies have been carried out with two catalases, HPII (and its mutants) and beef liver. Fluoride and formate are inhibitors of both enzymes, and their binding is modulated by the heme and by distal residues N201 & H128. Both HPII and beef liver enzymes form compound I with $H_2O_2$ or peracetate. The

reduction of beef liver enzyme compound I to II and the decay of compound II are accelerated by fluoride. The decay of compound II is also accelerated by formate, and this reagent acts as a 2-electron donor towards compound I of both enzymes.

It is concluded that heme d enzymes (*Penicillium* and HPII of *E. coli*) are formed by autocatalytic transformation of protoheme in a modified pocket which contains a characteristic serine residue as well as a partially occluded heme channel. They are less active than protoheme enzymes but also do not form the inactive compound II species. Binding of peroxide as well as fluoride and formate is prevented by mutation of H128 and modulated by mutation of N201.

## Acknowledgments

I would like to thank my M.Sc. research supervisor, Dr. Peter Nicholls, for allowing me the honor of earning my M.Sc. degree under his direction. The lessons learned under his guidance will no doubt follow me throughout my chosen careers. I would also like to thank Brenda Tattrie for advice and guidance both personal and professional. I would like to acknowledge Dr. Peter Loewen of the University of Manitoba for providing the HPII wild-type and mutant enzymes as well as unpublished crystallographic data. I would also like to acknowledge Dr. Garib Murshudov of The University of York for providing unpublished 3-dimensional coordinates of the PVC & MLC enzymes. Lastly, I would like to thank the Maj family for their support.

## Table of Contents

**Chapter III. Results**

## List of Figures

## List of Tables

## Abbreviations and definitions

### Abbreviations

| | |
|---|---|
| BLC | Beef liver catalase |
| HPII | *E. coli* hydroperoxidase II catalase |
| MLC | *Micrococcus lysodeikticus* catalase |
| PVC | *Penicillium vitale* catalase |
| PMC | *Proteus mirabilis* catalase |
| NADP | nicotinamide adenine dinucleotide phosphate |
| H, his | histidine |
| N, asn | asparagine |
| S, ser | serine |
| A, ala | alanine |
| I, ile | isoleucine |
| V, val | valine |
| P, pro | proline |
| L, leu | leucine |
| M, met | methionine |
| peracetate,pera | peroxoacetic acid |

### Definitions

catalatic reaction..... the decomposition of two molecules of hydrogen peroxide to two molecules of water and one molecule of oxygen

peroxidatic reaction.... the oxidation of a hydrogen donor (i.e. ethanol or formate) by hydrogen peroxide

# Chapter I

## Introduction

Catalase (EC 1.11.1.6) is an enzyme which is present in many evolutionarily distant respiring organisms. It belongs to the hydroperoxidase family which break down hydrogen peroxide (see eqns. 1-4, pp. 7-8), thereby protecting cells against the toxic effects of oxidants generated as a by-product of respiration. The most common form of catalase is a homo-tetramer heme protein. Generally the catalase subunit is approximately 470 amino acid residues long and is associated with a protoheme. The secondary and tertiary structures are highly conserved, and most residues at the active site are homologous among prokaryotes, plants, fungi and animals.

Five to three billion years ago, the amount of free oxygen in the atmosphere was virtually zero. The gradual introduction of free oxygen into the atmosphere is postulated to have occurred first by the radiolysis of water vapor by ultraviolet rays and later by the decomposition of water by photosynthetic cyanobacteria. The free oxygen produced was removed by oxygen sinks, mainly by the oxidation of Fe(II) to magnetite or hematite. Geological evidence suggests that formation of these iron deposits abruptly ceased approximately 2 billion years ago when the supply of Fe(II) was exhausted and the atmosphere became more oxygenic. Organisms began to utilize the strong oxidizing power of oxygen, evolving efficient aerobic metabolisms (Holland 1984, Veizer 1983,

Walker *et al.* 1983). Catalase is thought to have evolved at the same time as protection against oxidative stress due to the generation of hydrogen peroxide as a by-product of cellular metabolism and respiration. Catalases have remained highly conserved, animal/fungal and plant catalases still bearing strong similarity to those of prokaryotes (von Ossowski, Hausner and Loewen 1993).

The fact that catalases have retained high homology among evolutionary diverse organisms, may be indicative of their physiological importance. The number of known disease processes in which oxygen toxicity is involved continues to grow. Early findings have shown that peroxide will cause tumors in drosophila embryos (Plaine 1955). Damage to the lens of the eye in organ culture (Zigler *et al.* 1985), and DNA damage have been directly linked to the presence of peroxide (Tullis 1987). Peroxide causes cell death in fibroblasts (Simon *et al.* 1981) and age related damage in drosophila (Sohol *et al.* 1995). The potential therapeutic uses of catalase along with new techniques to engineer organism with increased tolerance to oxidative stress, have continued to drive a search for the use of protective enzymes in the treatment of human diseases (Greenwald 1990).

Catalase has been studied for more than a century, decades before the physiological importance of catalase had been elucidated. Catalase is a very stable enzyme, robust enough to have been

isolated from tobacco plants by Loew in 1901, and purified in the early 1920's. Much is known about the biochemistry of catalase, albeit the precise mechanism of catalytic action has yet to be clarified. The primary sequences for nearly 100 catalases from sources representing prokaryotes, fungi, animal and plants are available. The crystal structures have been determined for bovine liver catalase (BLC), *Escherichia coli* hydroperoxidase II catalase (HPII), *Micrococcus lysodeiktus* catalase (MLC), *Penicillium vitale* catalase (PVC) and *Proteus mirabilis* catalase (PMC). The tertiary structures of these catalases are very similar, but their activities, their reactivities with substrate analogues and hydrogen donors, and their sensitivities to inhibitors are all different.

Because of its robust protein nature catalase was one of the first enzymes purified, and because of its physiological importance it has remained of great interest. The objective of this study is to further characterize ligand binding by mammalian and bacterial catalases (wild-type and site directed mutants) and to relate the observed differences to structural differences, thereby furthering knowledge of the enzyme mechanism. Ultimately this knowledge may be applicable to the study of degenerative processes of the cell related to oxygen toxicity.

## General Features and Function

The catalytic reaction of catalase is a 2-electron transfer mechanism involving the dismutation of hydrogen peroxide to oxygen and water. Hydrogen peroxide has the unique ability to both oxidize and reduce the heme group of catalase. The first molecule of peroxide will execute a 2-electron oxidation of the heme to form compound I. A second molecule of peroxide will perform a 2-electron reduction of the heme back to the resting state. A 1-electron reduction of compound I will yield the inhibited intermediate form of the enzyme, compound II. Free enzyme, compound I and compound II are spectrally distinct. The transition of compound I to compound II and the decay of compound II is accelerated in the presence of high-spin ligands (Nicholls 1961). If high-spin ligands have the same affinity for the free enzyme, compound I and compound II, high-spin ligand complexes with the heme group may depend only on the heme pocket environment and not the oxidation state of the iron.

Evolutionarily distant catalases are composed of four identical subunits. Each subunit is a single polypeptide with a porphyrin containing a high-spin $Fe^{3+}$ as a prosthetic group (figure 1). Beef liver catalase (Fita and Rossman 1985b) and *Micrococcus lysodeikticus* (Vainstein *et al.* 1986) catalase contain protoheme whereas *Penicillium vitale* and *Escherichia coli* HPII catalases contain heme d (Murshudov 1996). HPII originally binds protoheme

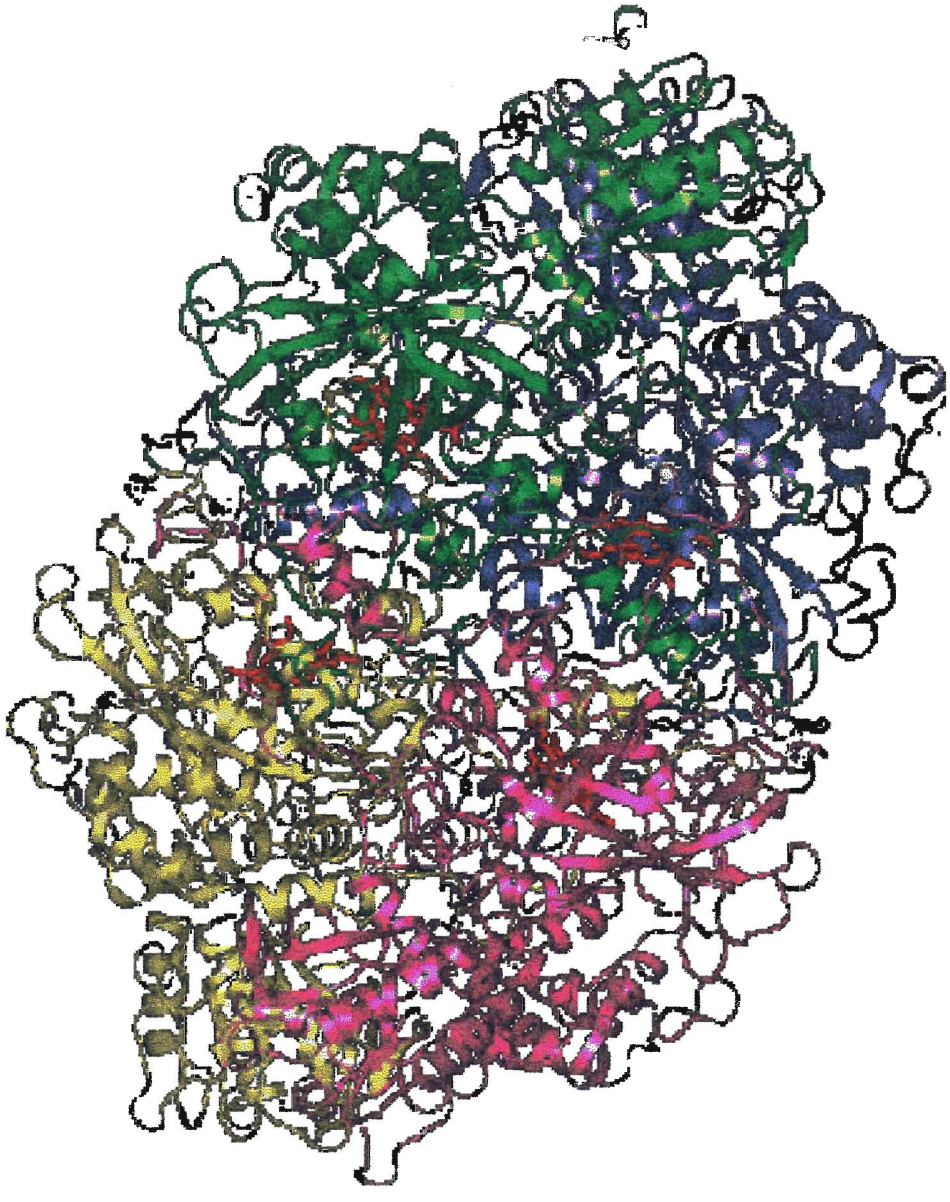

**Figure 1. Ribbon diagram of the HPII tetramer.**
The four identical subunits are arranged with a 222 symmetry. Each subunit is associated with a heme prosthetic group (shown in red). The secondary structures were determined from the torsion angles of the backbone.

All structural diagrams contained in this thesis were generated using QUANTA™ software on an SGI Indigo 2 system.

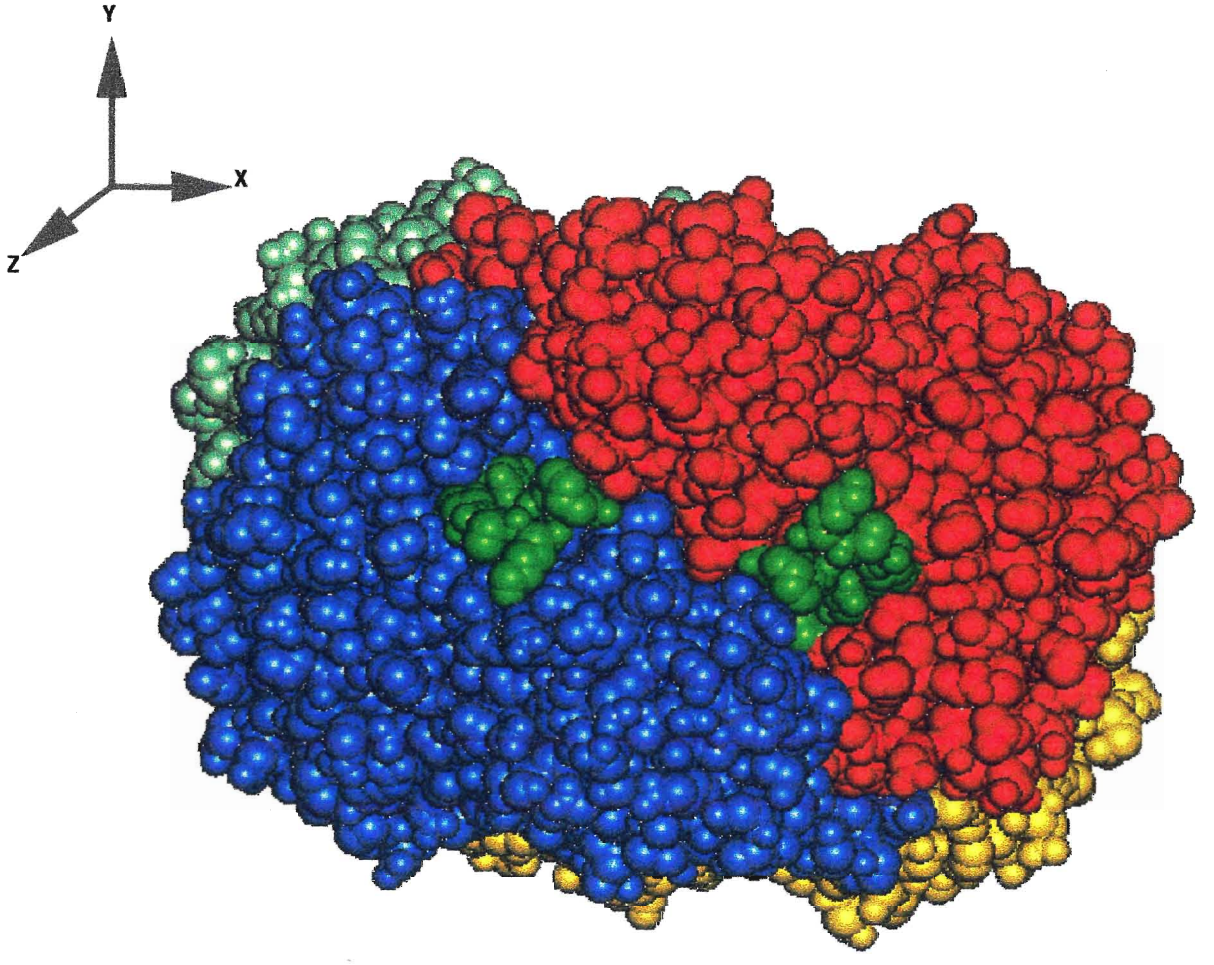


**Figure 2. Space filling model of the HPII tetramer.**
Each subunit is individually coloured, and the opening of the active site channel is coloured green. The size of the tetramer is 90X150X71 Å.

then catalyses the conversion to a heme $d_{cis}$ in the presence of hydrogen peroxide (Loewen *et al.* 1993). Amino acid sequences of the four enzymes show ≈70% homology and their tertiary structures are similar. The hemes are typically 20Å from the surface of the protein and are accessible to solvent by a largely hydrophobic channel (figure 2). All have the phenolate of a tyrosyl residue occupying the fifth coordination position of the heme iron (Fita and Rossman 1985b, Sharma *et al.* 1989). The heme iron is penta-coordinated with the sixth coordination site vacant (Fita and Rossman 1985b, Andersson *et al.* 1995). All have the distal residues histidine and asparagine which are essential to catalytic activity (Fita and Rossman 1985b, Loewen *et al.* 1993). Their activities, their reactivities with peroxide and their ligand binding affinities are all different. These differences may be due to the differences in heme type and heme pocket amino acid residues as well as differences in the accessibility to the heme group.

Catalase accelerates the rate of hydrogen peroxide decomposition. In the overall catalatic reaction (equation 1), two molecules of hydrogen peroxide are decomposed to molecular oxygen and water in successive two-electron reactions as shown below (equation 2 and 3):

$$2\ H_2O_2 \rightarrow 2\ H_2O + O_2 \quad (1)$$

$$\text{Catalase} + H_2O_2 \rightarrow \text{Compound I} + H_2O \quad (2)$$

$$\text{Compound I} + H_2O_2 \rightarrow \text{Catalase} + O_2 + H_2O \quad (3)$$

The first molecule of peroxide acts as a two electron oxidant forming the primary intermediate compound I (eqn. 2). Both catalases and peroxidases can form compound I, but only catalase compound I has the ability to oxidize a second molecule of hydrogen peroxide (eqn. 3). This ability is presumably related to tyrosinate ligation as well as to the nature of the distal heme pocket (Schonbaum and Chance 1976). A second function of catalase is the less specific peroxidatic decomposition of compound I (eqn. 4) via two-electron donors:

$$\text{Compound I} + AH_2 \rightarrow \text{Catalase} + A + H_2O \quad (4)$$

where $AH_2$ is a two-electron donor such as ethanol or formate. The peroxidatic reaction of catalase predominates in the presence of hydrogen donors and low hydrogen peroxide concentrations (Chance *et al.* 1952b, Keilin and Hartree 1955). Under suitable conditions, compound I can spontaneously react with a one-electron endogenous donor to form a second intermediate, compound II. Compound II is catalytically inert, and is formed slowly in the absence of added electron donors (Chance 1948). The conversion of compound I to compound II can be accelerated by anions (Nicholls 1961). Accumulation of compound II *in vivo* may occur under

abnormal conditions such as those associated with cell necrosis, tumor, or prolonged hypoxia (Oshino *et al.* 1973). Compound III is formed from compound II in the presence of excess hydrogen peroxide (Keilin and Hartree 1951) or from the association of the resting enzyme with superoxide (Kono and Fridovich 1982, Shimizu *et al.* 1984). Compound III does not participate in the normal catalatic or peroxidatic cycles and is inactive towards most electron donors (Chance *et al.* 1984).

## History

In 1901, Loew first introduced the term catalase. Most work with catalase from the turn of the century untill the mid-1930's was directed at purification of the enzyme (Sumner and Dounce 1937) and studies of the action of metals in biological systems. The history of catalase research is summarized in reviews by Nicholls and Schonbaum (1963), Deisseroth and Dounce (1970) and Schonbaum and Chance (1976). From the early 1930's to the end of the 1940's compounds of hemoproteins and their substrates were studied by visual spectroscopy. Using a concentrated preparation of liver catalase, Zeile and Hellstrom (1930) demonstrated the hematin nature of catalase as being similar to that of hemoglobin. It was impossible to ascertain whether the hematin of catalase was ferric or ferrous because neither sodium dithionite nor potassium ferricyanide had any effect on the absorption spectrum. By analogy with other hemoproteins, this was considered a

"remarkable" property of catalase (Zeile and Hellstrom 1930). They also showed that compounds which inhibited the activity of catalase (KCN and $H_2S$) also modified the absorption spectra of the hematin. The spectra of neither KCN-catalase nor $H_2S$-catalase were affected by the addition of small amounts of hydrogen peroxide, showing that KCN and $H_2S$ inhibited the formation of an intermediate enzyme-substrate compound (Keilin and Hartree 1936b). Another stable spectral derivative of catalase was reported by Stern in 1936. Stern identified a red intermediate of catalase and ethyl hydrogen peroxide, now known as compound II. Keilin and Hartree (1935) reported that the spectrum of catalase was not affected by the addition of peroxide, although an immediate decomposition of hydrogen peroxide did occur. In fact it was not till 1947 that Chance (1947a), using the stopped flow method and an improved sensitive spectrophotometer, discovered the primary compound of catalase (now known as compound I). Shortly after the discovery of compound I, Chance (1948) proposed that not only does hydrogen peroxide bind with catalase to form the primary enzyme-substrate complex but also reacts again with this complex to cause the decomposition of hydrogen peroxide and regenerating catalase, a mechanism first proposed by Albers in 1933 to explain the kinetics of catalase. Because the rate of hydrogen peroxide decomposition is directly proportional to peroxide concentration, no saturation effects were expected. Chance suggested that any decrease in enzyme activity in the presence of continuously supplied hydrogen peroxide is the result

of the slow conversion of compound I to the enzymatically inactive compound II (Chance 1948).

Very little direct evidence for a catalase reaction mechanism had been obtained before the rapid spectrophotometric methods used by Chance in 1947. It had been known since 1936 (Keilin and Hartree 1936a) that catalase had the ability, under certain conditions, to catalyse the oxidation of alcohols by hydrogen peroxide. In 1949, detailed spectroscopic studies to investigate the properties of the primary complex and the oxidation of alcohols were carried out. Chance (1949a) found that 1.2 ± 0.1 hematin groups are occupied by hydrogen peroxide using a method involving the reaction of the complex with cyanide. Chance (1949b) also measured the velocity constants for the reactions of compound I with various alcohols and formate, leading to the distinction between the catalatic and peroxidatic activity of catalase.

By the early 1950's, many of the intermediates of catalase had been well defined spectroscopically. The introduction of stopped and rapid flow methods with sensitive spectrophotometers, the development of the spectrophotometric technique for following the breakdown of hydrogen peroxide, and the invention of the electric analog computer allowed for quantitative methods for the study of catalase kinetics (Chance and Herbert 1950, Beers and Sizer 1952).

## Ligands and Intermediates

Historically, the oxidation state of the heme iron was determined by the reaction of the hemoproteins with sodium dithionite or ferricyanide. Neither compound had any effect on the absorption spectrum of catalase, but magnetometric measurements could be used for the elucidation of the electronic structure of the resting heme state, as well as reaction intermediates and derivatives of catalase. The magnetic suseptibility technique for the study of iron proteins was developed in the lab of Pauling (Coryell *et al.* 1936). Magnetic susceptibility is the ratio of the intensity of magnetization of a substance to the strength of the magnetic field. Substances are classified as to whether they are diamagnetic (negative, indicating fully paired electrons) or paramagnetic (positive, indicative of unpaired electrons) (Hartree 1947). Magnetic susceptibility measurements of horse liver catalase were first reported by Theorell and Agner in 1943. The iron of free catalase was determined to have 5 unpaired electrons, cyanide and $H_2S$ derivatives showed 1 unpaired electron with a "covalent" bond to the iron (low-spin) and both azide and fluoride derivatives contained 5 unpaired electrons. The azide and fluoride bond to the heme iron was suggested as being ionic (high-spin). Deutsch and Ehrenberg (1952) reported identical results with erythrocyte catalase. Theorell and Ehrenberg (1952) found that catalase compound II has 2 unpaired electrons, which might imply a low-spin complex with an extra unpaired electron

associated with its single oxidation equivalent (Nicholls and Schonbaum 1963). Deutsch and Ehrenberg (1952) also reported no change in the paramagnetism of the heme from pH 4.8 to 10.4. Catalase with 5 unpaired electrons has no oxidizing equivalents, compound I has 2 oxidizing equivalents and compound II has one oxidizing equivalent (Chance 1949b, Keilin and Nicholls 1958, Brill and Williams 1961). The spin state of the resting enzyme does not change with pH, nor is there any effect of pH on catalase activity. This suggests that there are no heme linked groups to be dissociated over the pH range between 5 and 10 (Chance 1952a). However, the binding of anions is dependent upon pH. It is normally the acid form and not the ion which binds at the active site, as shown for cyanide, fluoride and formate (Chance 1952b).

The visible spectrum of catalase reflects not only changes of heme iron ligands and spin state, but any transitions of the $\pi$ electrons of the porphyrin (Hartree 1946, Brill 1966). The absorption band of catalase in the Soret region is due to $\pi$-$\pi^*$ transitions of the aromatic system of the porphyrin ring, the 622 nm ($\alpha$) band and the 500-505 nm band are due to the metal to ligand charge transfers that increase in magnitude during excitation. The band at 535-540 nm is also thought to be due to a metal to ligand charge transfer (Brill and Williams 1961, Sanders *et al.* 1964).

Catalase can exist in three oxidation states. The peroxide intermediates, compounds I, II and III, are spectrally distinct. The formation of the primary complex can be observed by an absorption band in the visible region, and a decrease in optical density in the Soret region at 405 nm. The formation of the secondary intermediate from the primary compound can be observed as a red shift of the Soret band and a blue shift of the $\alpha$-band in the visible region. The transition of compound II to III affects the spectrum by blue shifting the Soret region band, as well as causing spectral changes in the visible region. These various oxidation states of catalase are interconvertable upon the addition of suitable oxidants and reductants to the resting form of the enzyme (Lardinois 1995).

Evolutionarily diverse catalases are efficient in the dismutation of hydrogen peroxide. Even though mammalian and bacterial catalases contain over 90% structural homology, their rate constants for the formation of the primary intermediate are different. The catalytic activity of the bacterial catalase MLC is nearly twice that of mammalian catalases. The rate of compound I decay in the presence of ethanol is very different, mammalian catalase being 100 times greater than that of MLC. The small differences in the active site residues may account for the differences in catalytic activity as well as peroxide and hydrogen donor reactivity.

Hydrogen peroxide performs both oxidation and reduction of the heme group. The first molecule of peroxide reacts with the heme of catalase to form compound I. Compound I is a strong oxidizing agent where the heme has been oxidized from $Fe^{3+}$ to $Fe^{4+}$=O. Compound II is formed by a 1-electron reduction of compound I. The nature of compound I is best studied with the use of hydrogen peroxide analogues which convert free catalase completely into compound I (Chance 1949a). The absorption spectrum of catalase compound I formed with ethyl hydrogen peroxide led Brill and Williams (1961) to suggest that the formation of compound I involves an attack on the porphyrin conjugated ring system at one methylene bridge. They concluded that the magnetic evidence allowed for a radical on the porphyrin combined with an Fe(IV) state. Direct evidence for a $\pi$-cation radical was reported by Dolphin and co-workers in 1971. The optical properties of cobaltous octaethylporphyrin cation radicals are analogous to those of catalase and peroxidase compound I. If the primary compound is a cation radical, and the one electron reduction of the porphyrin system results in the formation of compound II, then both compound I and II should contain Fe(IV). Mossbauer spectroscopy (Maeda and Morita 1968) has shown that the electronic configurations of compound I and compound II are the same. Dolphin and co-workers (1971) also suggest that a stable porphyrin cation radical permits transfers in the catalytic cycle to occur via the porphyrin ring.

High-spin ligands such as fluoride and formate bind to the free enzyme. The transition of compound I to compound II and the decay of compound II is accelerated in the presence of anions suggesting that anions form complexes with the heme even when the heme is in the form of compound I and II. High-spin ligands are thought to enhance the rate at which the endogenous donor can reduce compound II. These reactions are first order with respect to the enzyme concentration in the absence of external hydrogen donors.

The formation of compound II from compound I is accelerated by fluoride although fluoride is not thermodynamically capable of acting as a hydrogen donor. Fluoride accelerates the formation of compound II ten fold, from 0.012 $s^{-1}$ to 0.15 $s^{-1}$ at pH 5. The decay of compound II is increased a hundred fold, from 0.0009 $s^{-1}$ to 0.08 $s^{-1}$. Both free catalase, compound I and compound II have a similar affinity for fluoride, 3.0 mM, 3.5 mM and 4.4 mM respectively at pH 5 (Chance 1952b, Nicholls 1961). Formate is a unique high-spin ligand, as it has the ability to donate 2 electrons to compound I in a second order reaction. The reaction rate of formate with compound I is 470 $M^{-1}s^{-1}$. (Chance 1950b). Formate also increases the rate of compound II decay (Keilin and Nicholls 1958, Nicholls 1961). Free enzyme and compound II share a similar affinity for formate, 13 mM at pH 5 (Nicholls 1961).

Catalase compound II shows a much lower affinity for low-spin ligands such as cyanide. The low affinity of compound II for

cyanide is presumed to be a consequence of the heme iron already being covalently bound to substrate (George 1953, Nicholls 1961). Recent resonance Raman investigation of covalent HCN binding to the heme iron of catalase showed that HCN binds with two conformers. At physiological pH, the heme iron binds cyanide with a linear conformer with the proton presumably protonating the distal histidine imidazolium group. At higher pH when the imidazole is presumably deprotonated, cyanide binds to the iron in a bent conformer presumably stabilized by another distal residue (Al-Mustafu *et al.* 1995).

## Kinetics

In the first half of this century, only investigation of steady-state enzyme reactions were possible. In the early 1950's, using electric circuit technology from the second world war, analog computers were developed specially designed to solve mathematical equations representing the non-steady state reaction kinetics of complex enzyme systems and their substrates (Chance *et al.* 1952a). Chance and his coworkers (1952b) employed such a computer to study the peroxidatic and catalatic routes of compound I decay (Chance *et al.* 1952b). When catalase accelerates hydrogen peroxide decomposition to oxygen and water, the reaction rate is directly proportional to $H_2O_2$ and catalase concentrations.

$$\frac{dx}{dt} = -k_1' * e * x \qquad (5)$$

where x = [hydrogen peroxide], e = [catalase] and $k_1'$= velocity of hydrogen peroxide decomposition (Bonnichsen *et al.* 1947).
Catalase also accelerates the oxidation of alcohols and related compounds by $H_2O_2$. This reaction predominates at low peroxide concentrations:

$$\frac{da}{dt} = -k_4 * a * p \qquad (6)$$

where a = [alcohol], $k_4$ = alcohol oxidation and p = compound I (Chance 1947b).
Compound I forms at a rate proportional to the concentration of free catalase and hydrogen peroxide:

$$\frac{dp}{dt} = k_1 * (e - p) \qquad (7)$$

where p = compound I and $k_1$ is the rate of comp I formation (Chance 1947b).
The average number of hemes forming compound I with $H_2O_2$ is 30% (Chance 1947b, Chance 1949a). All hemes form compound I with alkyl peroxides:

$$\frac{dp}{dt} = k_1'' * x(e - p) \qquad (8)$$

where $k_1''$ is the rate of compound I formation, x = [alkyl peroxide], p = [compound I] and e = [hematin] (Chance 1949b).

Compound I will decompose in a first order reaction:

$$\frac{dp}{dt} = -(k_{-1} + k_4 * a)p \qquad (9)$$

where $k_{-1}$ is the spontaneous rate of decomposition, a = [alcohol] and $k_4$ is the rate of alcohol oxidation (Chance 1949b).

The following reaction mechanism adequately explains the catalatic and peroxidatic reactions:

$$E + S \underset{k_{-1}}{\overset{k_1}{\rightleftharpoons}} E + P \qquad (10)$$

$$ES + S \xrightarrow{k_4'} E + P \qquad (11)$$

$$ES + AH2 \xrightarrow{k_4} E + A \qquad (12)$$

where E = catalase, S = hydrogen peroxide, ES = compound I, $AH_2$ = donor molecules and P = products.

A third route available for the decay of compound I is the slow accumulation of the inactive second intermediate. Compound II is formed from compound I in a first order reaction (Keilin and Nicholls 1958) due to the presence of an internal donor. The endogenous donor reacts at a rate independent of catalase

concentration, suggesting a unimolecular decomposition of compound I, where compound II formation is the result of a transfer from the same protein molecule (Nicholls 1961). Sometimes the transitions among the intermediates are accelerated in the presence of reagents such as ascorbate and ferrocyanide (Chance 1950a), suggesting that these reagents react with compound I (Nicholls 1961). Alcohols and formate, if added at the beginning of a reaction, prevent the formation of compound II by keeping a low steady state concentration of compound I.

Compound III is produced from compound II in the presence of excess hydrogen peroxide, and seems to decompose to give compound II, therefore retaining at least one oxidizing equivalent. Compound III is rather inactive towards most hydrogen donors so it is an inhibited form of the enzyme (Chance 1952a).

**Reaction Mechanism**

The exact mechanism by which catalase dismutes cellularly generated hydrogen peroxide has yet to be defined. However, some conclusions have been drawn based on decades of biochemical investigation. The catalytic and peroxidatic cycles of catalase action, intermediates of these cycles and their oxidizing equivalents are summarized in figure 3.

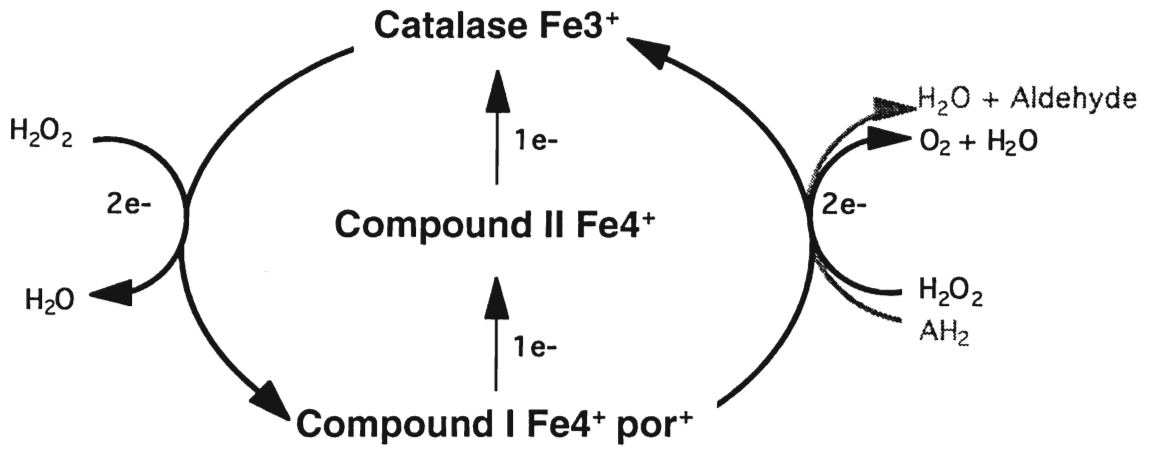


**Figure 3. The reaction cycle and principle redox reactions of catalase.** Catalytic reaction with hydrogen peroxide will occur in the absence of hydrogen donors (shown in black). The peroxidatic reaction (shown in gray) will occur in the presence of hydrogen donors ($AH_2$).One molecule of peroxide will induce the oxidation of the heme from $Fe^{3+}$ to $Fe^{4+}$ and a cation radical ($por^+$). A second molecule of hydrogen peroxide (catalytic) or a hydrogen donor (peroxidatic) will induce a 2-electron reduction of the heme regenerating the resting enzyme. Compound I can also undergo a 1-electron reduction via the porphyrin ring. This 1-electron reduction is due to the presence of an internal donor and can be accelerated in the presence of anions such as fluoride and formate.

The mechanism of the reaction at the active site is controlled by the influence of the phenolate oxygen of tyrosine at the fifth coordination site of the heme iron, as well as the effect of the basic distal residues histidine and asparagine in stabilizing substrate at the active site. The mechanism of the reaction is also controlled by the length, size and hydrophobicity of the active site channel (Bengal *et al.* 1989).

The role of tyrosine as the fifth ligand was investigated by Robert and coworkers in 1991. Their attempts to model catalase activity with simple iron porphyrin compounds indicated that oxygen donors (phenolate, tyrosinate & alcoholate) at the fifth

coordination site are less efficient in catalyzing the dismutation of hydrogen peroxide than if the fifth site is occupied by a nitrogen ligand such as imidazole (Bengal *et al.* 1989 and Robert *et al.* 1991). However a tyrosine residue as a proximal ligand will draw the heme iron out of the plane thereby increasing the probability of penta coordination (Hildebrand *et al.* 1995), leaving an open 6th ligand site more easily occupied during catalysis (Andersson *et al.* 1995). This suggests that penta coordination as well as distal residues at the active site are responsible for the catalytic efficiency of catalase (Bengal *et al.* 1989 and Robert et *al.* 1991).

Amino acid residues distal to the heme govern the events leading up to the formation of the primary complex of catalase. The events of compound I formation were computer-simulated by Fita and Rossman (1985b). They concluded that hydrogen bonding to the distal residues histidine and asparagine as well as electrostatic interaction with the heme iron stabilizes the substrate at the active site (figure 4). A general acid-base reaction can occur resulting in a single oxygen bound to the iron in the Fe(IV) state, a $\pi$-cation radical at a methylene bridge and the release of a water molecule. Compound II could be formed through the donation of an electron from the surrounding protein matrix (Fita and Rossman 1985b).

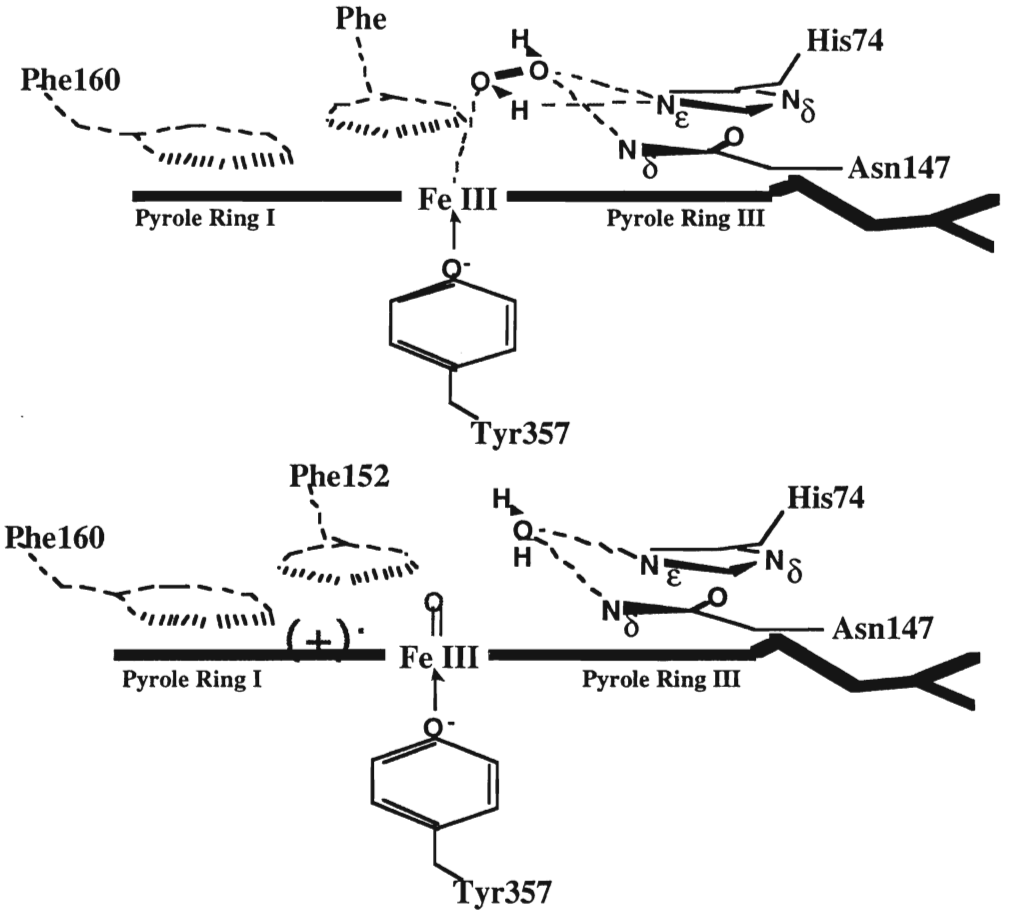


**Figure 4. The formation of BLC compound I.**
The events leading to the formation of compound I are governed by the stabilization of substrate at the active site by the distal histidine and asparagine. The electrostatic interaction of peroxide with $Fe3^{+}$ as well as hydrogen bonding to $N_{\varepsilon his74}$ will lower the pKa of the OH group of the peroxide inducing the oxygen to bind to the heme iron. The iron will increase in oxidation from $Fe^{3+}$ to $Fe^{4+}$ thereby decreasing the nuçleophilic nature of the distal histidine. The ensuing molecular rearrangement of the peroxide molecule will result in an oxygen covalently bound to the iron. One delocalized porphyrin electron will be utilized in creating this bond, resulting in a stable prophyrin π-cation radical. These events are based on the computer generation studies of Fita and Rossmann (1985b).

The active site channel is approximately 20Å long, is lined with hydrophobic residues and is rather narrow. Before the crystal

structure of catalase was known, biochemical data indicated that the heme of catalase was buried in the protein and that the heme was connected to the surface by a narrow channel. The reaction rates of catalase with alkyl peroxides decrease with increasing alkyl size (Jones and Middlemiss 1972) and compound I reacts less rapidly with higher alcohols (Chance 1947b) indicating that smaller molecules are more accessible to the active site. The protein channel acts as a filter preferring small neutrally charged molecules (figure 5). The acid form of anions bind at the active site suggesting that there is an electrostatic constraint on the access of substrate to the active site (Deiseroth and Dounce 1970). Recent site-directed mutagenesis experiments (Zamoky *et al.* 1995) relieved the narrow constraint of the yeast catalase A channel by replacing four channel phenylalanines with valines, and one valine with alanine. The result was an increase in the non-specific peroxidatic rates and a decrease in the catalytic rates. The difference in the protein moieties are responsible for the relative rates of specific catalytic and broad range peroxidatic reactions.

The mechanism of catalase activity is governed by at least three things. The first is tyrosine at the fifth coordination site inducing the penta-coordination of the heme iron. The next is the basic distal residues histidine and asparagine. The third factor is the control of substrate specificity by protein moities of the active site channel.

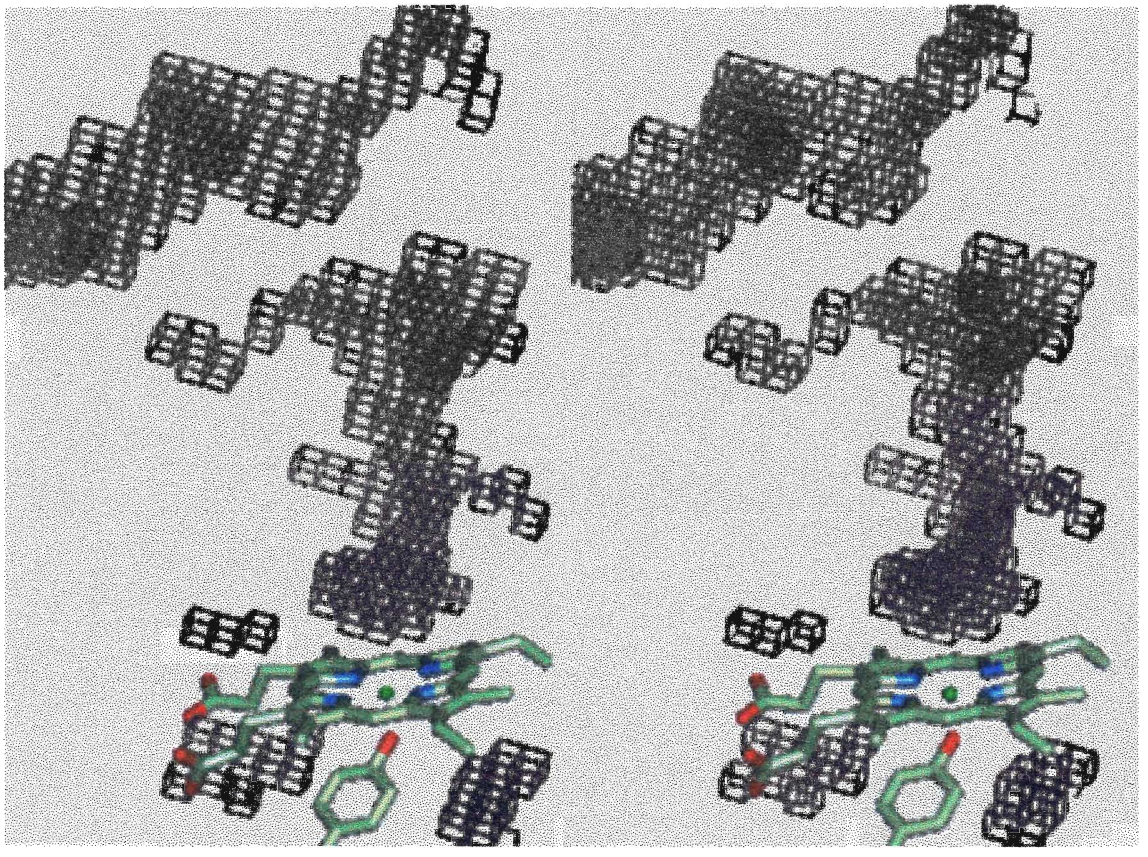

**Figure 5. Stereo view of the catalase active site channel.**
Show here is the accessibility of solvent to the active site. The active site channel is approximately 20 Å in length, and 5 Å in diameter at its most narrow region. The channel is lined with hydrophobic residues. The dimensions of each cube representing solvent accessibility is 1 cubic angstrom.

## Structure of Typical Catalases

The sequence and structure of catalases have been very highly conserved among diverse organisms. The active site residues and their secondary structures are nearly identical for animal, plant, fungal and bacterial catalases. Most catalases utilize protoheme IX (figure 6a) as the prosthetic group (e.g. BLC and MLC). Other enzymes originally associate with protoheme IX then biosynthesize a derivative of the heme upon turning over (Hansson and von Wachenfeldt 1993). HPII and PVC execute a cis-hydroxychlorin gamma-spiralactone derivative referred to as heme $d_{cis}$ (figure 6b). The protein surrounding the heme controls the heme bioconversion (Jacob and Orme-Johnson 1979, Varva *et al.* 1986, Chiu *et al.* 1989, Timkovich and Bondoc 1993, Loewen *et al.* 1993, Murshudov *et al.* 1996). The details of the heme modification are still unknown. Catalases share the distinctive feature of having the phenolate group of a tyrosine residue (figure 7a & b) coordinated to the heme as the fifth ligand (Reid *et al.* 1981, Dawson *et al.* 1991). Catalases also share a distal histidine and asparagine (figure 7a & b) which are necessary for efficient dismutation of hydrogen peroxide (Loewen *et al.* 1993). The distal histidine is at an angle unique to hemoproteins. The plane of the imidazole ring lies parallel to that of the porphyrin ring. This histidine has phi psi angles normally permitted for glycine only and may be stabilized by a strong interaction of the histidine carbonyl with the guanidium group of a nearby arginine.

6 a. protoporphyrin IX

6 b. heme $d_{cis}$

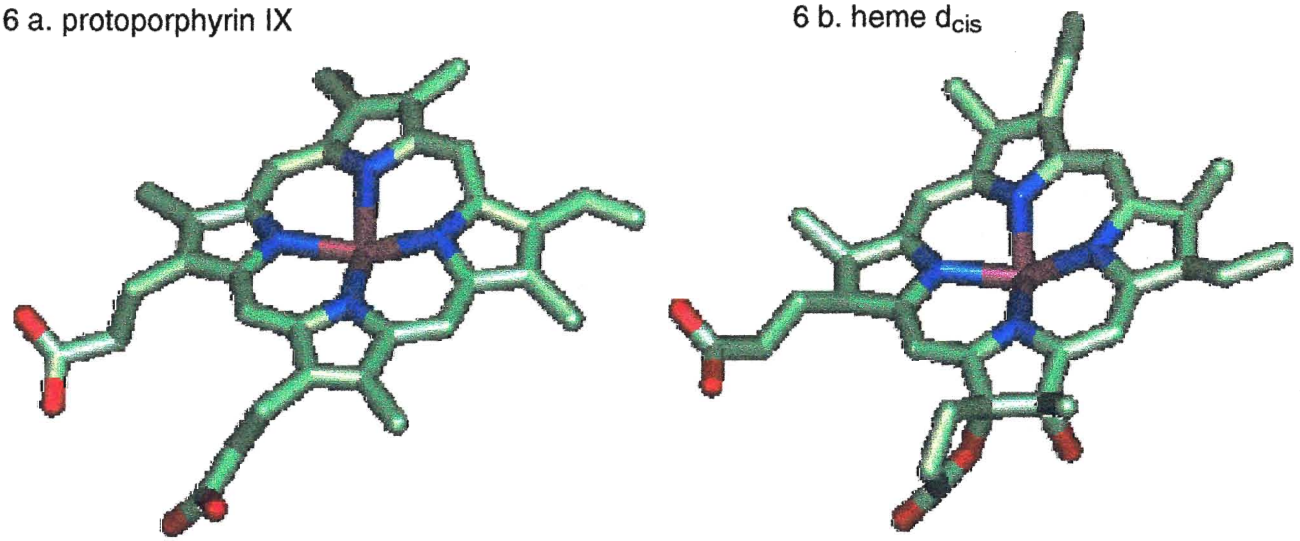

**Figure 6 a&b. Distal view of BLC protoporphyrin IX (a) and HPII heme $d_{cis}$ (b).** The orientation of the hemes are as viewed from the distal side.

7a) BLC protoporphyrin IX

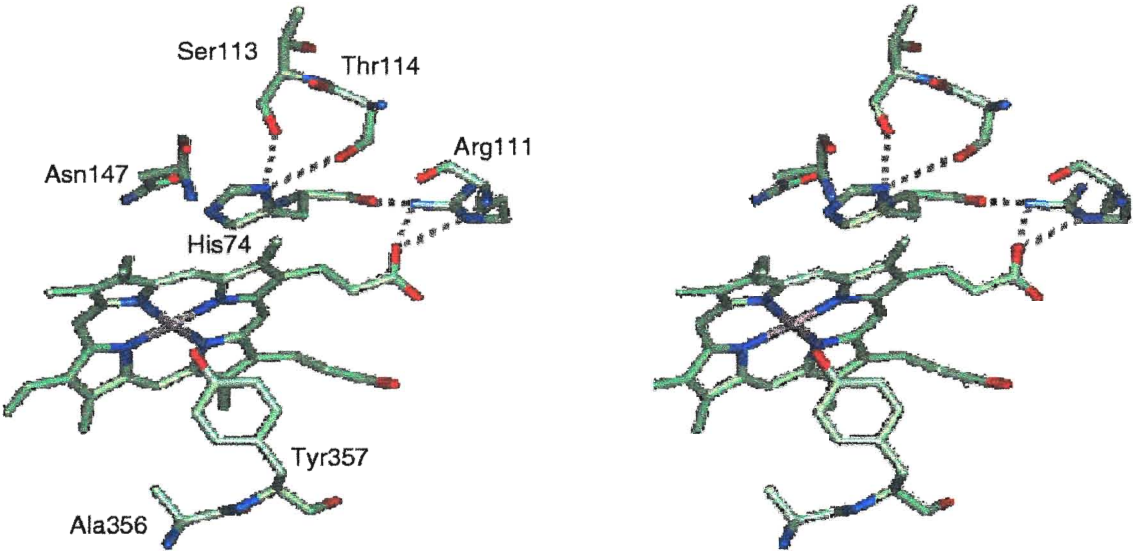


7b) HPII heme d (cis)

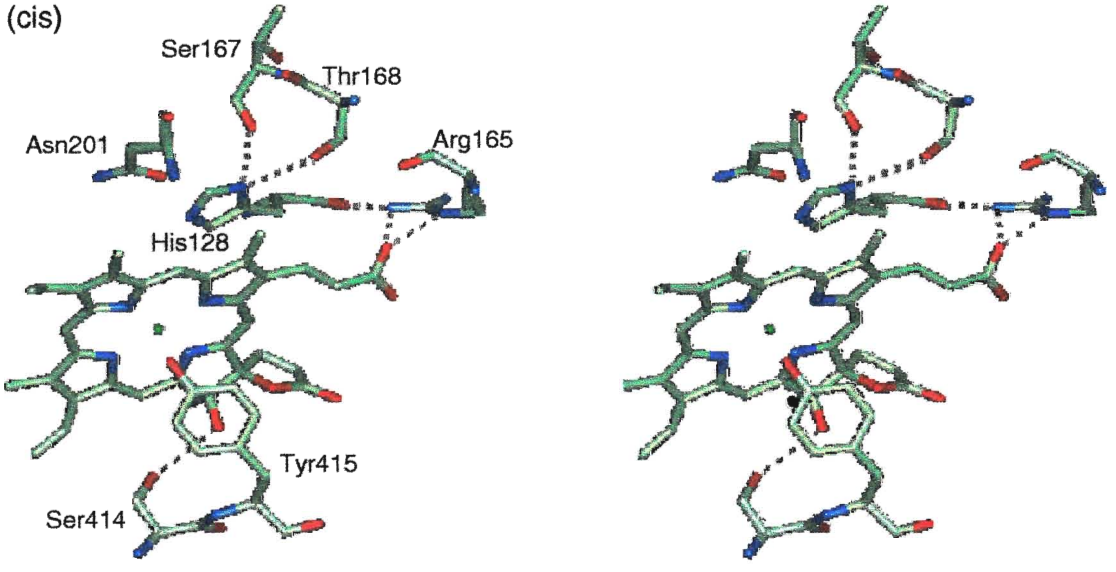


**Figure 7 a&b. Stereo views of catalase active sites.**
The veiw is from the proximal side of the heme showing the orientation of the proximal tyrosine as well as the distal histidine and asparagine for a)BLC and b)HPII. The unique conformation of the distal histidine is held in place by hydrogen bonding to other distal residues. Figure b) shows the hydrogen bond from the hydroxyl of heme d to ser414.This serine residue may assist in the bioconversion of protoheme to heme d (cis).

The carbonyl of a threonine points directly at the plane of the imidazole group of the distal histidine, thereby constraining the orientation of these distal residues (Fita and Rossman 1985b). The distal histidine is absolutely required for catalytic activity, whereas mutation of the distal asparagine produces an enzyme with limited activity. The distal asparagine stabilizes substrate at the active site during catalysis (Loewen *et al.* 1993).

The three dimensional structures of five catalases are known, PVC at a 1.8 Å resolution (Murshudov *et al.* 1996), HPII at 2.8 Å resolution (Bravo *et al.* 1995) BLC at 2.5 Å resolution (Fita *et al.* 1986) MLC at 1.5 Å resolution (Murshudov *et al.* 1992) and PMC at a 2.2 Å resolution (Gouet *et al.* 1995). These five catalases share four common domains per subunit (figure 8a & b). The first 70 residues form the first domain which is an arm that extends from the globular region of the subunit and interacts with the active site channel of a neighboring subunit. The next ≈ 250 residues form the second domain which is a large 8-stranded antiparrallel ß-barrel. The third domain (residues 300-450) is referred to as the wrapping domain in which the essential helix containing the proximal tyrosine is located. The fourth domain consists of α-helices on the external part of the molecule (figure 8a). Both PVC and HPII contain an additional c-terminal domain extension of about 250 residues with a flavodoxin-like topology (Bravo *et al.* 1995, Murshudov *et al.* 1996). This extension is located in a crevice between the ß-barrel domain and α-helical

8a) BLC

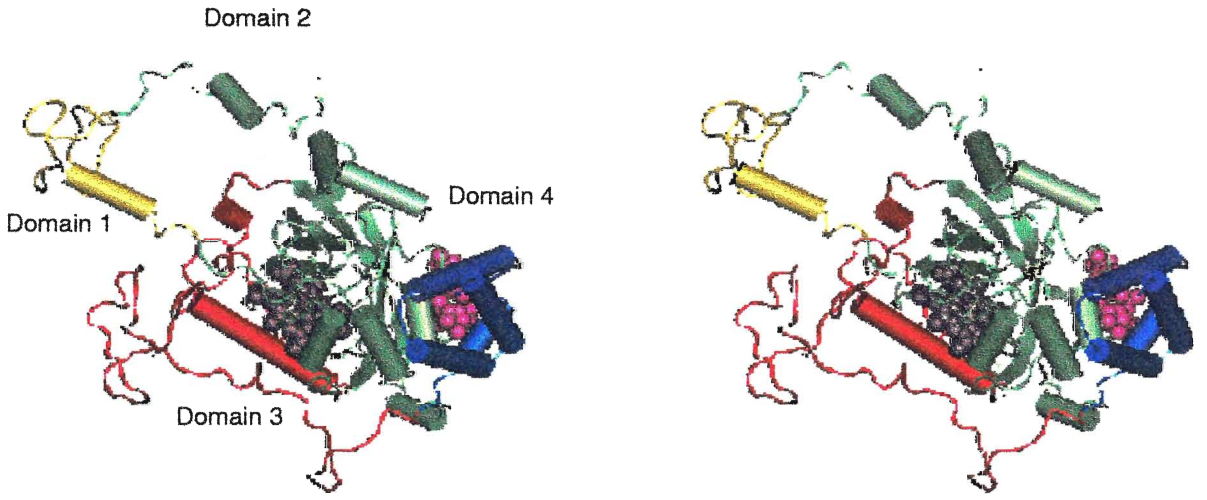


8b) HPII

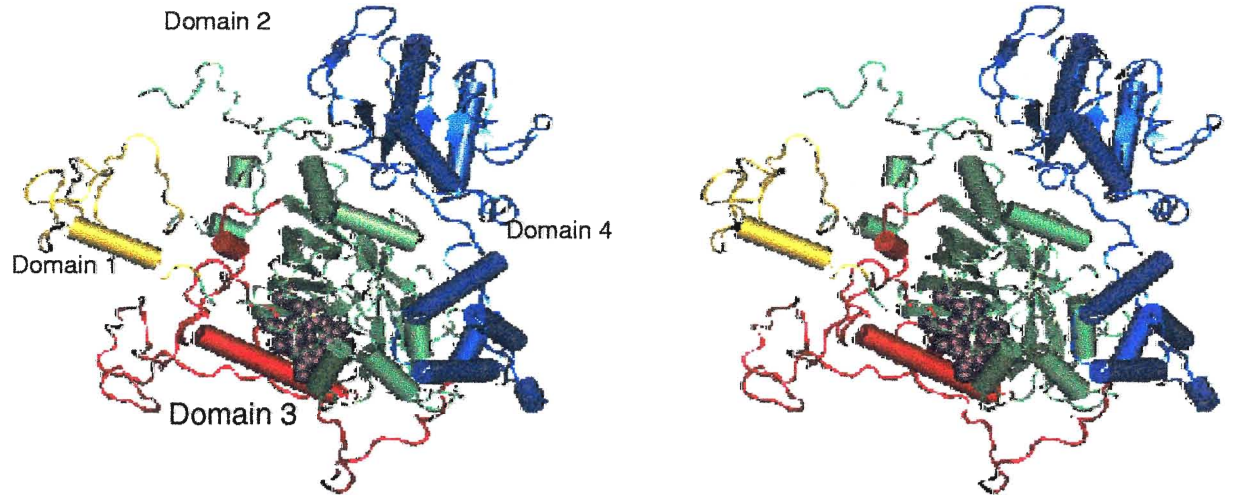


**Figure 8 a&b. Stereo domain diagram of a BLC (a) sununit and an HPII sununit (b).** All typical catalases share these four typical domains. Domain 1 (yellow) involves the first ~70 amino acid residues. Domain 1 is an extension from the globular region of the subunit which interacts with active site channel of a neighbouring subunit. The next ~250 residues (Domain 2,white) are involved in the formation of an 8–stranded anti–parallel beta barrel. The heme group (shown in grey) is contained in this domain. Domain 3 (red) is called the wrapping arm of the subunit which stabalizes the tetramer, and is composed of ~100 residues. Domain 4 (blue) is the carboxy terminus. BLC and MLC contain an NADPH binding site a) at the interface between domain 2 & 4 (NAPDPH shown in pink). HPII and PVC do not bind NADPH but they do contain an additional globular region b) of ~250 residues which has a flavodoxin–type binding site.

domain 4 (figure 8b). BLC tightly binds NADPH (figure 8a), one molecule per subunit (Kirkman and Gaetani 1984). The bases of NADPH (figure 9) are approximately perpendicular rather than parallel, and these bases are close to the helices of domain 4. The folded conformation of the NADPH is unlike the extended conformations found in other protein structures (Fita and Rossman 1985a). Most mammalian catalases (Kirkman *et al.* 1987) as well as MLC (Murshudov *et al.* 1992) and PMC (Jouve *et al.* 1989) bind NADPH. Bound NADPH protects catalases from forming the inactive compound II peroxide complex (Eaton *et al.* 1972, Kirkman et *al.* 1987, Hillar *et al.* 1994). Table 1 summarizes the structural information for MLC, BLC, PVC and HPII. The four tetramers crystallize in the same space group. The molecular sizes are close to 240000 MW per tetramer for the protoheme containing enzymes (BLC and MLC) but larger for the heme d enzymes (PVC and HPII). The channels leading to the heme pocket differ in length, with BLC (eukaryotic) enzyme having the shortest path and MLC (prokaryotic) the longest. There is no correlation between the heme type and channel length, however there may be a correlation between the heme type and molecular size.

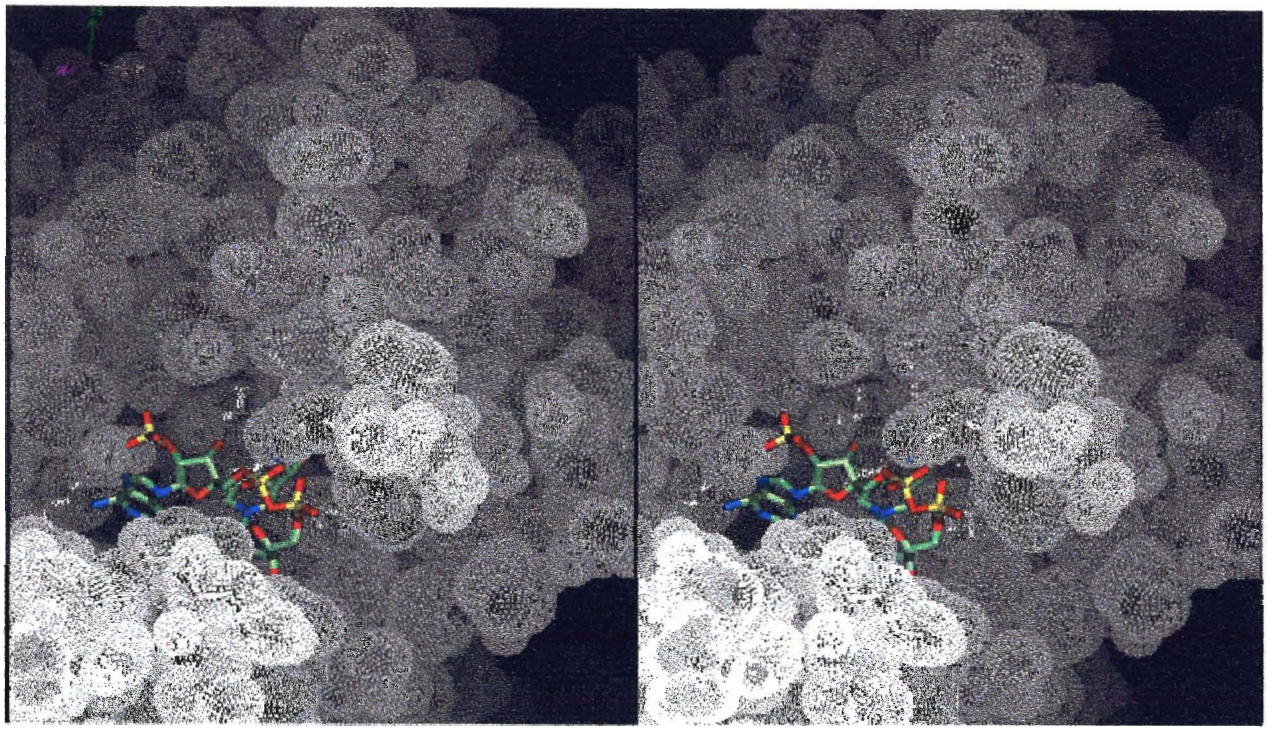

**Figure 9. Stereo view of the BLC NADPH binding site.**
The folded conformation of the NADPH molecule is shown. The bases face into the protein crevice. The crevice is at the surface of the protein at the interface between domain 2 and 4 (cf. fig. 8a).

**Table 1. A summary of the information concerning the structure of BLC, PVC, MLC and HPII.**

| Physical properties | Eukaryotes | | Prokaryotes | |
|---|---|---|---|---|
| | **BLC** | **PVC** | **MLC** | **HPII** |
| **Structure and crystal form** | tetramer; 222 symmetry[1] 2.0 Å resolution | tetramer; 222 symmetry[2] 2.0 Å resolution | tetramer; 222 symmetry[2] 1.5 Å resolution | tetramer; 222 symmetry[3] 2.8 Å resolution |
| **M.W. and subunit Md** | 506 residues 60x80x90 Å Md 57550 Da | ≈670 residues 67x90x127 Å Md 71200 Da | 492 residues 66x90x93 Å Md 55645 Da | 753 residues 71x90x150 Å Md 84200 Da |
| **Heme group** | protoheme[4] | heme d[2] | protoheme[5] | heme d[6] |
| **NADPH site** | yes[7] | no[8] | yes[5] | no[3] |
| **Channel length** | 20 Å | 25 Å | 30 Å | 23 Å |

[1]Murthy et al. 1981, [2]Murshudov et al. 1996, [3]Bravo et al. 1995, [5]Murshudov et al. 1992, [6]Chiu et al. 1989, [7]Kirkman and Gaetani 1984, [8]Vainshtein et al. 1986.

## *Escherichia coli* hydroperoxidase II

### Heme d catalases

*Escherichia coli* is a gram-negative, facultatively anaerobic, rod-shaped bacteria. *E. coli* has two distinct catalases, HPII which is a monofunctional catalase coded for by the katE gene (von Ossowski *et al.* 1991), and HPI which acts as both a catalase and a peroxidase which is coded for by the katG gene (Clairborne and Fridovich 1979). HPII of *E. coli* K12 is purified using a protocol that also allows the purification of HPI in large amounts. HPII is very stable and is maximally active between pH 4-11 (Loewen and Switala 1986). HPI and HPII are induced independently, HPII during bacterial growth into stationary phase and HPI during logarithmic growth (Loewen *et al.* 1985). HPI contains protoheme as the prosthetic group and is found in both the periplasmic and

cytoplasmic membrane fractions. HPII contains heme $d_{cis}$ as the prosthetic group, and is found only in the cytoplasm (Heimberger and Eisenstark 1988). A visible and fluorescent library of heme d, its derivatives and complexes of heme d, compiled from biochemical analysis of the terminal oxidase complex of *E. coli* (Varva *et al.* 1986), was used to prove the presence of the heme d in HPII catalase (Chiu *et al.* 1989).

HPII from aerobically grown *E. coli* normally contains heme d but cultures grown with poor or no aeration produce a mixture of heme d and protoheme catalases. It was concluded that heme d found in HPII catalase is formed by the cis-hydroxylation of protoheme in a reaction catalyzed by HPII using peroxide as the substrate (Loewen *et al.* 1993). The distal amino acid residue histidine 128 is absolutely required for the protoheme to heme d conversion. Two mutants of the distal histidine, H128A and H128N, are catalytically inactive and contain only protoheme which is unaffected by treatment with peroxide. Mutation of the distal residue asparagine 201 indicates that it is not absolutely required for the heme conversion. The mutant N201A contains mostly heme d ,and is partially active, though mutation of the distal asparagine to histidine has been shown to interfere with heme conversion. The N201H enzyme is isolated containing protoheme and has very limited activity. There is, however, a reversible conversion to a heme d like species which occurs in the presence of continuously generated peroxide (Loewen *et al.* 1993).

The crystal structures of PVC (Murshudov et al. 1996) and HPII (Bravo *et al.* 1995) show the stereochemistry of the two heme d chiral carbon atoms as being identical (figure 7b). The heme prosthetic groups for PVC and HPII are found at similar depths and orientation in the protein, however electron density maps for PVC and HPII indicate that the prosthetic group of PVC and HPII are rotated 180° relative to that of BLC (figure 10). Residues which are within contact distance of the heme are different between heme d and protoheme enzymes. The heme contacting residues for PVC are ile41, val209, pro291 and leu342. The corresponding residues for HPII are ile114, ile279, pro356 and leu407. Analogous residues for BLC are met60, ser216, leu298 and met349, and for MLC are his43, ser198, leu280 and met341. These differences may govern the orientation of the heme at the active site (Murshudov *et al.* 1996). Heme d catalases also have a unique serine residue located just below pyrole ring d. A hydrogen bond is formed between the hydroxyl group of the heme d (figure 7b) and the O-$\gamma$ of a serine residue (349 PVC, 414 HPII). This serine is also hydrogen bonded to the carboxylate oxygen of an aspartic residue located in domain 1 of a neighboring subunit (53 PVC, 118 HPII). These interactions may stabilize heme d with the hydroxyl oxygen pointing toward the proximal side. The crystal structure of the inactive HPII mutant N201H indicates that the prosthetic group remains as protoheme but its orientation is the same as that of the wild type enzyme (180° with respect to the heme of BLC). This

10a.Protoporphyrin IX

10b. Heme $d_{cis}$

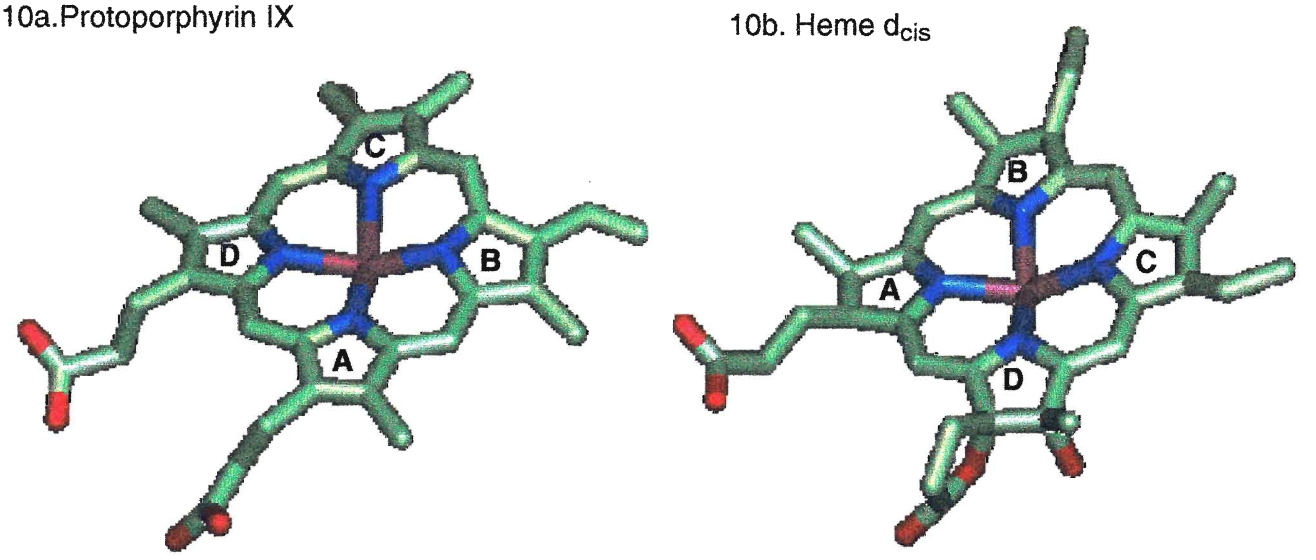


**Figure 10 a&b. The orientation of heme d (b) is reversed with respect to protoporphyrin IX of BLC (a).**
There are 6 residues of HPII (conserved in PVC) which differ from those found in BLC. These 6 residues may be responsible for the inversion of the heme, as well as the conversion of HPII protoheme to heme d (Murshudov *et al.* 1996).

confirms the idea that HPII originally associates with protoheme which is then bioconverted to heme d upon turning over with hydrogen peroxide (Loewen *et al.* 1993, Murshudov *et al.* 1996).

Heme d enzymes appear to be more resistant to oxidative damage than are protoheme enzymes during turnover. Protoheme enzymes, such as BLC and MLC, become inactivated by the slow formation of compound II during catalytic activity. The binding of NADPH (figure 11 a & b) is thought to protect against this formation of compound II (Hillar *et al.* 1994). PVC and HPII both possess a flavodoxin like domain and lack the ability to bind NADPH (figure 11 c & d). Heme d is a weaker lewis base than protoheme (Varva *et al.* 1986), and heme d catalases do not react with one electron donors to give the inactive compound II (Hillar *et al* 1994, Murshudov *et al.* 1996). Therefore there may be an evolutionary correlation between the extra c-terminal domain and heme d.

**Evolution of catalases**

Catalase has been isolated from a large number of respiring organisms, and their amino acid sequences are essentially the same. Because these catalases from evolutionarily distant sources are fundamentally similar, it appears that the enzyme is of some antiquity, and is potentially useful for phylogenetic reconstruction (von Ossowski *et al.* 1993). Melik-Adamyan and coworkers (1986) proposed that the high degree of structural

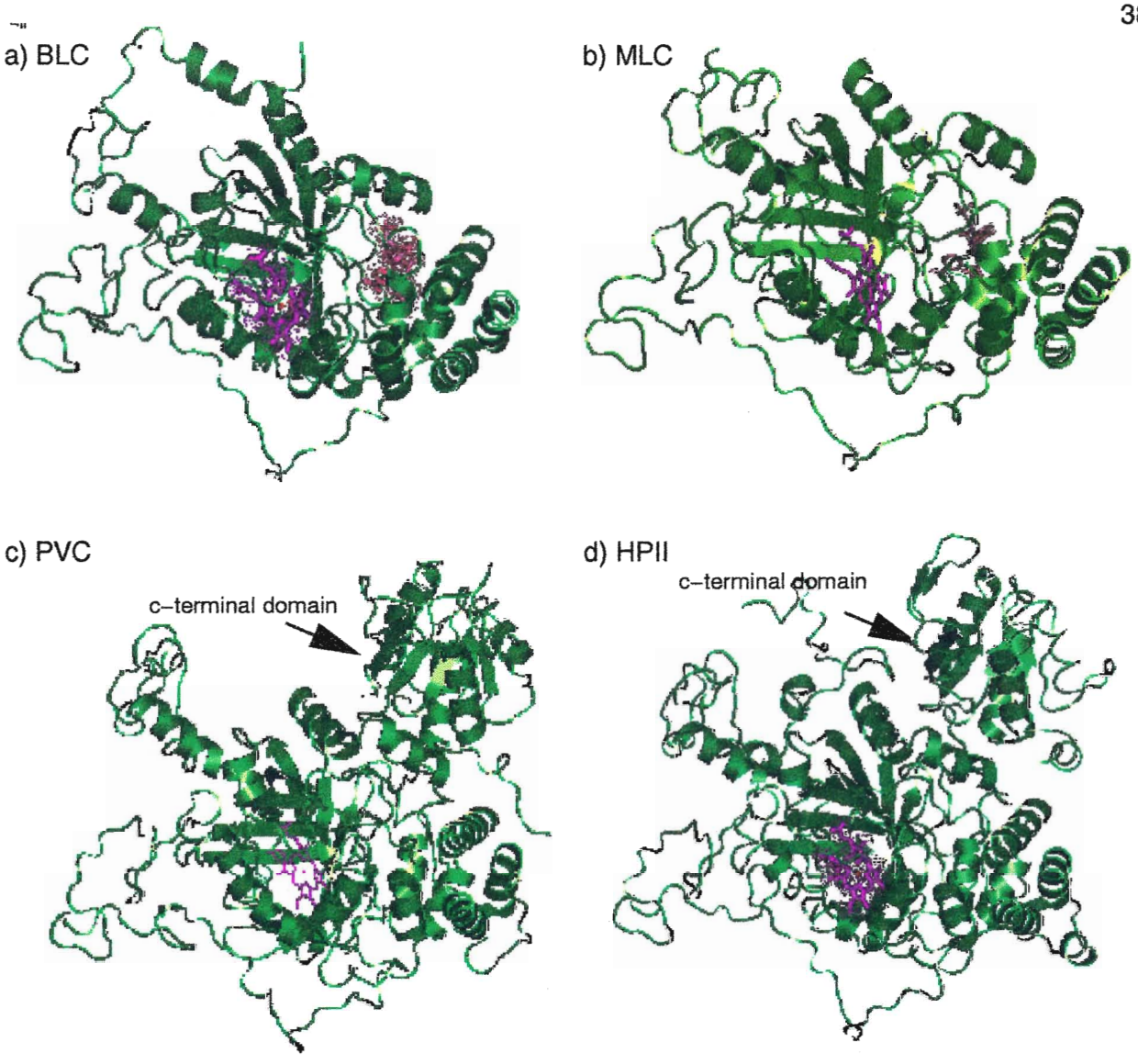


**Figure 11 a, b, c&d. Ribbon diagrams of catalase subunits**.
a) BLC and b) MLC both contain protoheme as the prosthetic group (shown in purple). Each subunit of BLC and MLC bind one molecule of NADPH (shown in pink). NADPH is thought to prevent these catalases from self–inactivation. The heme d catalases c) PVC and d) HPII have an extra c–terminal domain which is located at the same crevice where the protoheme enzymes bind NADPH.Heme d catalases are not known to form the inactive compound II.

homology between mammalian and fungal catalases makes it probable that they have diverged from a common ancestor more than $10^9$ million years ago. A phylogenetic analysis of heme containing catalase sequences from prokaryotes, fungi, plants and animals was reported in 1993 by von Ossowski, Hausner and Loewen. Of the 20 organisms studied, it was determined that catalase may be polyphyletic, and that animal/fungal catalases are derived from a single prokaryotic ancestor. Plant catalases appear to form a second class of catalase, arising independently from a different prokaryotic ancestor. However there is still a very high degree of homology between animal/fungal and plant catalases. This is attributed to the fact that eukaryotic proteins which are compartmentalized in peroxisomes are not exposed to the same evolutionary pressures as are cytosolic proteins, and evolve slowly (Ingual *et al.* 1992). The investigation of 15 bacterial heme catalases by Ingual and coworkers (1992) shows the same polyphyletic character as shown by von Ossowski and colleagues. Catalases show no clear divergence between gram positive and gram negative bacteria (Rocha and Smith, 1995). The evolution and potential origin of catalases may become more evident as more sequences from archaebacteria and cyanobacteria become available (von Ossowski *et al.* 1993).

## Peroxisomes

Peroxisomes are cellular microbodies which contain a number of peroxide producing oxidases ( e.g. urate oxidase and d-amino acid oxidase) and large amounts of catalase. Peroxisomes are organelles with diameters ranging from 0.1-1.7 μm, and are bound by a single membrane. Catalase typically constitutes as much as 40% of the

total peroxisomal protein (de Duve *et al.* 1966). Kidney and liver tissues have much higher catalase activities than most other mammalian tissues. Catalase is renewed at a rapid rate in the liver and the enzyme is synthesized by rough surfaced microsomes and then rapidly transferred to peroxisomes (de Duve 1966). The peroxisomal rat liver catalase and catalase A of *Saccharomyces cervisiae* contain at least six carboxy terminal amino acids which appear to direct the proteins into peroxisomes (Furuta *et al.* 1986, Kragler *et al.* 1993).

Up to 10% of oxygen uptake is converted to hydrogen peroxide (Boveris *et al* 1972). Under normal physiological conditions catalase controls the peroxide concentration so that this does not reach toxic levels (Tolbert and Essner 1981, del Rio *et al.* 1992). 40 - 80% of the peroxide generated in peroxisomes is destroyed inside the organelle. The remaining 20 - 60% diffuses to the surrounding medium (Boveris *et al.* 1972). Very low amounts of peroxide is maintained in the medium surrounding the peroxisomes because of the permeability of peroxide to the peroxisomal membrane. The permeability coefficient is estimated at 0.2 cm $min^{-1}$ (de Duve 1965) which is 5.5 times larger than that estimated by Nicholls (1965) for the red blood cell. The diffusion of peroxide into blood circulation is regulated at concentrations below $10^{-7}$ M by cytosolic catalase and glutathione peroxidase (Sies *et al* 1973).

**Oxygen toxicity**

Cellular oxidative stress occurs in all aerobically respiring organisms. Active oxygen species such as superoxide, hydrogen

peroxide and $OH^{\bullet}$ occur as a by-product of cellular respiration and metabolism. High levels of these active oxygen species can result in metabolic impairment and cell death (McCormick *et al.* 1976). Studies over the last few decades have begun to show the extent of damage caused by active oxygen species. Oxidative stress has been associated with aging (Sohol *et al.* 1995), carcinogenesis (Cerutti 1985), cell damage due to ischemia-reperfusion (Conner *et al.* 1992) and degenerative processes such as Alzheimer's disease (Luft, 1994). The action of catalases, superoxide dismutases and peroxidases keep the intracellular levels of active oxygen species acceptably low (Chance *et al.* 1979, Sies 1993). Cellular response to high levels of hydrogen peroxide is the increased synthesis of at least 21 proteins (Toyokuni *et al.* 1995). Both superoxide dismutase and catalase are essential components of the biological defense against oxygen toxicity. In the absence of catalase, superoxide dismutase decreases activity after turnover suggesting that superoxide dismutase is inhibited by peroxide (Hodgson and Fridovich 1975), and catalase is inhibited by superoxide in the absence of superoxide dismutase (Shimizu *et al.* 1984). Superoxide dismutase and catalase are currently being exploited being as therapeutic agents in the treatment these human diseases (Szelgi *et al.* 1986, Greenwall 1990, Darley-Usmar *et al.* 1995).

## Molecular Modeling

The method of x-ray diffraction to study large molecules was developed mainly in the lab of Perutz and Kendrew. The first three dimensional protein structure solved by x-ray crystallography was that of myoglobin in 1958. Physical models of proteins were used for

the three dimensional representation of proteins up until the 1970's when computer models began to be used. Computer models are mathematical representations based on atomic positions, bond lengths, angles and torsions. Molecular surfaces are mathematical functions based on atomic position and radii. Atomic energies are based on equations involving atomic distances, the atom type and bonding arrangements. Dynamic systems such as vibrations, diffusion and conformational changes can be modeled as well. The current applications of molecular modeling include drug design (Lybrand 1995), the study of enzyme structure and folding (Shakhnovich 1996) as well as enzyme interaction during catalysis (Jones and Willet 1995, Stoll *et al.* 1996). Computer modeling and simulations have also become a valuable tool in relating the function of proteins to their structure.

The crystal structures of five catalase enzymes from diverse organisms have been elucidated. Biochemical information is available for all of these enzymes with the exception of PVC. The differences in catalysis and ligand binding affinities between protoheme and heme d catalases may be correlated to the differences in heme types. The pockets and substrate access channels of protoheme (beef liver & *Micrococcus*) and heme d (HPII and *Penicillium*) catalases have been analysed using Quanta ™ and CharmM ™ molecular modeling packages on a Silicon Graphics Iris Indigo 2 computer. Experimental studies have been carried out with two catalases, HPII (and its mutants) and beef liver. Fluoride and formate are inhibitors of both enzymes. The reduction of beef liver enzyme compound I to II and the decay of compound II are accelerated by fluoride. The decay of compound II is also accelerated by formate, and this reagent acts as a 2-electron

donor towards compound I of both enzymes. The differences in residues that comprise the heme pockets and the channel walls may be correlated with the observed differences both in enzymatic activity towards peroxide and in sensitivity to ligation by anions such as fluoride and formate.

*The focus of this study is to answer the following questions:*

1. What are the differences in high-spin ligand binding between protoheme and heme d containing catalases?

2. What are the differences in high-spin ligand binding between three catalytic states of eukaryotic catalase?

3. What are the differences in high-spin ligand binding between wild-type HPII and HPII mutants with modified residues distal to the porphyrin ring?

4. What are the relationships between high-spin ligand binding and the catalytic activity of different catalases?

5. What is the most important factor determining the differences in reactivity of different catalases, the heme group chemistry or the residues in the heme pocket?

# Materials and Methods

## Materials

The beef liver catalase (EC 1.11.16, 65000U/mg) was supplied by Boehringer Mannheim Biochemica Canada. The crystalline suspension was diluted to ≈ 80 μM in sodium borate/HCl buffer (pH 8.24) and centrifuged at high speed for 3 minutes to remove any insoluble material. This suspension was used as a stock solution. Hematin concentration was determined spectrophotometrically with the extinction coefficient of 120 $M^{-1}cm^{-1}$ at 406 nm (Nicholls and Schonbaum 1963).

*Escherichia coli* HP II catalases were obtained courtesy of P. Loewen, Dept. of Microbiology, University of Manitoba, Winnipeg, Manitoba. Purification of HP II is described by Loewen and Switala (1986). Catalase hydroperoxidase II (HPII) was isolated from *E. coli*, purified from strain UM255 and transformed with pAMkatE22 a plasmid containing the katE gene which encodes for the 753 amino acid protein. Oligonucleotide-directed mutants of HPII were prepared as described by Loewen and Switala (1993). The oligonucleotides were synthesized on a PCR-Mate synthesizer. Asn201 mutants replace the sequence AAT at 1421. The sequence was confirmed by the Sanger method on single-stranded DNA from the same phagemids. The mutagenized fragments were reincorporated into pAMkatE72 and transformed into UM255 for expression. The concentrations of HP II hematin

were estimated using the millimolar extinction coefficient as reported by Dawson *et al*, (1991) of 118 $M^{-1}cm^{-1}$ at 405 nm. The lyophilized protein was diluted in potassium phosphate buffer and centrifuged to remove insoluble material.

Fisher Scientific supplied the 30% hydrogen peroxide. Peroxoacetic acid (30% wt) was supplied from Aldrich (St. Lewis, USA). Pre-treatment of the peracetate was carried out to remove any presence of $H_2O_2$ from the solution (Jones and Middlemiss 1972). The stock solution of peracetate was brought to pH 5 and 2 nM catalase was added. The solution of peracetate was then diluted to 10 mM with distilled water and left for 30 minutes before use. $KH_2PO_4$ was a product of Baker Chemicals and $K_2HPO_4$ a product of Caledon Laboratories. All other chemicals were of analytical grade and had been purchased from BDH (Darmstadt, Germany) or Sigma (St. Lewis, USA).

## Methods

## Spectrophotometry

Electronic spectral properties of beef liver catalase, compound I, compound II, HPII wild-type and HPII mutants upon the addition of fluoride were monitored by recording the absorption with a Beckman DU-7000 diode array spectrophotometer. The concentrations of catalase varied from 4-10 μM. Peracetic acid

was used to form a large steady-state concentration of compound I. Potassium ferrocyanide is a one-electron reductant of compound I and was used to create a large steady-state concentration of compound II. Ethanol was added to compound II to remove residual compound I. All experiments were carried out at 23°C at pH5.0 in 100 mM potassium phosphate buffer.

Spectral properties of beef liver catalase, HPII wild-type and HPII mutants upon the addition of formate were monitored by recording the absorption with a Beckman DU7 standard single beam spectrophotometer linked to a Apple IIGS for data transfer. The concentrations of catalase varied from 3-7 μM. All experiments were carried out at 23°C in 100 mM potassium phosphate buffer at pH 5.8 and 6.8 except where stated.

**Catalase Assay**

Kinetics

The decay of BLC (11μM hematin) compound II in presence of formate was monitored on the Aminco™ dual wavelength double beam DW2 spectrophotometer linked to a Compaq™ 286 device with Olis™ fitting routines for various exponential reactions. The experiment was performed at 23°C in 50 mM potassium phosphate buffer at pH 5.8. BLC compound II was generated by the addition of 800 μM peracetate followed by 33 μM ferrocyanide.

Rapid Kinetics

Rapid kinetic measurements were performed using the Durrum™ D-100 stopped flow spectrophotometer linked to a Ancom™ Top 286 computer with Olis™ fitting routines. The rate of BLC (3μM hematin) complex formation with fluoride (pH 5.8) and formate (pH 7.4) as well as the decay of compound I in the presence of formate (pH 7.4, 10μM $H_2O_2$) were carried out at 23°C in 50 mM potassium phosphate buffer. BLC compound I formation with peracetate (pH 5.0) and HPII wild-type compound I formation with $H_2O_2$ (pH 7.0) were performed at 23°C in 100 mM potassium phosphate buffer.

Subsequent spectral and kinetic data analysis was performed using the DeltaGraph™ 2.0 application software.

**Molecular Modeling**

Catalase structures were displayed and distances and configurations calculated using Quanta™ release 4.1.1 version 95.0320 software (1984-1994 The University of York, York, England, Molecular Simulations Inc.) which functions on the UNIX operating system, Silicon Graphics Indigo2™ R4400 workstation. Quanta allows for the manipulation of a molecule in 3-D space. It also allows for selective displaying, coloring and overlaying structures as well as creating graphical objects. Quanta release

4.1.1 includes CHARMm™ dynamics calculations whose simulations include energy minimization and hydrogen bond calculations.

# Results

## Spectral comparisons of beef liver catalase, compound I and compound II

When peracetate is added to a solution of beef liver catalase there is an immediate decrease in absorbance of the Soret region band at 405nm and a red shift of the $\alpha$-band from 622 (ferric enzyme) to 660 nm, indicating the formation of compound I (Figure 12A). Upon addition of ferrocyanide to compound I, absorbance peaks appear at 425, 535 and 568 nm, characteristic of compound II (Figure 12B). Compound I and II have isosbestic points at 408 and 602 nm. Ethanol when added to such a mixture removes any residual compound I and induces a slow reversion of compound II back to the ferric form of the enzyme (Figure 12C). Figure 12C shows isosbestic points for compound II and the native enzyme at 434, 520 and 604 nm. Absorbance data for the ferric enzyme, compound I and compound II are summarized in table 2.

## Spectral comparisons of HPII wild-type and its mutants N201D and N201Q

The spectrum of the HPII wild-type catalase shows high similarity to the absorbance spectrum of other heme d enzymes, such as the catalase of *Neurospora crassa* (Jacob and Orme-Johnson 1979) and the terminal oxidase complex of *Escherichia coli* (Varva et al. 1986). The spectra of HPII wild-type and its

mutants (Figure 13) all contain an absorbance peak in the Soret region at approximately 405 nm characteristic of $\pi-\pi^*$ transitions of the porphyrin ring. Both wild-type and N201Q mutant enzymes show an $\alpha$-band at approximately 715 nm which is characteristic of heme d, analogous to the 622 nm peak of the ferric beef liver enzyme. In addition, the heme d HPII spectra show an intense peak at 590, corresponding to the 480-500 nm peak of mammalian catalases, and characteristic of heme d. For the N201D enzyme, these maxima are shifted to 690 and 580 nm which may be intermediates of the spontaneous cyclization of a diol during the bio-conversion to heme d (Chiu *et al.* 1989). Small absorption shoulders at ≈535 and 630 nm may indicate that the N201D mutant preparation has a small population of enzymes containing protoheme. Protoheme containing enzymes such as HPI show absorption maxima at approximately these wavelengths (Loewen *et al.* 1993). Absorbance data for HPII wild-type, HPII N201D and N201Q are summarized in table 2.

## The kinetics of Compound I formation

*Beef liver catalase*

Peracetate (pera) is an analog of hydrogen peroxide and forms a stable primary intermediate with beef liver catalase and when used in excess will convert all heme groups to compound I (refer to introduction page 18). The kinetics of beef liver catalase compound I formation with peracetate were monitored at 660 nm.

Typical traces of beef liver catalase compound I formation in the presence of increasing amounts of peracetate are shown in Figure 14A. Figure 14B shows the reaction rates plotted against peracetate concentration. A calculated linear fit of the data allows an estimate of the second-order rate constant $k_1''$ of 1.1 x $10^4$ $M^{-1}s^{-1}$. A first-order decomposition rate constant $k_{-1}''$ of 0.3 $s^{-1}$ was estimated from the ordinate intercept. The maximum change of absorbance for each assay was plotted against peracetate concentration (Figure 14C). The data was fitted to the equation:

$$A = \frac{A_{max} * S}{\left(\frac{k_{-1}''}{k_1''} + S\right)} \qquad (13)$$

where A is the absorbance, $A_{max}$ is the maximum absorbance change, S is the concentration of substrate and $\frac{k_{-1}''}{k_1''}$ is the apparent dissociation constant.

The data of Figure 14C show a value of 33μM for $\frac{k_{-1}''}{k_1''}$ in agreement with the values obtained for Figure 14B.

**Table 2. Spectral peaks of Beef liver catalase, intermediates, HPII wild-type and its mutants.**
Spectral analysis performed at pH 5.0 in 100 mM potassium phosphate buffer at 23°C. Spectral peaks were obtained from data collected in Figures 12 & 13.

| Catalase | Ferric | | Compound I | | Compound II | |
|---|---|---|---|---|---|---|
| | Soret (nm) | visible (nm) | Soret (nm) | visible (nm) | Soret (nm) | visible (nm) |
| BLC | 405 | 500, 537, 622 | - | 660 | 425 | 534, 568 |
| HPII | 406 | 590, 630, 711 | - | - | - | - |
| N201D | 408 | 580, 610, 695 | - | - | - | - |
| N201Q | 405 | 588, 625, 710 | - | - | - | - |

Figure 12. *Spectra of BLC catalase, compound I and compound II: formation of compound I and II from native enzyme*

The analysis was performed using the diode array spectrophotometer in 100 mM potassium phosphate pH 5.0 at 23°C. Spectral changes during the transition of intermediates are indicated by arrows.
A) The first intermediate, compound I, is almost immediately formed by the addition of 200 μM of peracetate to a suspension of 10μM beef liver catalase.
B) Compound II is formed from compound I by the addition of 33 μM ferrocyanide (plus 5 mM ethanol).
C) Compound II decays back to the native enzyme over a period of 60 minutes after the addition of ethanol.

Figure 12.

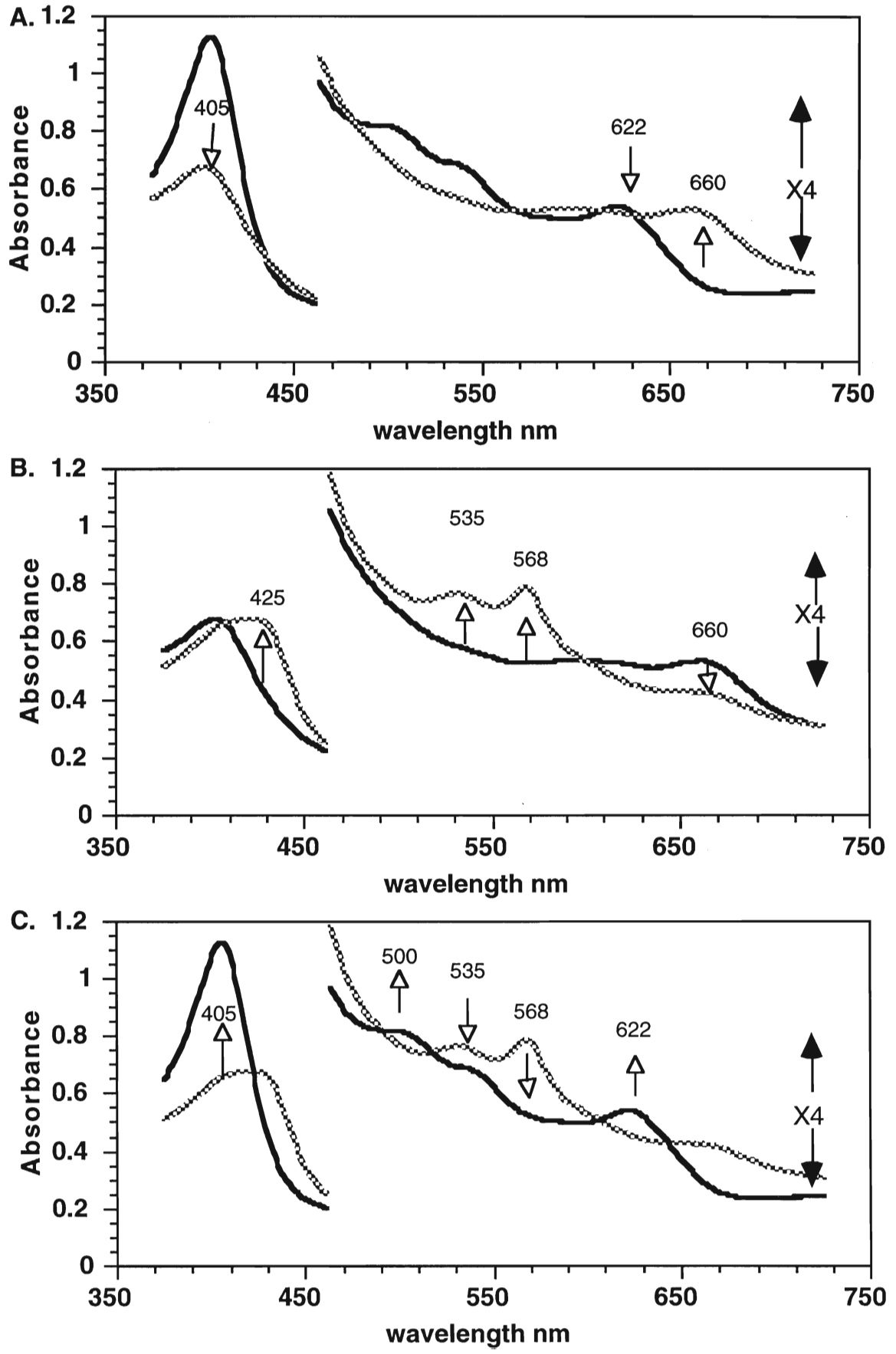
A.
B.
C.
Absorbance
wavelength nm
405
622
660
X4
425
535
568
500
0
0.2
0.4
0.6
0.8
1
1.2
350
450
550
650
750

Figure 13. *Spectra of HPII wild-type and mutants N201D and N201Q.*

Absolute spectra of HPII wild-type (black), HPII N201D (dark gray) and HPII N201Q (light gray). The spectra were obtained on the diode array spectrophotometer at pH 5.0 in 100 mM potassium phosphate buffer at 23°C.

Figure 13.

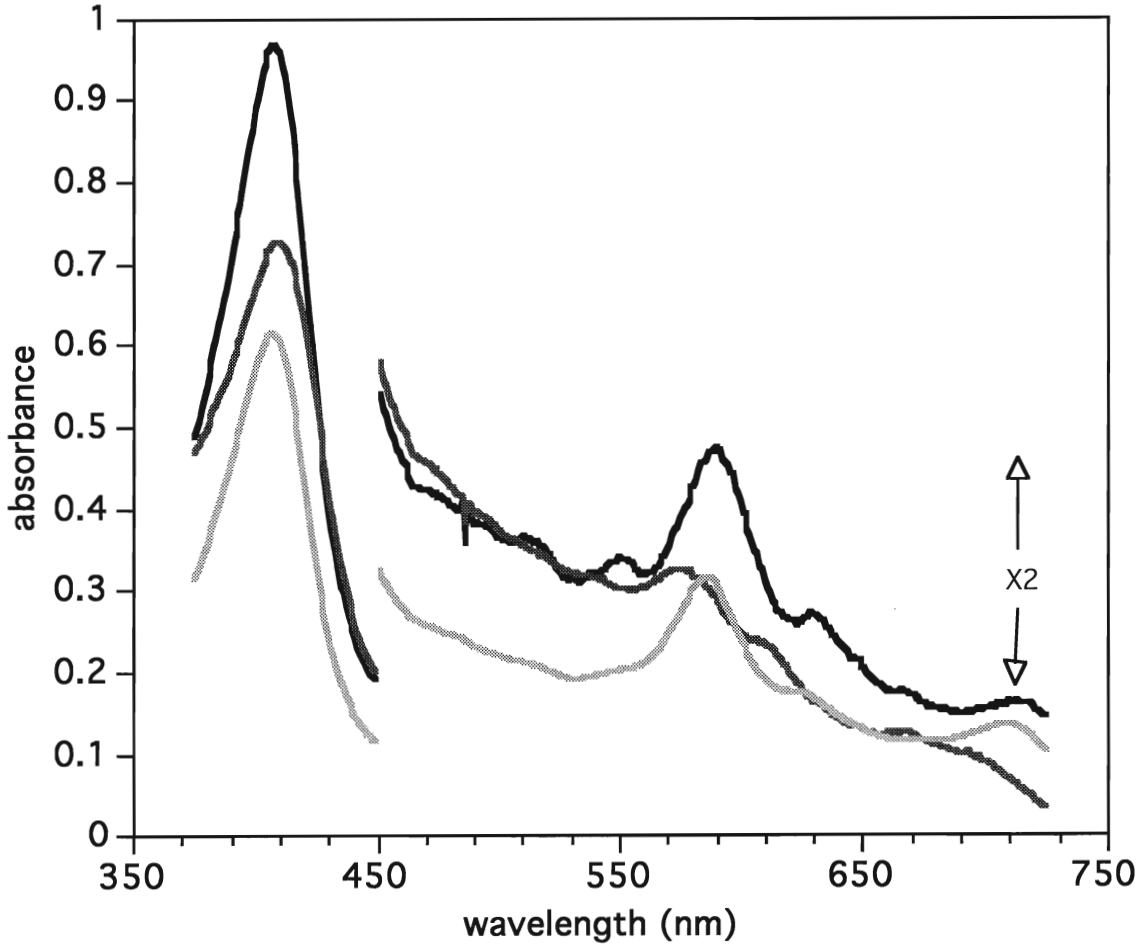
absorbance
1
0.9
0.8
0.7
0.6
0.5
0.4
0.3
0.2
0.1
0
350
450
550
650
750
wavelength (nm)
X2

Figure 14. *The rate of BLC compound I formation with peracetic acid.*

The rate of compound I formation was followed at 660 nm on the stopped flow spectrophotometer at pH 5.0 in 100 mM potassium phosphate buffer at 23°C. A) The change in absorbance is followed at 660 nm for various sequential additions of peracetate up to 200 μM. B) The exponential fits are plotted against peracetate concentration. C) the maximum change in absorbance at 660 nm is plotted against peracetate concentration and fitted to a Michaelis-Menten equation to determine Kd.

Figure 14.

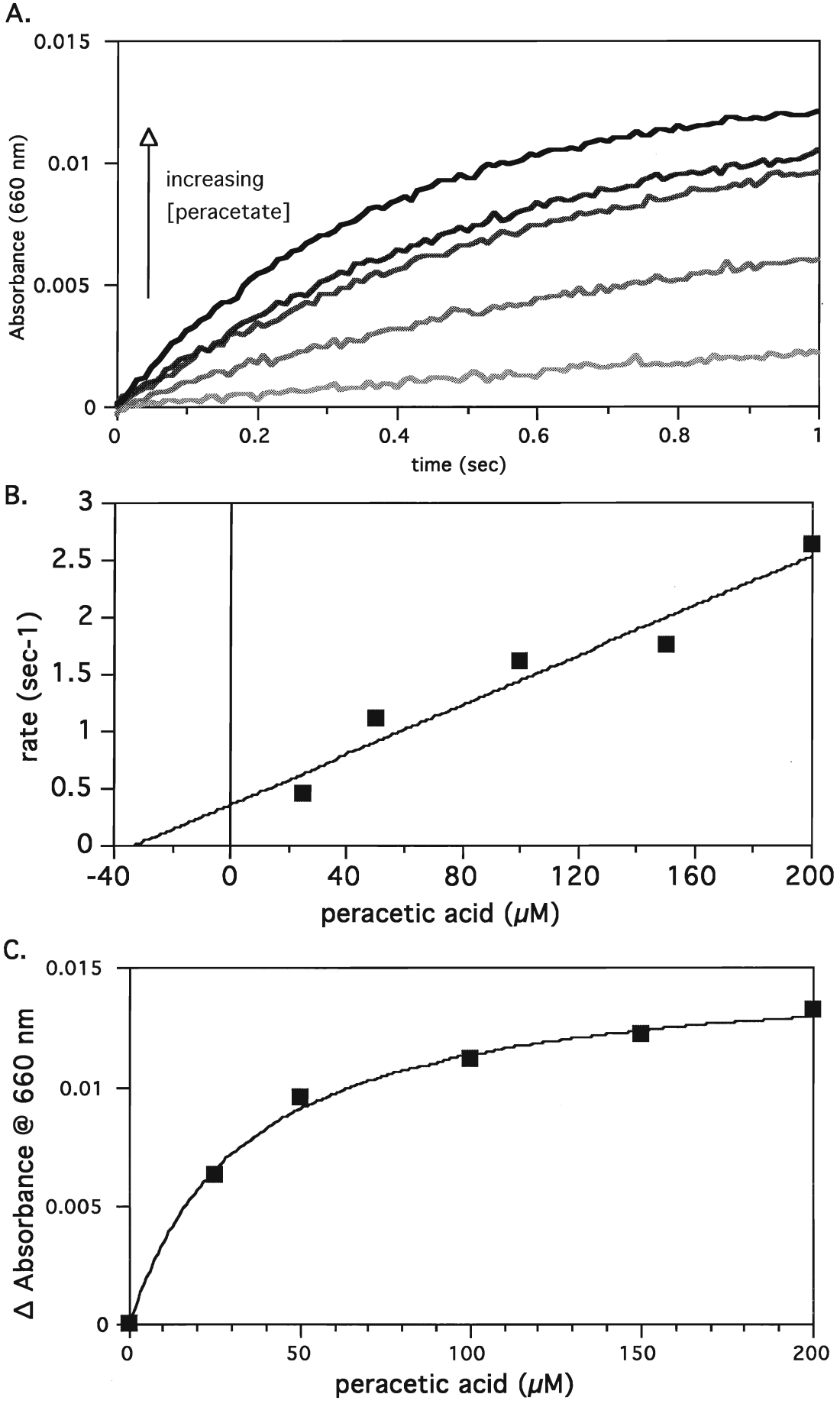
A.
0.015
0.01
0.005
0
Absorbance (660 nm)
increasing
[peracetate]
0
0.2
0.4
0.6
0.8
1
time (sec)
B.
3
2.5
2
1.5
1
0.5
0
rate (sec-1)
-40
0
40
80
120
160
200
peracetic acid (μM)
C.
0.015
0.01
0.005
0
Δ Absorbance @ 660 nm
0
50
100
150
200
peracetic acid (μM)

*Reduction of Compound I*

Compounds such as ethanol and formate accelerate the 2-electron reduction of compound I to the ferric enzyme. The reduction of catalase compounds I formed with hydrogen peroxide and with peracetate was investigated. Assays were performed at pH 7.4 which is favorable for the formation of compound I. Typical traces of compound I (pera) reduction by formate are shown in Figure 15A. The first-order rates were plotted with respect to formate concentration and fitted to a straight line as shown in Figure 15B. The second-order rate constant $k_4$ of 161 $M^{-1}s^{-1}$ was determined for compound I (pera) decay. The maximum rate of compound (pera) decay in the presence of formate was estimated to be 0.07 $s^{-1}$ with a spontaneous decay $k''_{-1}$ of 0.007 $s^{-1}$ estimated from the y-axis intercept.

Typical traces of compound ($H_2O_2$) reduction by formate are demonstrated in Figure 16A The reaction rates were plotted against formate concentration. The linear dependence of the decay rate on formate concentration is shown in Figure 16B. The second-order rate constant of compound I ($H_2O_2$) reduction by formate $k_4$ was calculated as 237 $M^{-1}s^{-1}$, and the maximum rate of decay in the presence of formate was estimated to be 3.5 $s^{-1}$. The spontaneous decay $k''_{-1}$ of 0.1 $s^{-1}$ was estimated from the y-axis intercept, suggesting that compound ($H_2O_2$) decay proceeds at an appreciable rate in the absence of added donors. Compound I

(pera) is ≥100 times more stable than compound I formed with hydrogen peroxide.

*HPII wild-type*

The kinetics of HPII compound I formation with hydrogen peroxide were investigated. Typical traces of the decrease in optical density at 405 nm in the presence of increasing amounts of hydrogen peroxide are shown in Figure 17A. Figure 17B shows the corresponding reaction rates plotted against hydrogen peroxide concentration. The linear fit of the data allows for an estimation of the second-order rate constant of $2.8 \times 10^6$ $M^{-1}s^{-1}$. A first-order decomposition rate of less than 10 $s^{-1}$ was estimated from the ordinate intercept. The first-order rates at higher hydrogen peroxide concentrations shown in brackets, which do not appear to be linearly dependent on peroxide concentration, are attributed to rates approaching the upper limit detectability of the stopped-flow spectrophotometer.

The decomposition of compound I can proceed through one of three paths, catalytic turnover, one electron or two electron reduction. Since compound I of HPII does not undergo the one electron reduction to form the inactive compound II (Hillar *et al.* 1993), the decomposition of compound I can occur either through reaction with a second molecule of hydrogen peroxide, or via reaction with hydrogen donors such as ethanol (i.e. peroxidatic

reaction). The disappearance of compound I in the presence of increasing amounts of ethanol was followed at 405 nm. Typical traces are shown in Figure 18A. A second-order rate constant $k_4$ of 3.5 $M^{-1}s^{-1}$ was estimated from the slope of the line as shown in Figure 18B. A spontaneous rate of compound I decay not greater than 0.02 $s^{-1}$ was estimated from the intercept in the absence of ethanol. The second-order rate constant of the peroxidatic reaction for HPII wild-type compound I and ethanol is 100 times lower than that reported in the literature for mammalian catalase.

Figure 15. *Formation of peracetate compound I and its reduction by formate.*

The formation and reduction of compound I (formed with peracetate) were monitored on the DW-2 spectrophotometer at pH 7.4 in 50 mM potassium phosphate buffer at 23°C. Compound I was also formed by the addition of 200 μM peracetate to 7 μM beef liver catalase.
A) Typical traces of the formation and decay of compound I (405-425 nm) in the presence of increasing amounts of formate are shown. The reaction curves were fitted exponentially to give rates.
B) The rates of reduction are plotted against formate concentration to give the apparent rate constants for spontaneous and formate catalysed decays.

Figure 15.

A.

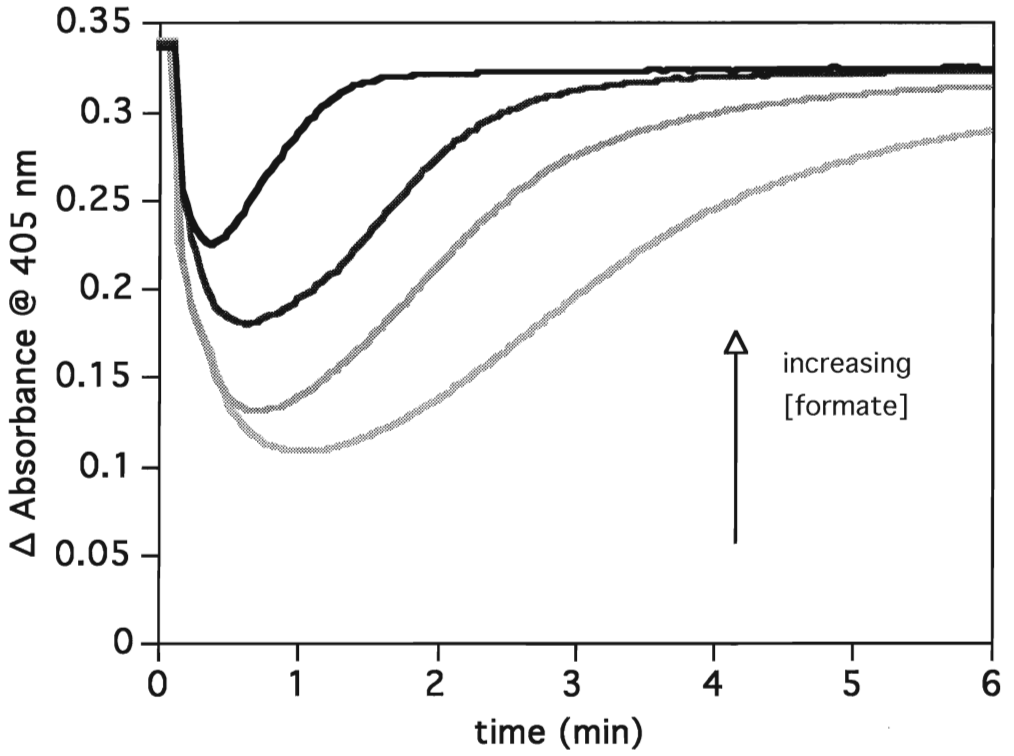
0.35
0.3
0.25
0.2
0.15
0.1
0.05
0
Δ Absorbance @ 405 nm
0
1
2
3
4
5
6
time (min)
increasing
[formate]

B.

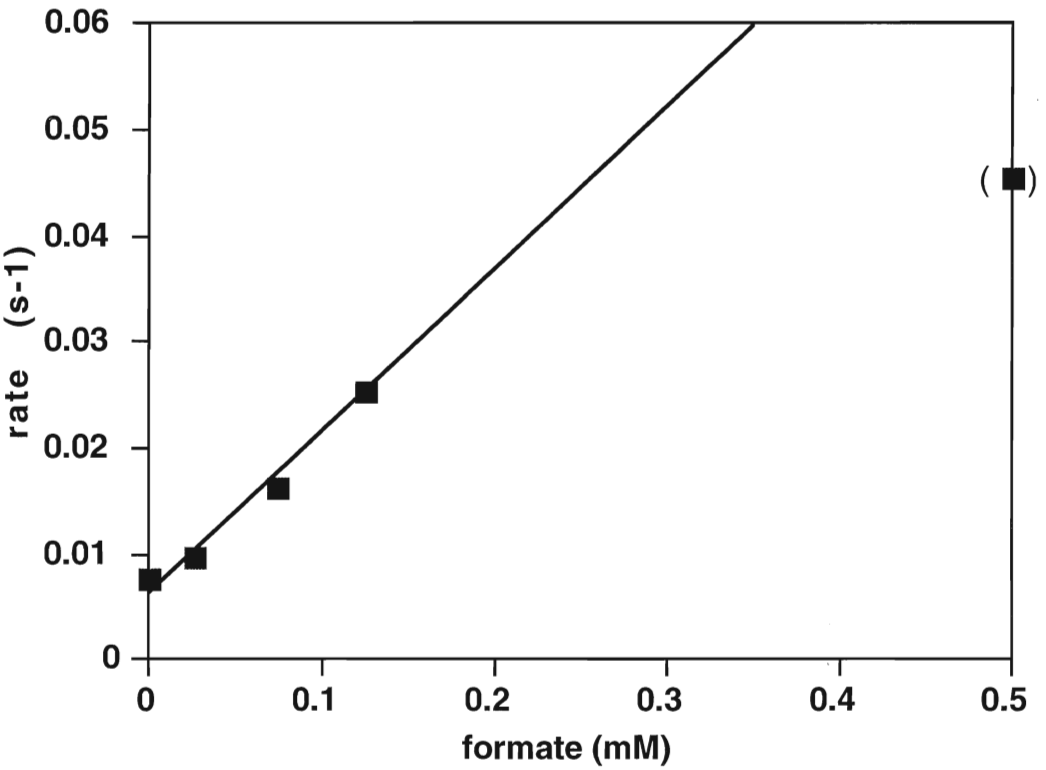
0.06
0.05
0.04
0.03
0.02
0.01
0
rate (s-1)
0
0.1
0.2
0.3
0.4
0.5
formate (mM)

Figure 16. *The formation of hydrogen peroxide compound I and its reduction by formate.*

The formation and reduction of beef liver catalase compound I were monitored at 405 nm on the stopped-flow spectrophotometer at pH 7.4 in 50 mM potassium phosphate buffer at 22°C. Compound I was generated by the addition of 10 μM hydrogen peroxide to 3 μM enzyme.
A) Compound I reduction by formate in concentrations ranging from 0.5-15 mM. The reaction curves were fitted exponentially to give rates.
B) The rates of reduction are plotted against formate concentration to give apparent rate constants for spontaneous and formate catalysed decays.

Figure 16.

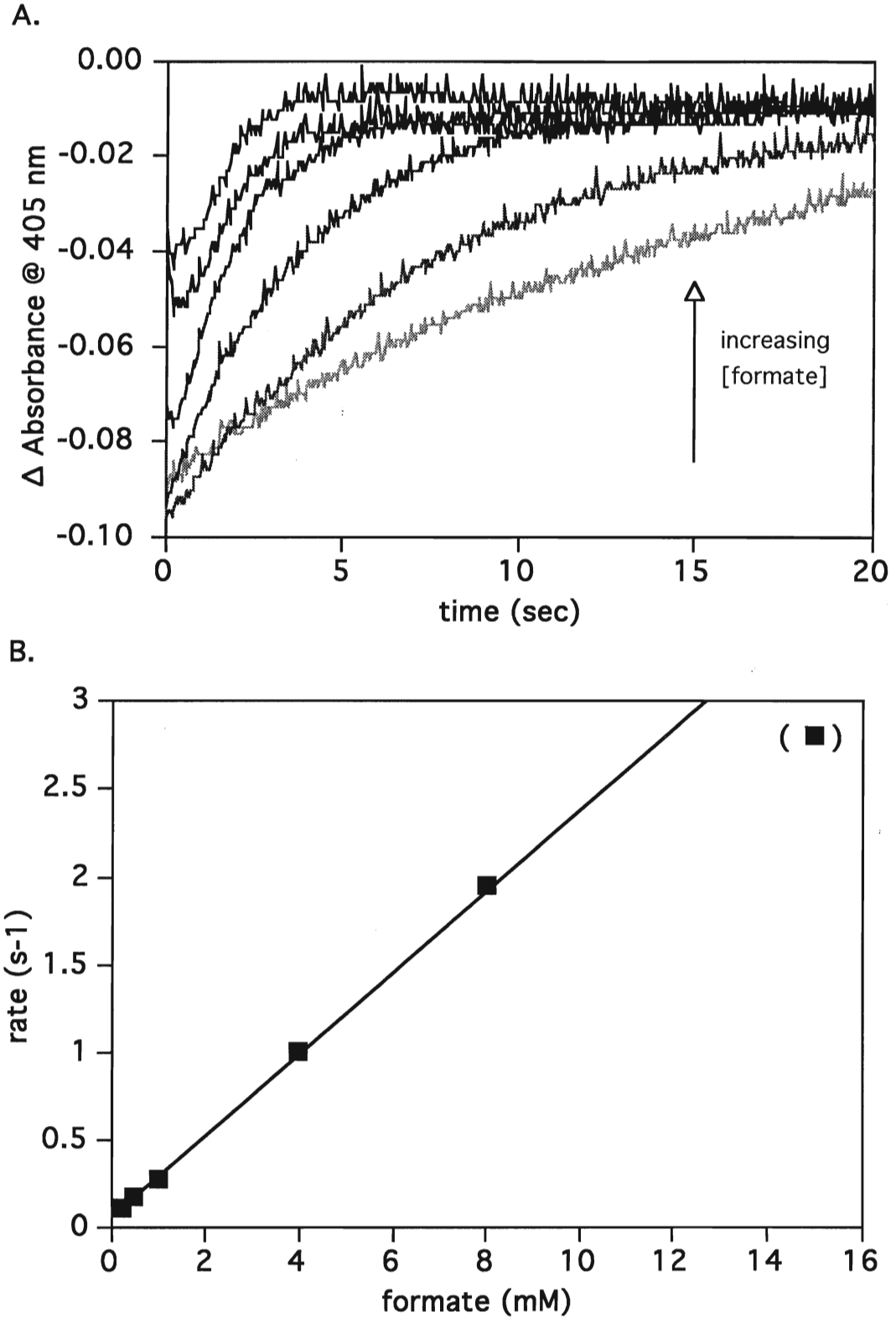
A.
0.00
-0.02
-0.04
-0.06
-0.08
-0.10
Δ Absorbance @ 405 nm
0
5
10
15
20
time (sec)
increasing
[formate]
B.
3
2.5
2
1.5
1
0.5
0
rate (s-1)
0
2
4
6
8
10
12
14
16
formate (mM)
( ■ )

Figure 17. *The formation of HPII wild-type compound I with hydrogen peroxide.*

The reaction of 3 μM HPII wild-type catalase compound I formation with hydrogen peroxide is monitored on the stopped-flow spectrophotometer at pH 7.0 in 100 mM potassium phosphate buffer at 23°C. A) The reaction is followed at 405 nm for various sequential additions of hydrogen peroxide up to 300 μM. The reaction curves were fitted exponentially to give rates. B) The reaction rates are plotted against $[H_2O_2]$ to give the rate constant of compound I formation.

Figure 17.

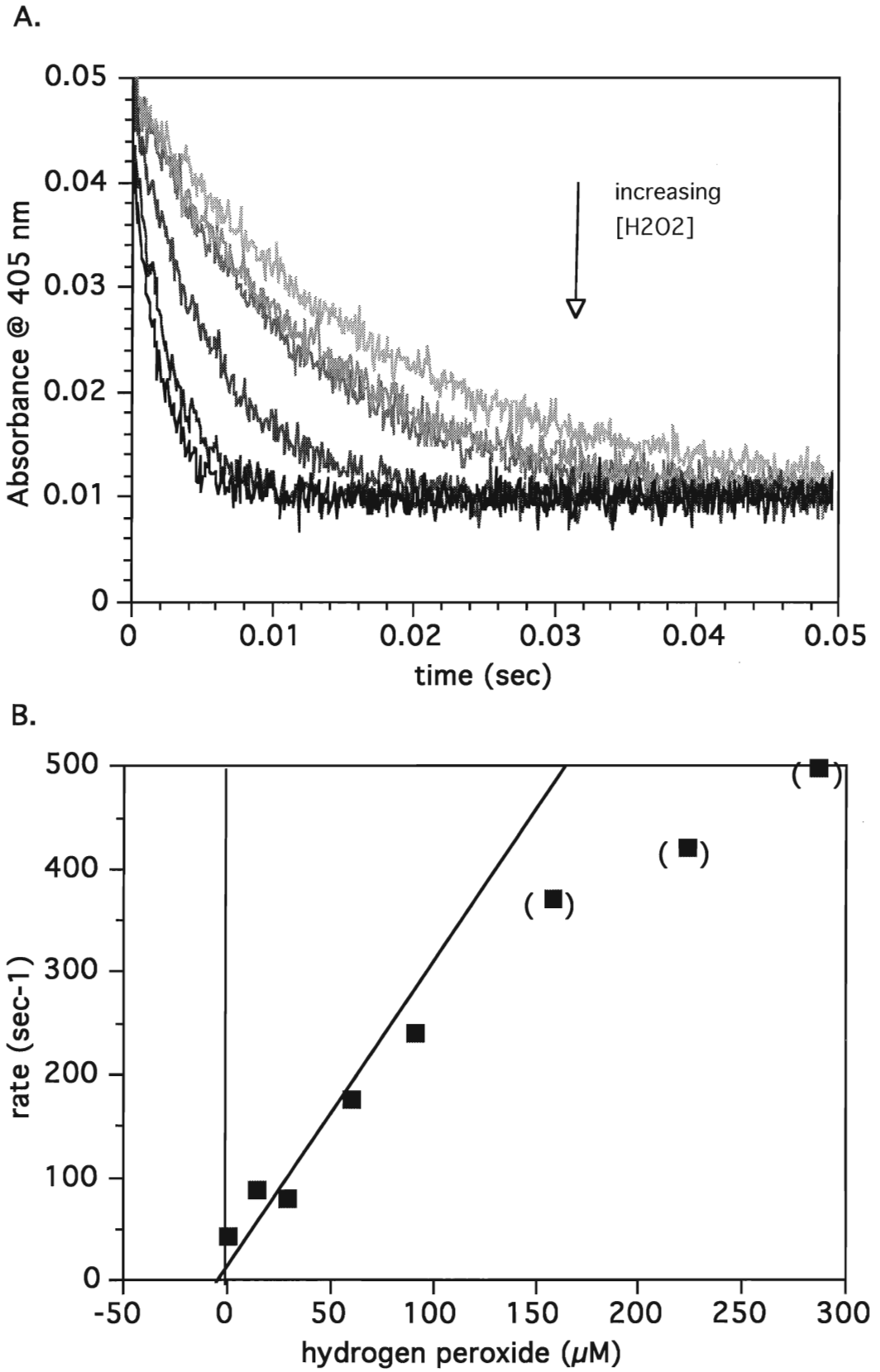
A.
0.05
0.04
0.03
0.02
0.01
0
Absorbance @ 405 nm
increasing
[H2O2]
0
0.01
0.02
0.03
0.04
0.05
time (sec)
B.
500
400
300
200
100
0
rate (sec-1)
-50
0
50
100
150
200
250
300
hydrogen peroxide (μM)

Figure 18. *The decay of HPII compound I.*

The reaction of HPII wild-type catalase compound I reduction by ethanol is monitored on the stopped-flow spectrophotometer at pH 7.0 in 100 mM potassium phosphate buffer at 23°C. A) Compound I reduction is followed at 405 nm for various step-wise additions of ethanol (10-267 mM) to a reaction mixture of 3 μM HPII enzyme and 100 μM hydrogen peroxide. The reaction curves were fitted exponentially. B) The reaction rates of decay are plotted against ethanol concentration to give the rate of compound I decay.

Figure 18.

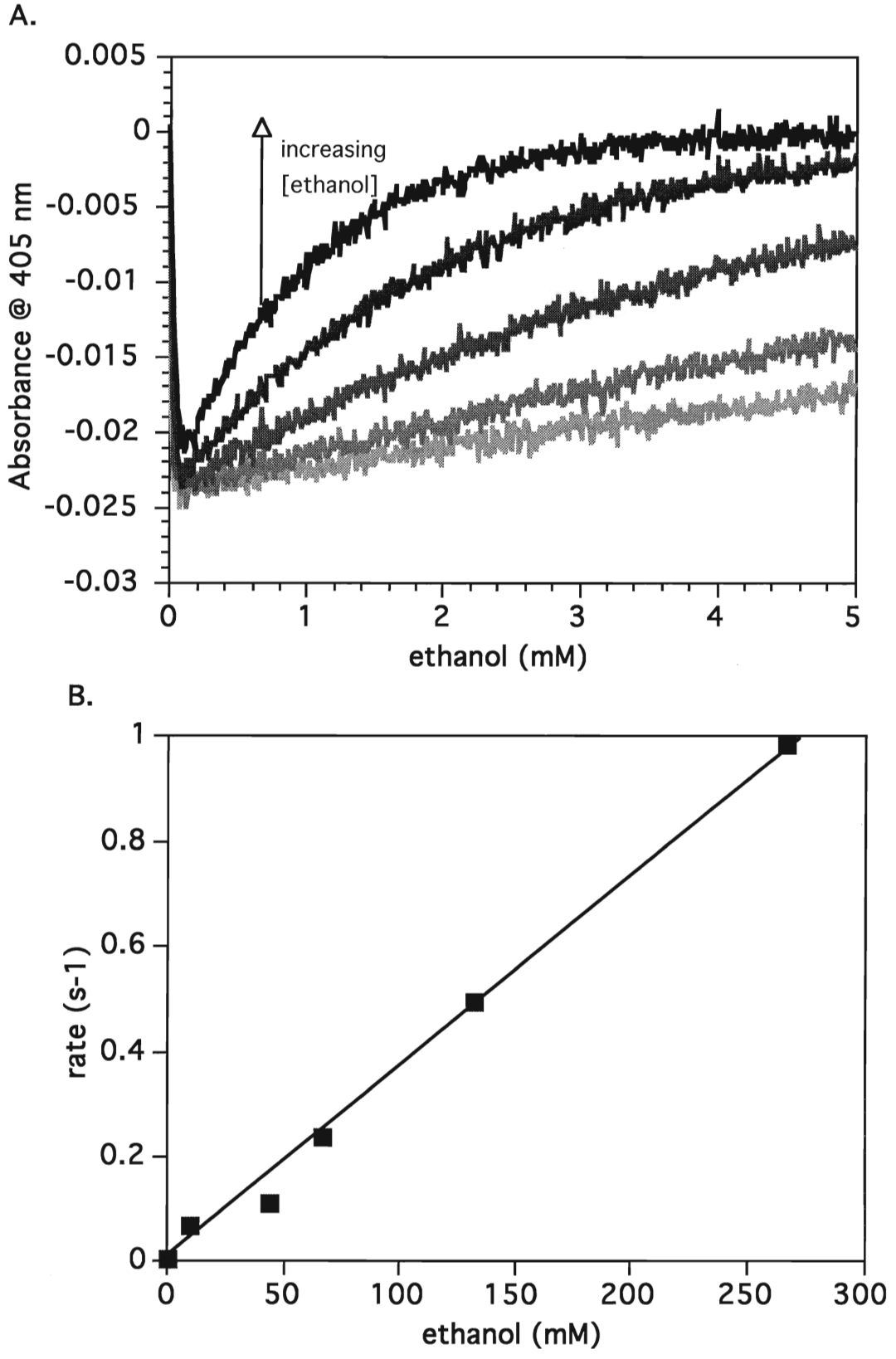
A.
0.005
0
-0.005
-0.01
-0.015
-0.02
-0.025
-0.03
Absorbance @ 405 nm
increasing
[ethanol]
0
1
2
3
4
5
ethanol (mM)
B.
1
0.8
0.6
0.4
0.2
0
rate (s-1)
0
50
100
150
200
250
300
ethanol (mM)

## Fluoride

*Spectral modifications of catalase upon binding fluoride*

The binding of fluoride by catalase is pH dependent, and the pK of hydrofluoric acid is 3.45 (Linde, 1990a). The binding of fluoride alters the absorbance spectrum of the catalases. Absorbance spectra of catalase/fluoride complexes are shown in Figure 19. The $\alpha$-band of the beef liver enzyme , which is due to metal to ligand charge transfer, is blue shifted (Figure 20A) and the Soret band is slightly red-shifted, indicative of high-spin ligand binding. Upon binding fluoride, the Soret band of the HPII catalase is red-shifted 4 nm from that of the resting enzyme. HPII wild-type and N201Q catalases (Figures 20B and D) show a blue-shift in the $\alpha$-band from $\approx$710 to $\approx$670 nm. The $\alpha$-band of the N201D (Figure 20C) mutant is blue-shifted from 695 to 665 nm. The magnitude of the 670 nm absorbance band is not as pronounced for the N201D mutant as seen for the $\alpha$-band of wild-type and N201Q enzymes suggesting that full complex formation with fluoride may not have been attained for the N201D enzyme (Figure 20C). The HPII catalases show the formation of additional bands at 550 and 625 nm. Analogous absorbance bands are not seen for the fluoride complex of mammalian catalase. A summary of absorbance data for the catalase/fluoride complexes are shown in table 3.

**Table 3. Absorption bands of Catalase/fluoride complexes**

Spectral analysis performed at pH 5.0 in 100 mM potassium phosphate buffer at 23°C. Spectral peaks were obtained from data collected in Figure 19.

| Catalase | Soret region (nm) | visible region (nm) |
|---|---|---|
| BLC | 407 | 596 |
| HPII wild-type | 410 | 551, 628, 671 |
| N201D | 411 | 540, 612, 665 |
| N201Q | 409 | 549, 625, 670 |

**Table 4. Dissociation constants for HPII catalase/fluoride complexes.**

Spectral analysis performed at pH 5.0 in 100 mM potassium phosphate buffer at 23°C. Dissociation constants were obtained from fitted data collected from Figures 21 (pH 5.0) and 22D (pH 5.8). Equations and fits used to determine dissociation constants are shown in appendix D table D-1.

| Catalase | Dissociation constants (mM) | |
|---|---|---|
| | pH 5.0 | pH 5.8 |
| BLC | 3.5 | 23 |
| HPII wild-type | 0.2 | - |
| N201D | 4.0 | - |
| N201Q | 0.9 | - |

*Catalase/fluoride equilibria*

Difference spectra for sequential additions of fluoride to catalases are shown in Figure 20. The change in the absorbance spectrum of catalase upon the addition of fluoride was used to determine the dissociation constant for catalase/fluoride. The absorbance changes at appropriate wavelength pairs were plotted against the log of fluoride concentration (Figure 21). The secondary plot for the beef liver enzyme shows a sigmoidal curve for the data collected in both the visible and Soret regions (Figure 21A). To determine the catalase affinity for fluoride, the sigmoidal curves were fitted to the equation:

$$1 - Y = \frac{\exp(2.303 * (\log F - \log K_d))}{1 + \exp(2.303 * (\log F - \log K_d))} \quad (14)$$

where Y is the fraction of free enzyme, 1-Y is the absorbance of the complexed enzyme, $K_d$ is the dissociation constant and F is the concentration of fluoride. Derivation of equation 14 is shown in appendix D.

The $K_{d\ fluoride}$ for the beef liver enzyme at pH 5.0 is calculated as 4.0 mM. The HPII enzymes show a double sigmoidal curve for the data collected at wavelength pairs in the Soret region suggesting a heterogeneous population. However the HPII catalases show a single sigmoidal relationship in the visible region. Data collected in the visible region (Figure 21B, C and D) were fitted to equation 14. The fluoride dissociation constants for HPII wild-type and mutants N201D and N201Q are calculated to be 0.22 mM, 4.0 mM and 0.93 mM respectively. The dissociation constant for the ND

mutant may have been underestimated as full complex formation with fluoride may not have occurred (cf. Figure 20C). A summary of dissociation constants for catalase/fluoride complexes are shown in table 4.

*Rate of fluoride binding to Beef liver catalase*

The kinetics of fluoride binding to beef liver catalase were investigated. The rate of fluoride complex formation was monitored at 595 and 634 nm. Typical traces collected on the stopped-flow spectrophotometer at a milli-second time scale are shown in Figure 22A. The first order rates at both wavelengths were plotted against fluoride concentration (Figure 22B) to give second-order rate and dissociation constants of 5000 $M^{-1}s^{-1}$ and 23 mM respectively and a $k_{off}$ constant of 120 $s^{-1}$ at pH 5.8.

*The formation and decomposition of Beef liver catalase compounds I and II in the presence of fluoride*

The transitions of compound I to II and compound II to the native enzyme are accelerated by fluoride suggesting that fluoride complexes with heme group intermediates as well as the ferric form. This hypothesis was tested by comparing the effect of fluoride on the ferric enzyme and on compounds I and II at pH 5.0. The change in absorbance of the ferric enzyme upon the addition of fluoride was plotted against fluoride concentration (Figure

23A). The dissociation constant of the native enzyme with fluoride is 6.5 mM at this pH in both the visible and Soret regions.

The first-order rates of both the 1-electron reduction of compound I and the 1-electron reduction of compound II in the presence of fluoride were collected on a diode array spectrophotometer and plotted against fluoride concentration (Figure 23B). These rates were fitted to an equation of the Michaelis-Menten type (eqn. 13). The dissociation constants were estimated from the fitted data, $K_d$ = 1.1 mM with $k_{max}$ of 0.25 $s^{-1}$ for compound I and $K_d$ = 4.6 mM with $k_{max}$ of 0.08 $s^{-1}$ for compound II. The spontaneous first-order rates of compound II formation and decay were obtained from the intercepts for the reaction occurring in the absence of fluoride, 0.03 $s^{-1}$ and 0.003 $s^{-1}$ respectively. A summary of fluoride reactions with ferric beef liver catalase and intermediates are shown in table 5.

**Table 5. The reactions of ferric beef liver catalase and intermediates with fluoride**

Spectral analysis performed at pH 5.0 in 100 mM potassium phosphate buffer at 23°C. Dissociation constants were obtained from data collected from Figures 23A and B fitted to eqn. 13.

| Catalase | $k_{min}$ ($s^{-1}$) | $k_{max}$ ($s^{-1}$) | $K_d$ (mM) |
|---|---|---|---|
| BLC | - | - | 6.5 |
| comp I | 0.03 | 0.25 | 3.1 |
| comp II | 0.003 | 0.08 | 4.6 |

Figure 19. *Absolute spectra of catalase/fluoride complexes*

The absolute spectra of catalase/fluoride complexes for beef liver (black), HPII wild-type (dark gray), HPII N201D (medium gray) and HPII N201Q (light gray) were recorded on the diode array spectrophotometer at pH 5.0 in 100 mM potassium phosphate buffer at 23°C.

Figure 19.

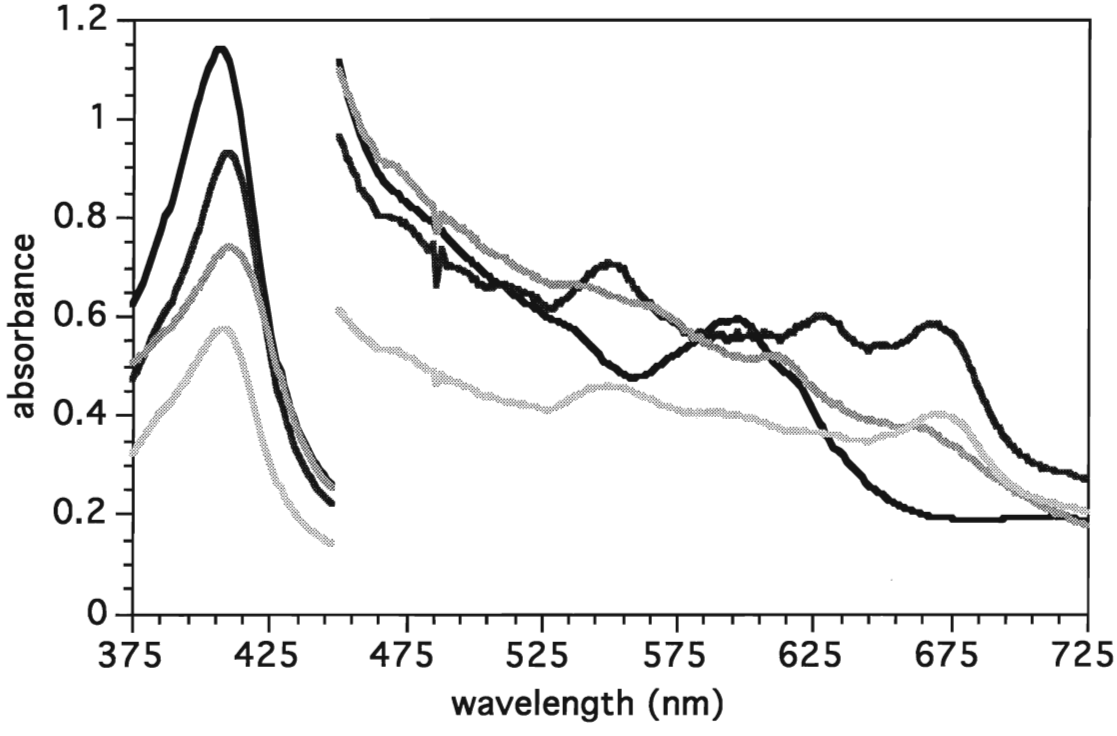
1.2
1
0.8
0.6
0.4
0.2
0
absorbance
375
425
475
525
575
625
675
725
wavelength (nm)

Figure 20. *Difference spectra of catalase/fluoride complexes*

Difference spectra were derived from the spectra of catalases upon the sequential additions of fluoride additions to catalase. The spectra of catalase/fluoride complexes were recorded on the diode array spectrophotometer at pH 5.0 in 100 mM potassium phosphate buffer at 23°C. A) 10 μM beef liver catalase, fluoride additions from 0.18-19 mM; B) 4 μM HPII wild-type, fluoride additions from 0.005-19 mM; C) 5 μM HPII N201D, fluoride additions from 0.045-4.3 mM; D) 7 μM HPII N201Q, fluoride additions from 0.005-24 mM.

Figure 20.

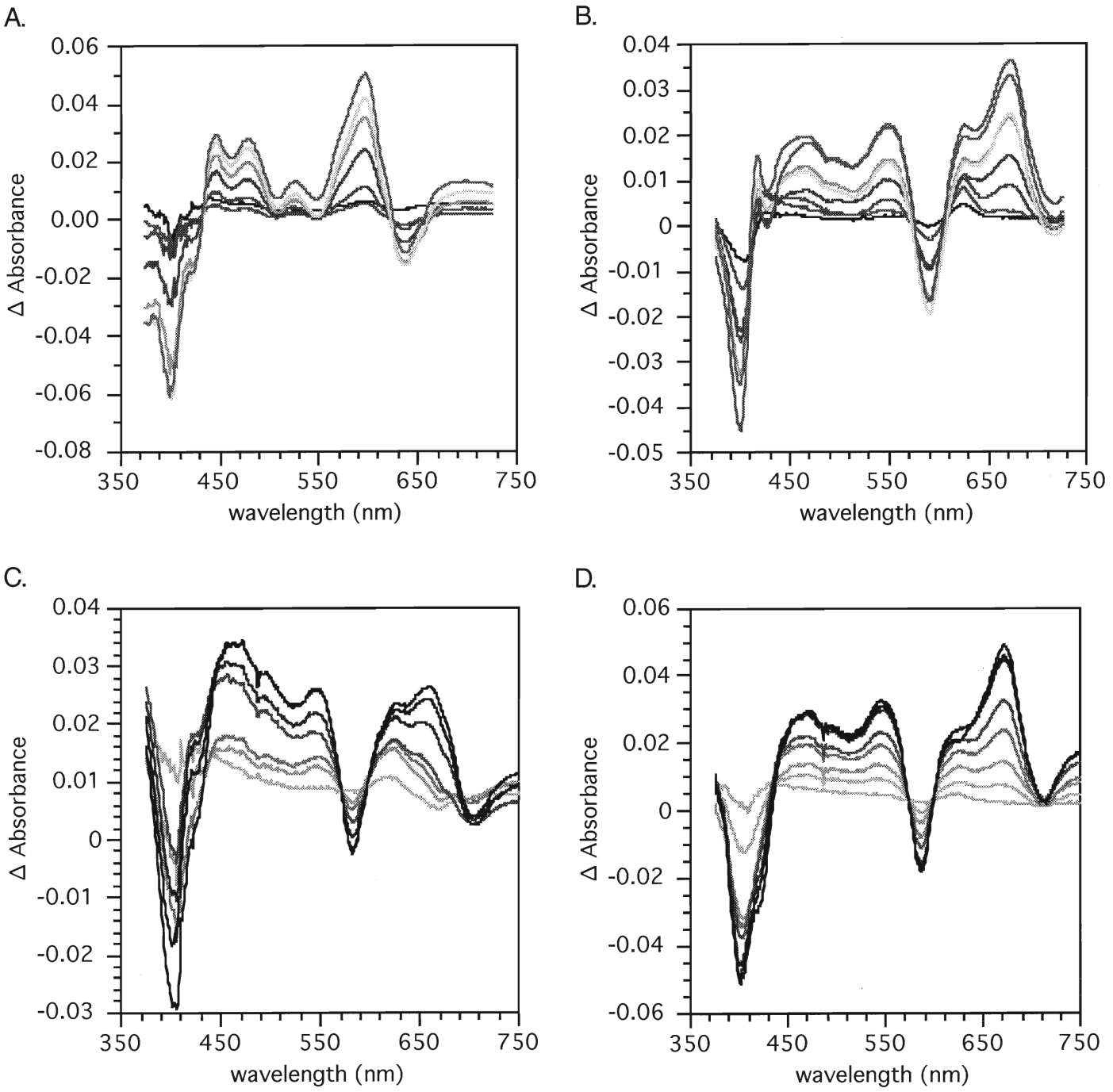
A.
0.06
0.04
0.02
0.00
-0.02
-0.04
-0.06
-0.08
Δ Absorbance
350
450
550
650
750
wavelength (nm)
B.
0.04
0.03
0.02
0.01
0
-0.01
-0.02
-0.03
-0.04
-0.05
Δ Absorbance
350
450
550
650
750
wavelength (nm)
C.
0.04
0.03
0.02
0.01
0
-0.01
-0.02
-0.03
Δ Absorbance
350
450
550
650
750
wavelength (nm)
D.
0.06
0.04
0.02
0
-0.02
-0.04
-0.06
Δ Absorbance
350
450
550
650
750
wavelength (nm)

Figure 21. *Fluoride binding by catalase*

The assay conditions were as described in the legend of Figure 20. The absorbance changes are plotted against the log of fluoride concentrations for A) beef liver catalase, wavelength pairs 445-399nm (■) and 596-636 (●); B) HPII wild-type, wavelength pairs 470-400nm (■) and 670-710nm (●); C) HPII N201D, wavelength pairs 450-400 (■) and 655-700nm (●); D) HPII N201Q, wavelength pairs 470-400nm (■) and 670-710nm (●). The equations used to fit the data is shown in appendix D, table D-1.

Figure 21.

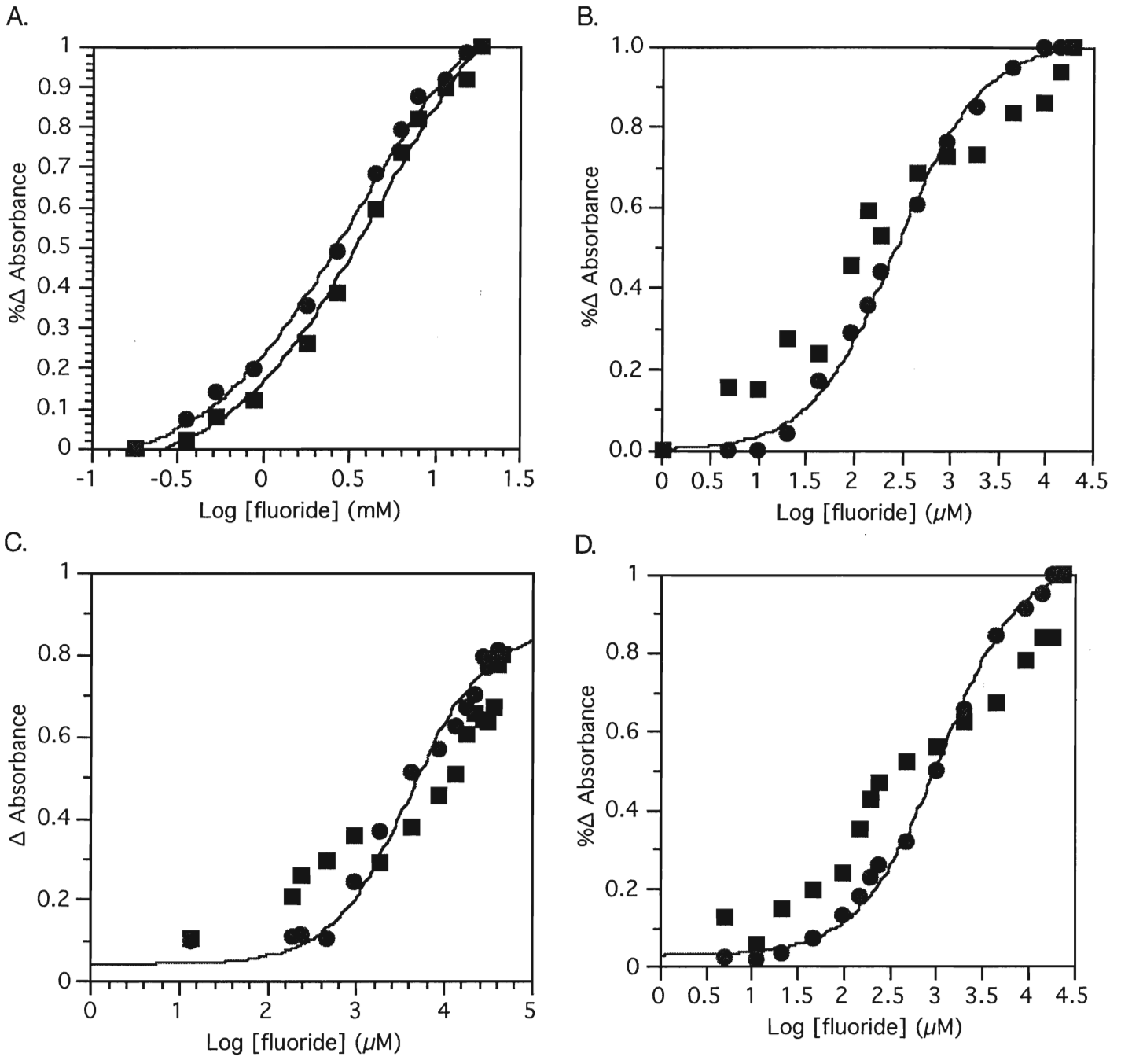
A.
%Δ Absorbance
Log [fluoride] (mM)
B.
%Δ Absorbance
Log [fluoride] (μM)
C.
Δ Absorbance
Log [fluoride] (μM)
D.
%Δ Absorbance
Log [fluoride] (μM)

Figure 22. *The kinetics of fluoride binding to Beef liver catalase*

The exponential rate of fluoride binding to 9 μM catalase was monitored at 595 (■) and 634 nm (●) on the stopped flow spectrophotometer at pH 5.8 in 50 mM potassium phosphate buffer at 23°C. A) The reaction curves at 595 nm with step-wise fluoride additions from 1-100 mM; B) The reaction rates are plotted against fluoride concentration.

Figure 22.

A.

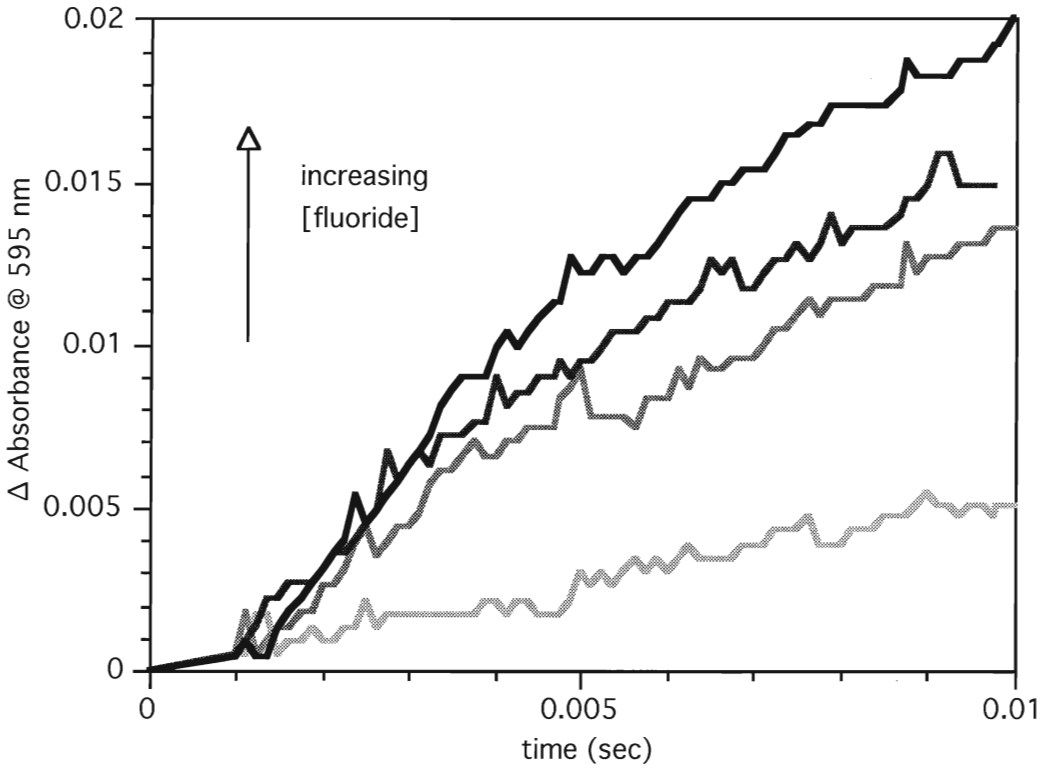
0.02
0.015
0.01
0.005
0
Δ Absorbance @ 595 nm
increasing
[fluoride]
0
0.005
0.01
time (sec)

B.

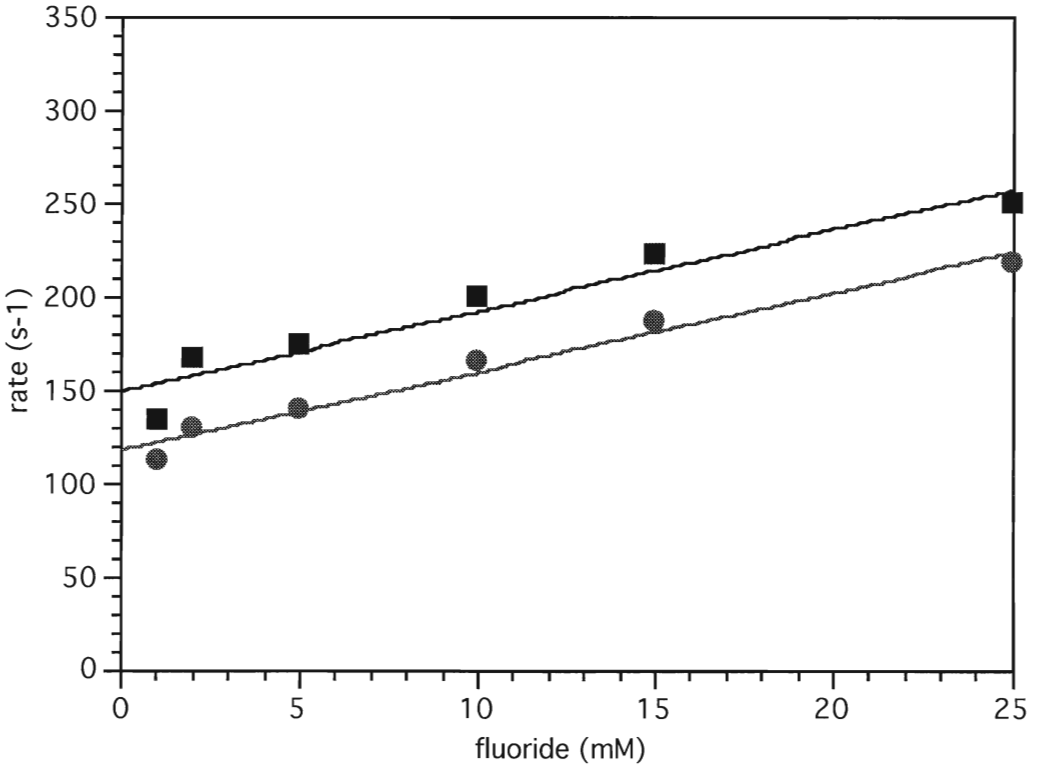
350
300
250
200
150
100
50
0
rate (s-1)
0
5
10
15
20
25
fluoride (mM)

Figure 23. *The formation and decomposition of BLC compounds I and II in the presence of fluoride.*

The experiments were performed on the diode array spectrophotometer at pH 5.0 in 100 mM potassium phosphate buffer at 24°C with 10 μM BLC. A) Fluoride binding to native enzyme. The maximum spectral changes upon the step-wise additions of fluoride (0.5-10 mM) are plotted against fluoride concentrations for the wavelength pairs 445-399 nm (Soret, ■) and 596-636 nm (visible, ●). B) The rates of fluoride binding to compounds I and II rates are plotted against fluoride concentration. Compound I was generated by the addition of 200 μM peracetate. The transition of compound I to compound II was monitored at the wavelength pairs 434-408 nm (▲) and 570-602 nm (◆) for a range of fluoride concentrations from 0.1-10 mM. The reaction rates were plotted against fluoride concentration. The decomposition of compound II back to the native enzyme was followed at the wavelength pairs 434-405 nm (■) and 570-622 nm (●) for a range of fluoride concentrations from 0.5-8 mM. The reaction rates were plotted against fluoride concentration. Compound II was generated by the addition of 200 μM peracetate, 100 μM ferrocyanide and 4 mM ethanol.

Figure 23.

A.

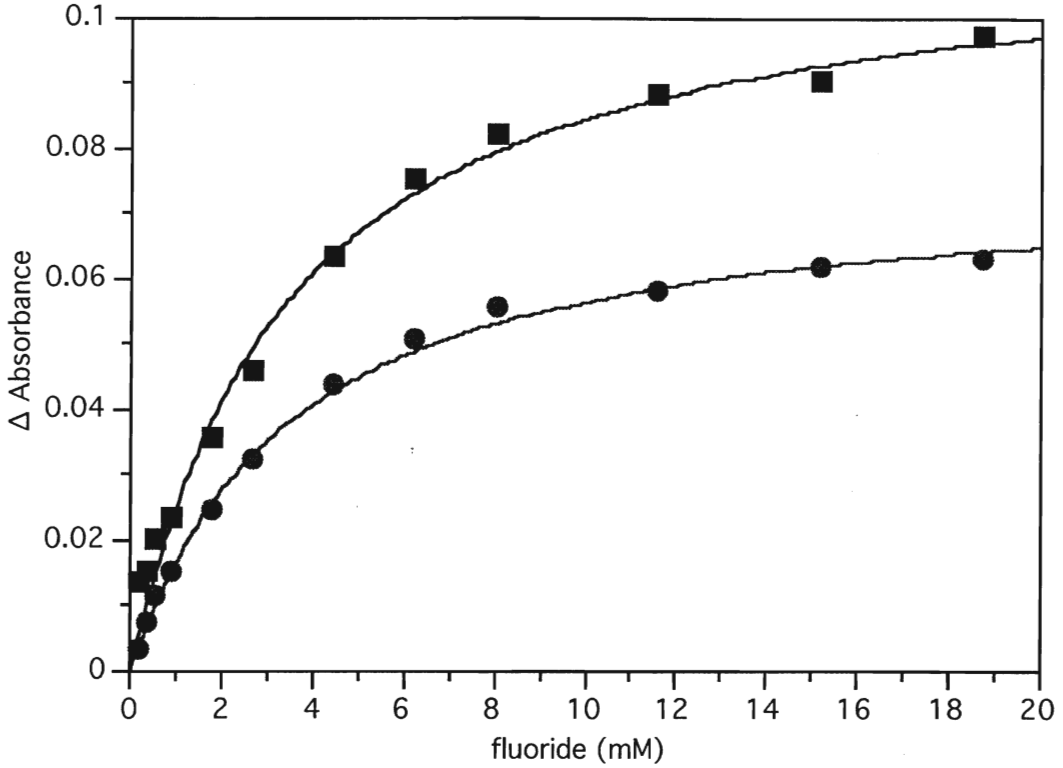
0.1
0.08
0.06
0.04
0.02
0
Δ Absorbance
0
2
4
6
8
10
12
14
16
18
20
fluoride (mM)

B.

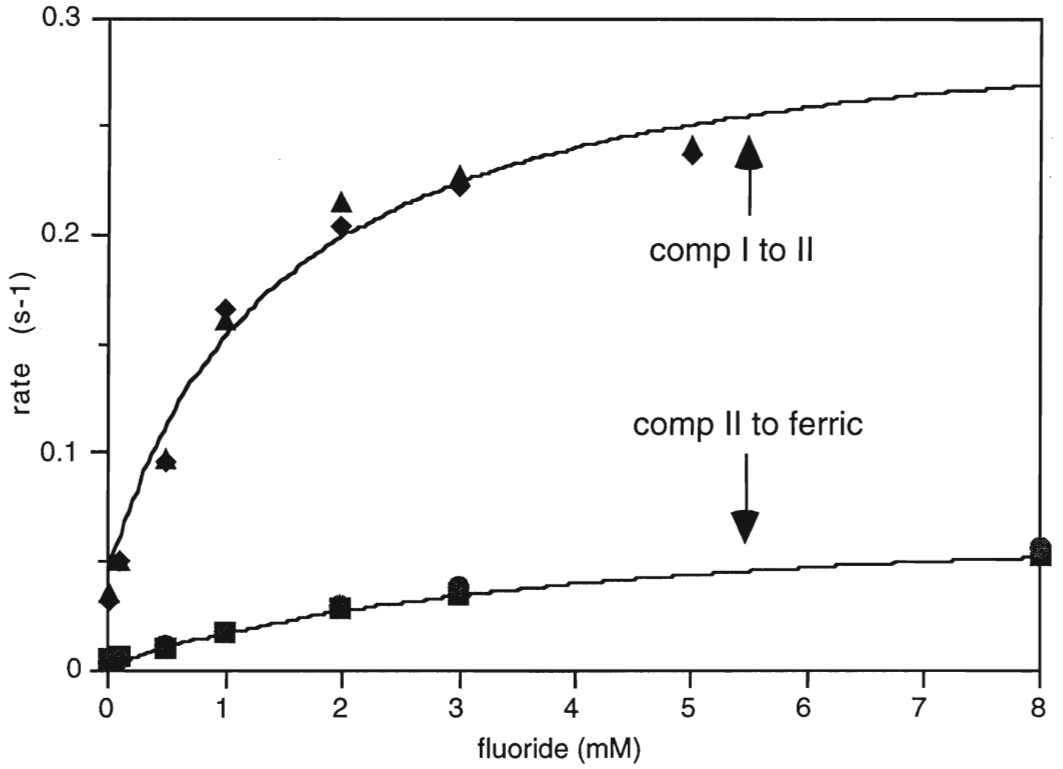
0.3
0.2
0.1
0
rate (s-1)
comp I to II
comp II to ferric
0
1
2
3
4
5
6
7
8
fluoride (mM)

## Formate

*Spectral modifications and equilibria constants of formate binding to catalases*

Beef liver catalase

The reaction of catalase with formate is pH dependent. The pK of formate is 3.75 (Linde, 1990b). Formate binding alters the absorbance spectrum of catalase as shown in Figure 24A. Upon complexing with formate, the $\alpha$-band is slightly blue-shifted and the Soret band is slightly red-shifted, indicative of high-spin ligand binding. Difference spectra for sequential additions of formate to catalase are shown in Figure 24B. The changes in absorbance at wavelength pairs in both the Soret (418-380 nm) and visible (612-648 nm) regions were plotted against formate concentration (Figure 24C) to determine a catalase/formate dissociation constant ($K_d$) at pH 6.8 equal to 3.9 mM.

HPII catalase

Absolute spectra of HPII wild-type, N201D and N201Q enzymes complexed with formate are shown in Figure 25A, B, and C. The $\alpha$-band of each of the three enzymes is blue shifted 10 nm and each Soret band is red shifted by about 1 nm upon complexing with formate. The absorbance peaks of ferric N201D and the formate complex are broader than their wild-type and N201Q counterparts, perhaps indicating a heterogeneous population of

hemes (cf. results page 50). A summary of the absorption peaks for the catalase/formate complexes are shown in table 6. Difference spectra for sequential additions of formate to catalases at pH 6.8 are shown in Figures 26A, B and C. Using data determined from the difference spectra, the changes of absorbance at wavelength pairs in the Soret region (420-400 nm) and in the visible region (580-600 nm) were plotted against formate concentration (Figure 27A, B and C).

In order to determine dissociation constants for the catalase/formate complexes, the data were fitted to equation 13 (results of all fitted data are presented in the appendix tables D-1 and D-2). HPII wild-type enzyme binding of formate (Figure 27A), like that of the beef liver enzyme, followed typical high-spin ligand type binding, with a dissociation constant of 7.7 mM at pH 6.8. Data for formate binding to HPII mutant enzymes could not be fitted to a simple equation. In order to fit the data, it was assumed that mutant enzyme samples contained at least two populations, each with a different binding affinity.

The data collected for the mutant enzymes in both the Soret and visible regions (Figures 27B and C) could then be fitted to the equation:

$$A = \frac{A_{max1} * F}{(K_{d1} + F)} + \frac{A_{max2} * F}{(K_{d2} + F)} \qquad (15)$$

where A is the absorbance, $A_{max1}$ and $A_{max2}$ are the maximum change of absorption for populations 1 and 2, F is the concentration of formate and $K_{d1}$ and $K_{d2}$ are the apparent dissociation constants for populations 1 and 2 respectively.

Based on the fitted data (cf. appendix table D-1), the contribution of population 1, for both N201D and N201Q, was less than 15% overall absorbance change upon binding formate. Therefore, the dissociation constants for the majority population, population 2 were used for comparative purposes. Data collected in the Soret and visible regions for each of the mutants enzyme failed to give similar dissociation constants. The dissociation constants at pH 6.8 for N201D/formate complex in the Soret region were 134 mM and 57 mM in the visible region. The dissociation constants for the N201Q/formate complex at pH 6.8 were 57 mM in the Soret region and 13.5 in the visible.

*Cyanide binding by HPII catalase/formate complexes*

The low-spin ligand cyanide was chosen for competitive binding with formate as BLC, HPII wild-type, N201D and N201Q all have similar affinities for cyanide (ref. to M. Maj B. Sc. thesis and Maj *et al.* 1996). The differences between the heme and the heme pocket environments among these catalases have little effect on their affinity for cyanide. The HPII catalase/formate complexes were titrated by step-wise additions of cyanide. Difference spectra for sequential additions of cyanide to catalase/formate complexes at pH 6.8 are shown in Figures 28A, B and C. The changes in absorbance for appropriate wavelength pairs were

plotted against cyanide concentration (Figure 29B and C). The competitive cyanide dissociation constants for HPII wild-type, N201D and N201Q at pH 6.8 are 46μM, 47.6μM and 57.3 μM respectively.

*Cyanide binding by HPII catalase and site-directed mutant forms*

The HPII enzymes were also titrated with cyanide in the absence of formate as described by Maj *et al.* 1996. Difference spectra for HPII catalase/cyanide complexes at pH 6.8 are shown in Figures 30A, B and C. The change in absorbance at appropriate wavelength pairs were plotted as a function of cyanide concentration (Figure 31A, B and C). $K_{d\ (cyanide)}$ for HPII wild-type, N201D and N201Q at pH 6.8 are 4.5 μM, 16 μM and 18 μM respectively.

*Formate binding by HPII catalase and site-directed mutant forms*

Summary Dixon-type plots were constructed for each of the HPII enzymes (Figure 32A, B and C). The apparent $K_d$ values for cyanide binding as well as competitive cyanide binding of HPII wild-type catalase were plotted as a function of formate concentration. The linear dependence of $K_{d\ (cyanide)}$ on formate concentration is shown in Figure 32A. The linear fits were extrapolated through the origin to give apparent dissociation constants for formate at zero cyanide. The $-K_{d\ (formate)}$ estimated from the x-axis intercept

reflect those determined experimentally (Figures for experiments performed at pH 5.8 are presented in appendix C).

The experimental values of $K_{d\ (cyanide)}$ in the presence and absence of formate were plotted as a function of formate concentration and fit to a straight line. Experimentally determined $K_{d\ (formate)}$ for data collected in the Soret region and visible region were plotted at zero cyanide along the negative x-axis. Extrapolation of the fitted line indicate the probable $K_{d\ (formate)}$ for the N201D enzyme (Figure 32B) is 137 mM at pH 6.8 and for the N201Q enzyme is 9mM at pH 5.8 (Figure C-2B)and 57 mM at pH 6.8 (Figure 32C). A summary of catalase equilibria constants are summarized in table 7.

**Table 6. Absorption peaks of Catalase/formate complexes**

Spectral peaks were obtained from data collected in Figures 24 & 25. Spectral analysis of BLC was performed at pH 5.8 in 100 mM potassium phosphate buffer at 23°C. Spectral analysis of HPII enzymes were performed at pH 6.8 in 100 mM potassium phosphate buffer at 23°C.

| Catalase | Soret region (nm) | visible region (nm) |
|---|---|---|
| BLC | 406 | 612 |
| HPII wild-type | 407 | 550, 630, 701 |
| N201D | 409 | 565, 610, 685 |
| N201Q | 406 | 582, 630, 700 |

**Table 7. Summary of catalase equilibria constants with formate: Eukaryotic and *E. coli* enzymes**

Data for dissociation constants for the beef liver enzyme at pH 6.8 from Figure 24C. Data for the HPII enzymes at pH 6.8 from Figure 32. Experiments at pH 5.8 are shown the appendix Figure C-1. Data fitting shown in appendix table D-1.

| Catalase | Dissociation Constants (mM) | |
|---|---|---|
| | pH 5.8 | pH 6.8 |
| BLC | 0.53 | 3.9 |
| HPII wild-type | 0.9 | 7.7 |
| N201D | - | 134 |
| N201Q | 4.1 | 57 |

Figure 24. *Formate binding by Beef liver catalase*

Spectra of beef liver catalase upon the addition of formate were collected on the DU-7 spectrophotometer at pH 6.8 in 100 mM potassium phosphate buffer at 30°C. A) The absolute spectra of 7 μM beef liver catalase and 95 mM formate. B) Difference spectra were derived for the formate complexes. Increasing amounts of formate were added in a step-wise fashion up to 95 mM. C) The absorbance changes were plotted against formate concentrations for wavelength pairs 418-380 nm (■) and 612-648 nm (●).

Figure 24.

A.

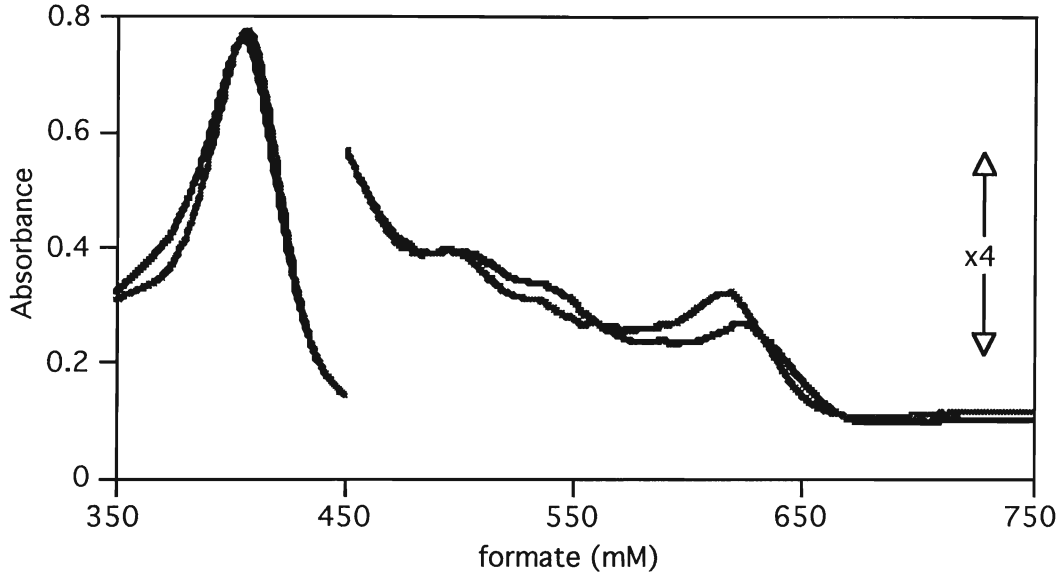


B.

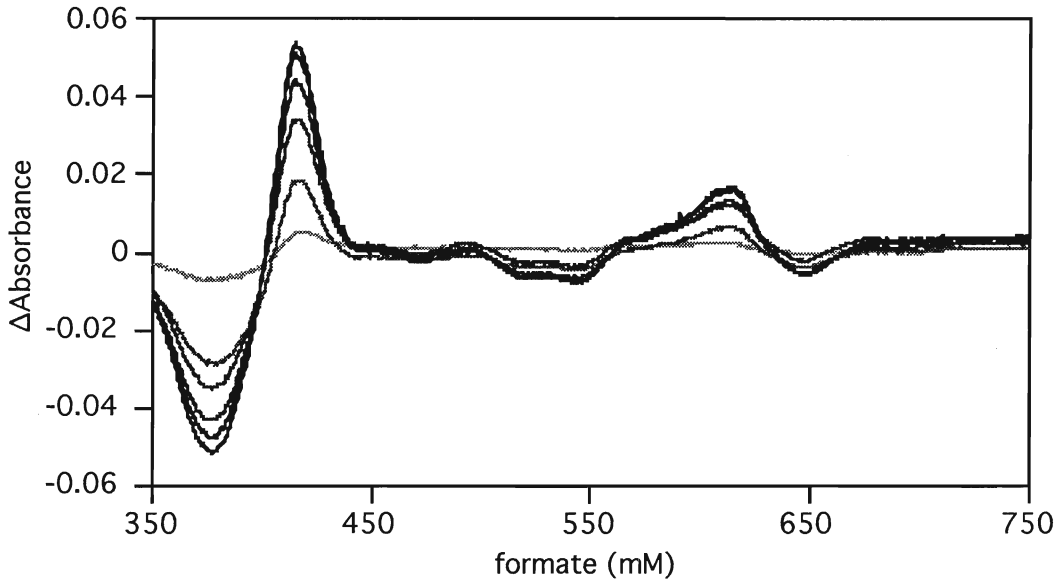


C.

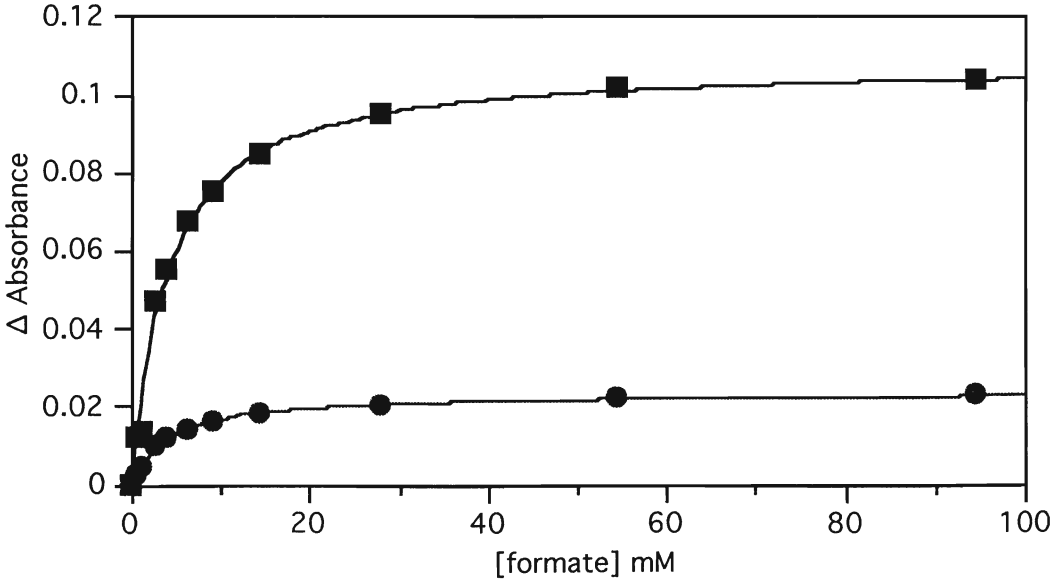

Figure 25. *Absolute spectra of HPII enzymes complexed with formate.*

The absolute spectra of HPII catalase/formate complexes (grey) for (A) HPII wild-type (black), (B) HPII N201Q (black) and (C) HPII N201D (black) were recorded on the DU-7 spectrophotometer at pH 6.8 in 100 mM potassium phosphate buffer at 30°C.

Figure 25.

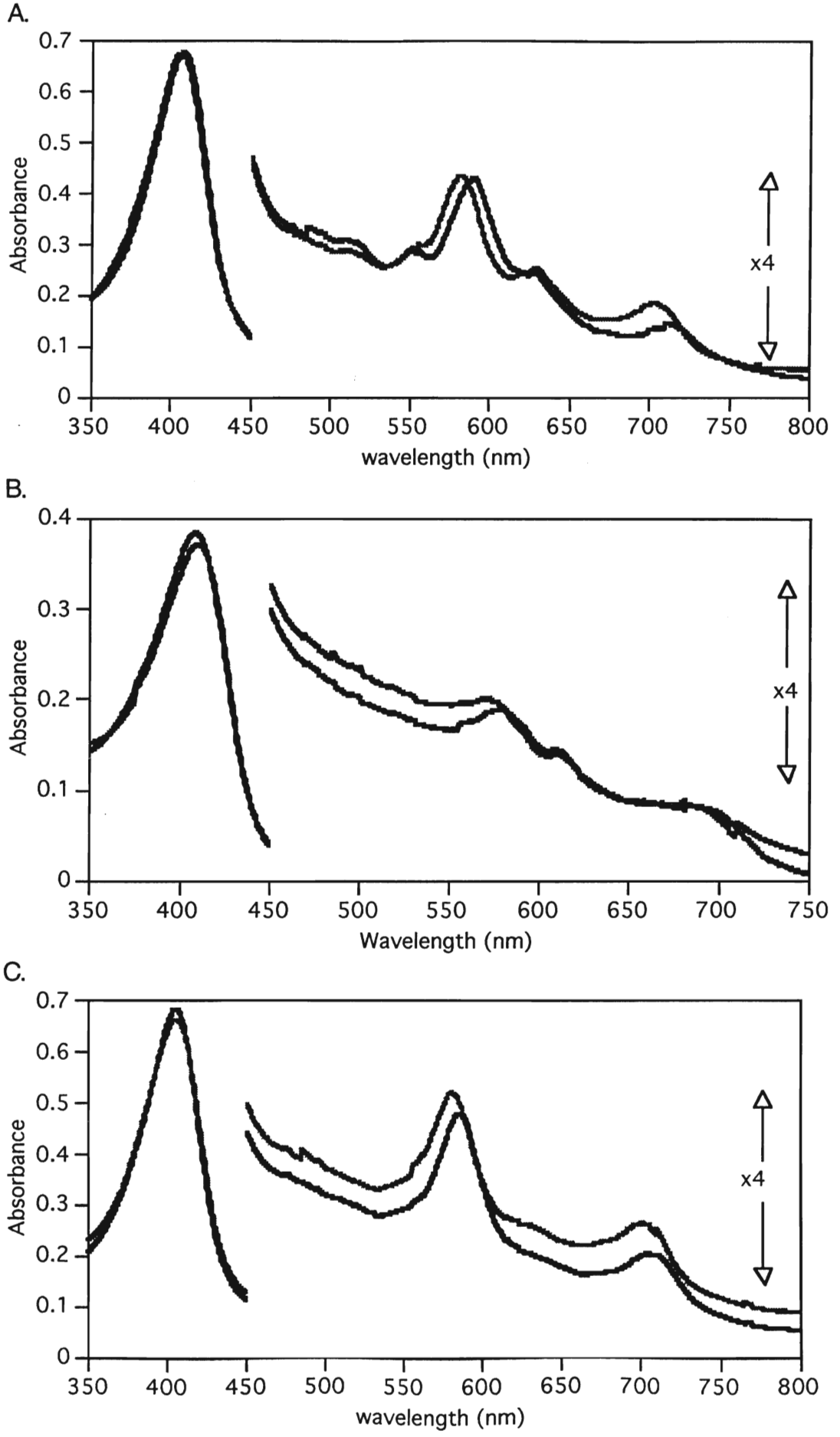
A.
Absorbance
0.7
0.6
0.5
0.4
0.3
0.2
0.1
0
x4
350 400 450 500 550 600 650 700 750 800
wavelength (nm)
B.
Absorbance
0.4
0.3
0.2
0.1
0
x4
350 400 450 500 550 600 650 700 750
Wavelength (nm)
C.
Absorbance
0.7
0.6
0.5
0.4
0.3
0.2
0.1
0
x4
350 400 450 500 550 600 650 700 750 800
wavelength (nm)

Figure 26. *Difference spectra of HPII catalase/formate complexes.*

Experiments were performed on the DU-7 spectrophotometer at pH 6.8 in 100 mM potassium phosphate buffer at 30°C. Increasing amounts of formate were added in a step-wise fashion. A) 5 μM HPII wild-type, formate concentrations from 0.1-75 mM; B) 3 μM N201D, formate concentrations from 1-335 mM; C) 7 μM N201Q, formate concentrations from 0.1-75 mM.
(HPII experiments performed at pH 5.8 are presented in appendix C).
*note: Due to the limited availability of the ND mutant, a low concentration of enzyme was used, resulting in light-scattering effects and baseline shifts at high formate concentrations. Difference spectra for ND/formate complex in the presence of 335 mM formate is not shown.

Figure 26.

A.

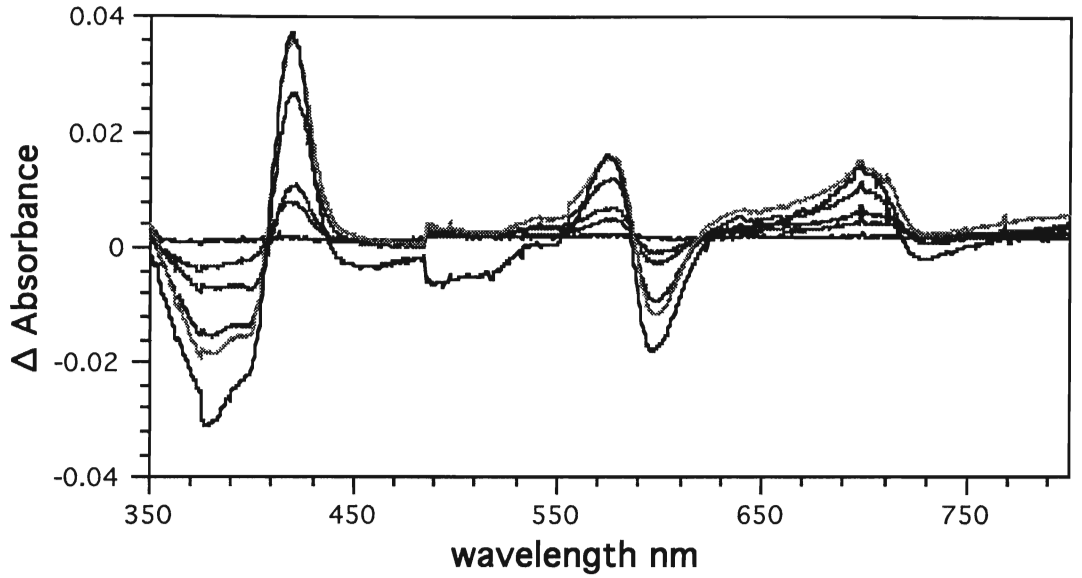


B.

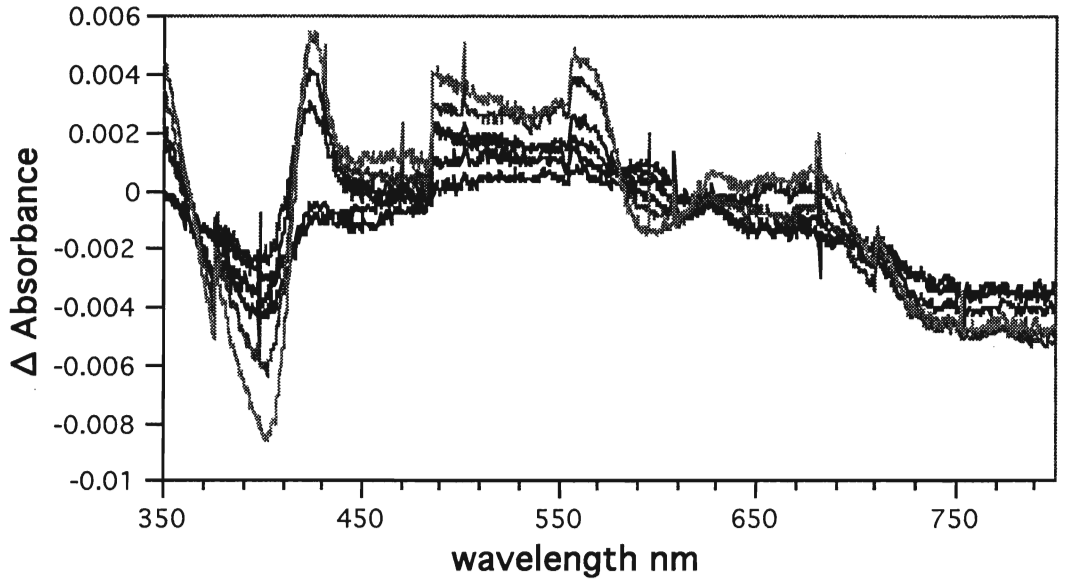


C.

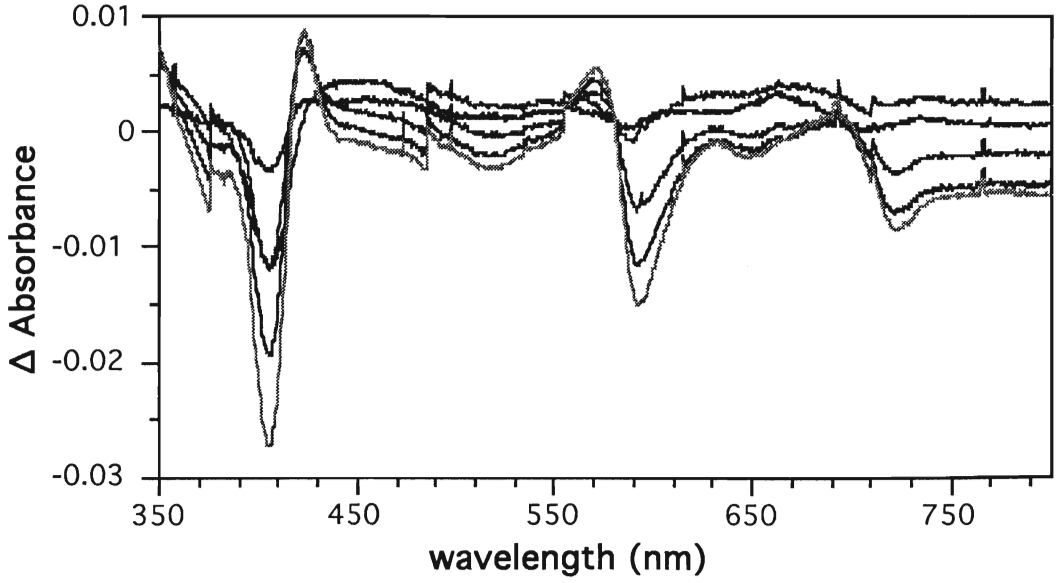

Figure 27. *Formate binding by HPII catalases*

The assay conditions are as described in the legend of Figure 26. The absorbance changes were plotted against formate concentrations for wavelength pairs 420-400 nm (■) and 580-600 nm (●): A) HPII wild-type; B) HPII N201D; C) HPII N201Q. The data was fitted to determine $K_d$. The equations used to fit data are shown in appendix D, table D-1.

Figure 27.

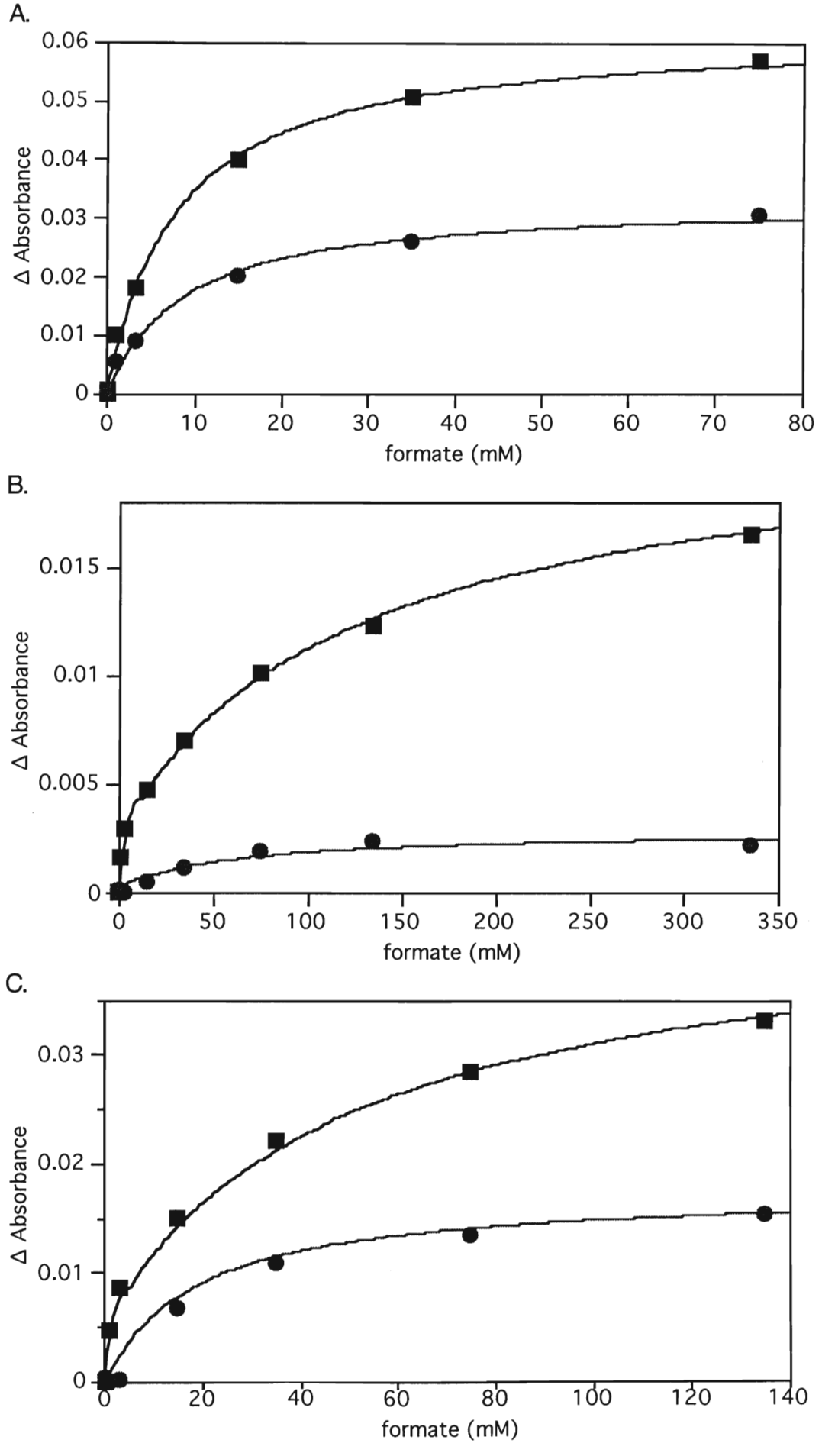
A.
0.06
0.05
0.04
0.03
0.02
0.01
0
Δ Absorbance
0
10
20
30
40
50
60
70
80
formate (mM)
B.
0.015
0.01
0.005
0
Δ Absorbance
0
50
100
150
200
250
300
350
formate (mM)
C.
0.03
0.02
0.01
0
Δ Absorbance
0
20
40
60
80
100
120
140
formate (mM)

Figure 28. *Difference spectra of HPII catalase/formate complexes titrated with cyanide*

Difference spectra were derived for HPII enzymes fully complexed with formate upon the addition of increasing amounts of cyanide. Experiments were performed on the DU-7 spectrophotometer at pH 6.8 in 100 mM potassium phosphate buffer at 30°C. A) 5 μM HPII wild-type complexed with 75 mM formate. Cyanide was added up to a concentration of 450 μM; B) 3 μM N201D complexed with 335 mM formate. Cyanide was added up to a concentration of 950 μM; C) 7 μM N201Q complexed with 75 mM formate. Cyanide was added up to a concentration of 1950 μM.

Figure 28.

A.

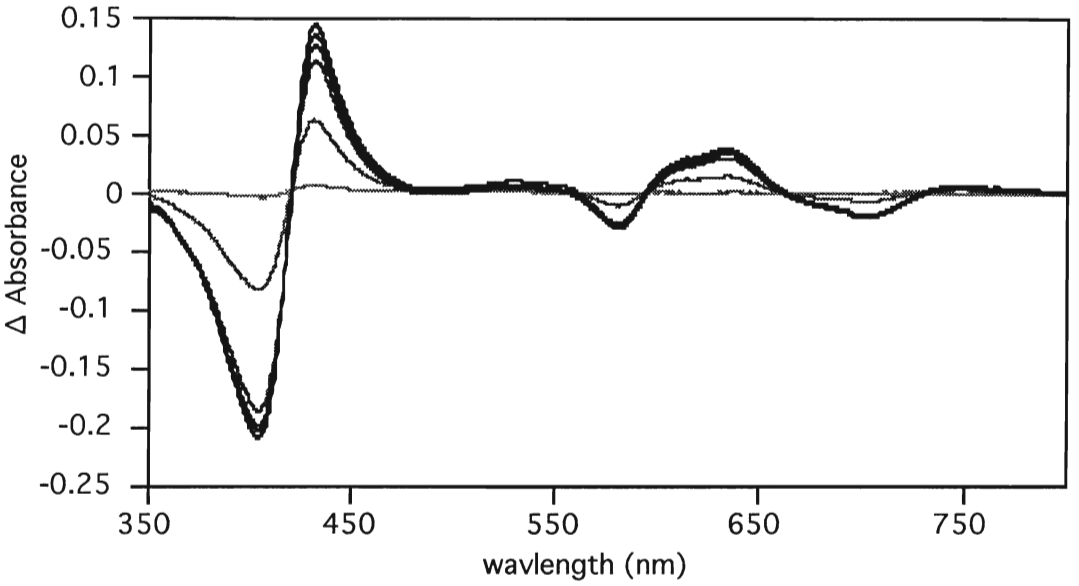


B.

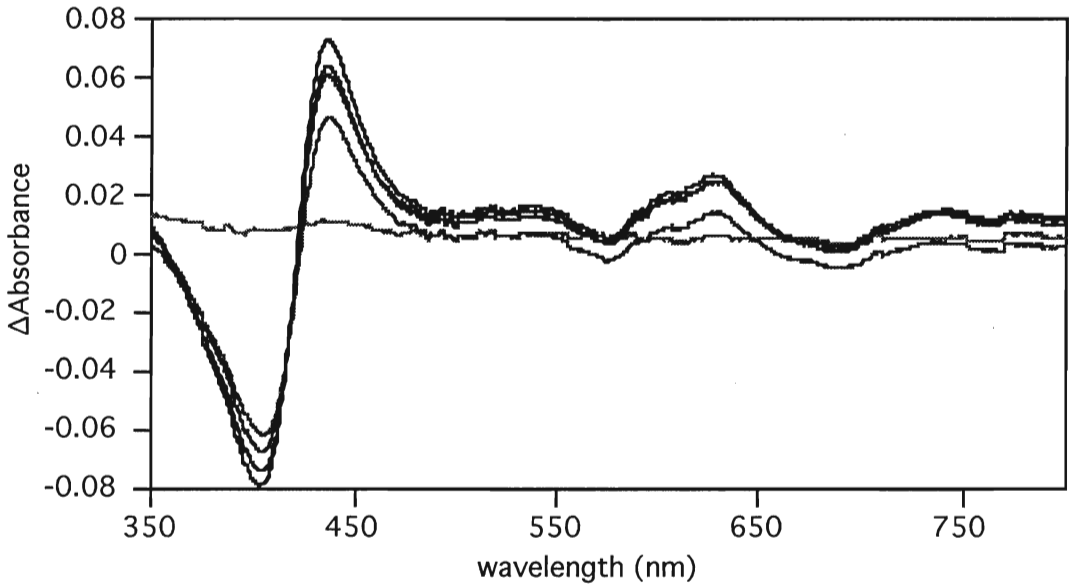


C.

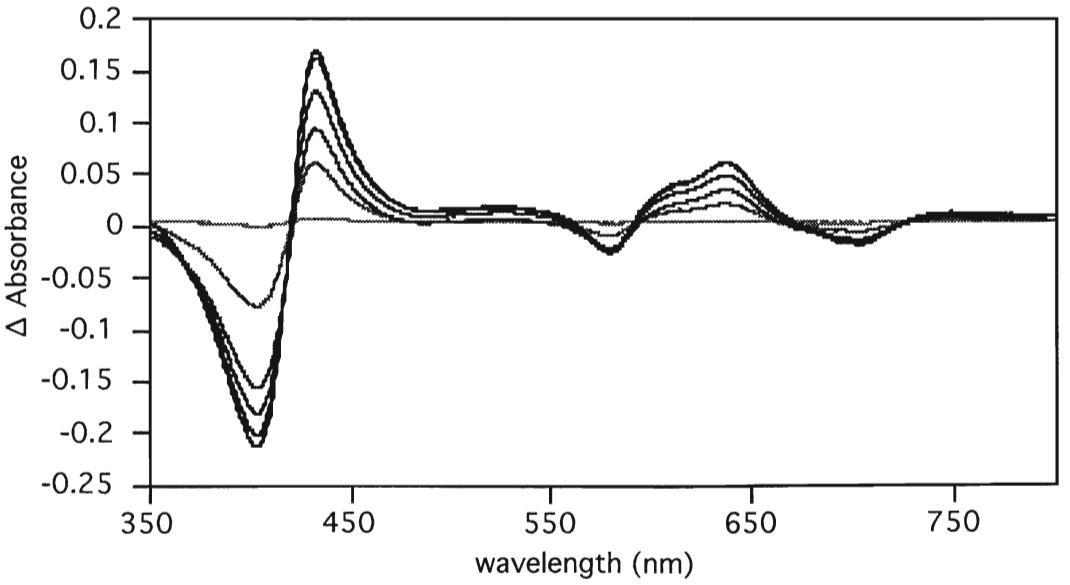

Figure 29. *Cyanide binding by HPII catalase/formate complexes*

The assay conditions are as described in the legend of Figure 26. The absorbance changes were plotted against cyanide concentrations for wavelength pairs 430-400 nm (■) and 630-580 nm (●). A) HPII wild-type; B) HPII N201D; C) HPII N201Q. The data was fitted to determine competitive dissociation constants for cyanide. The equations used to fit data are shown in appendix D, table D-2.

Figure 29.

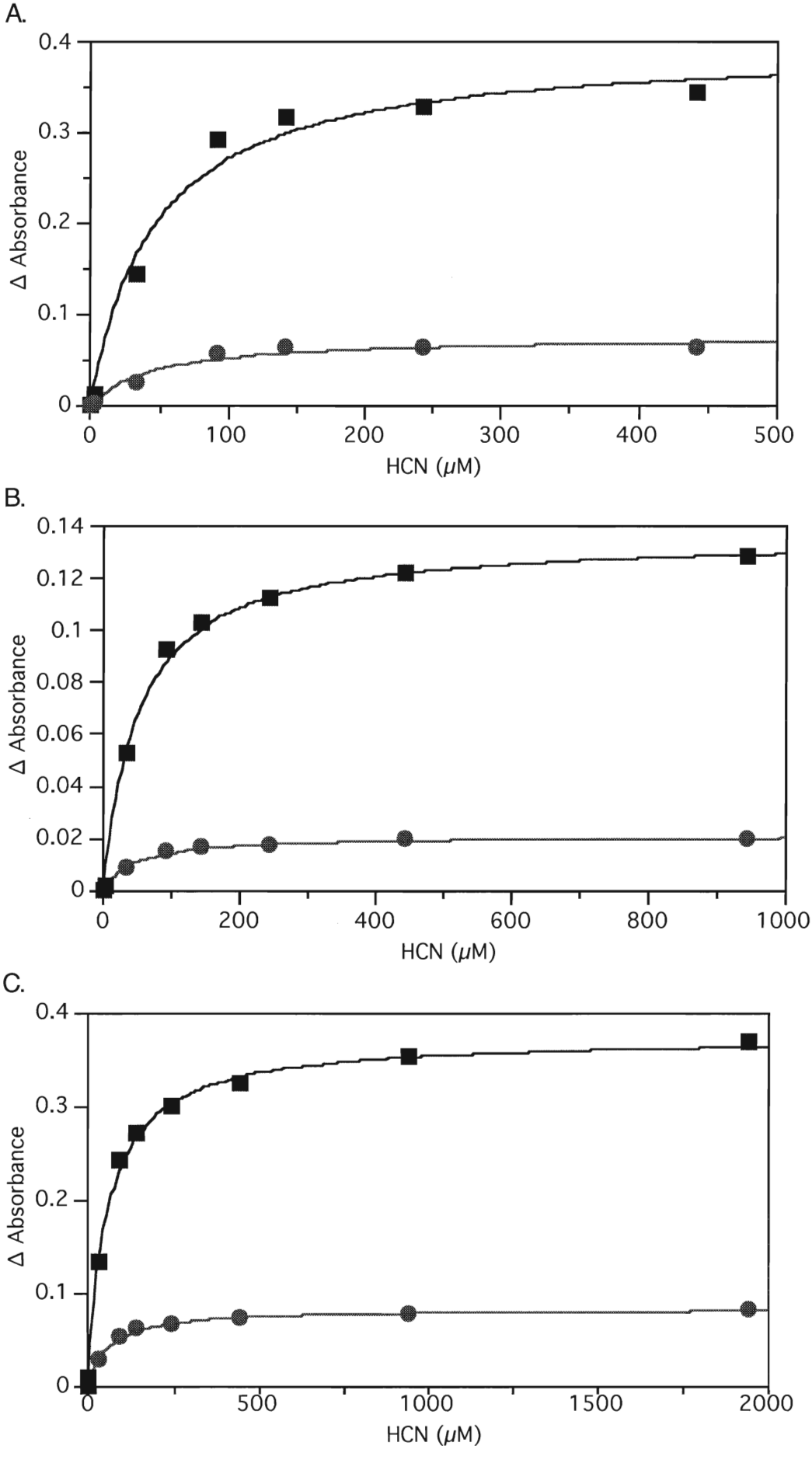
A.
0.4
0.3
0.2
0.1
0
Δ Absorbance
0
100
200
300
400
500
HCN (μM)
B.
0.14
0.12
0.1
0.08
0.06
0.04
0.02
0
Δ Absorbance
0
200
400
600
800
1000
HCN (μM)
C.
0.4
0.3
0.2
0.1
0
Δ Absorbance
0
500
1000
1500
2000
HCN (μM)

Figure 30. *Difference spectra of HPII Catalase cyanide complexes*

Difference spectra were derived for HPII enzymes upon the addition of increasing amounts of cyanide. Experiments were performed on the DU-7 spectrophotometer at pH 6.8 in 100 mM potassium phosphate buffer at 30°C. A) step-wise additions of cyanide up to 140 μM was added to 5 μM wild-type enzyme; B) step-wise additions of cyanide up to 1150 μM were added to 3 μM N201D enzyme; C) step-wise additions of cyanide up to 1650 μM was added to 7 μM N201Q enzyme.

Figure 30.

A.

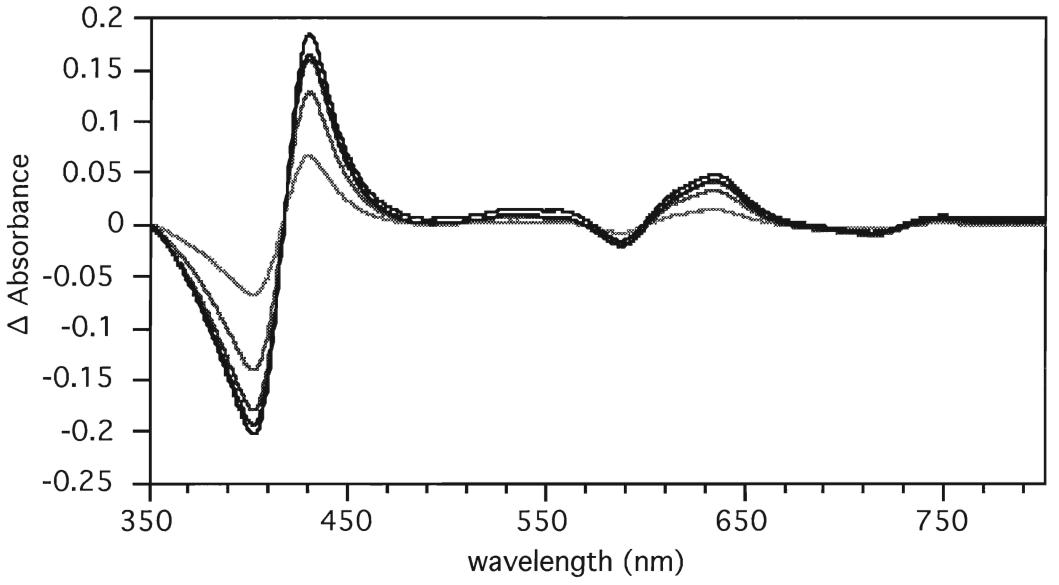


B.

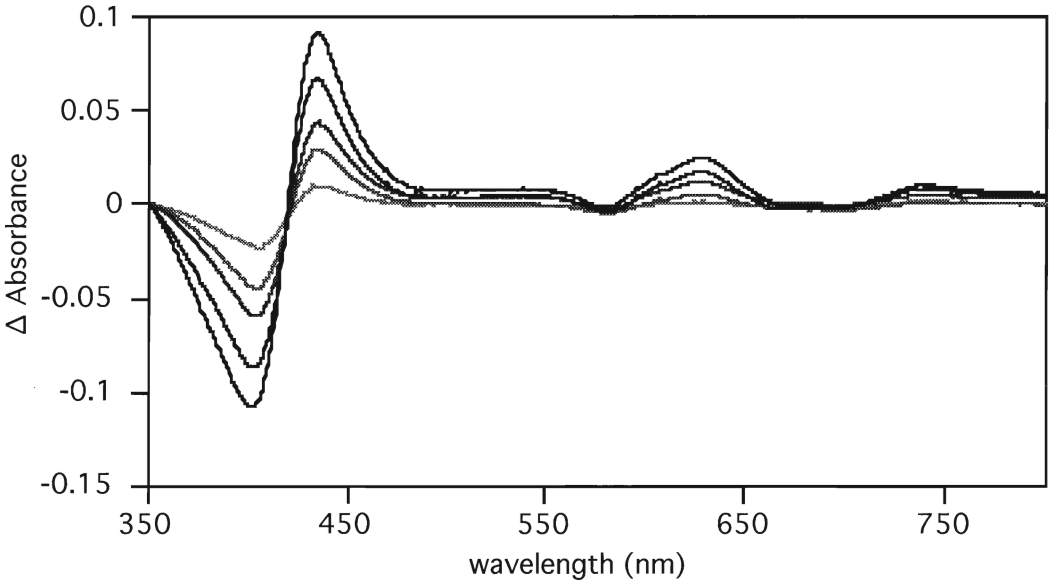


C.

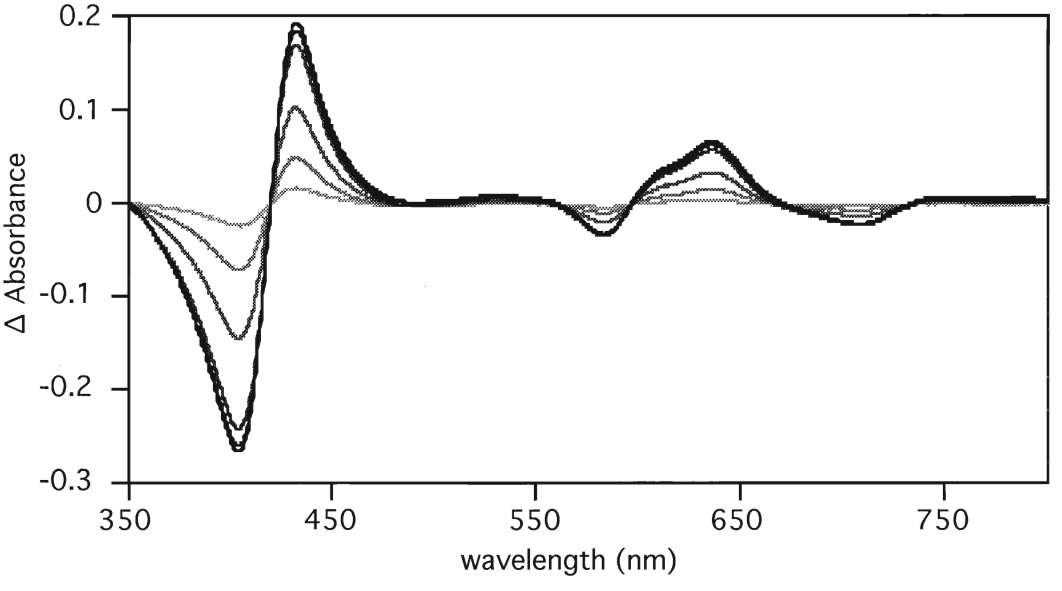

Figure 31. *Cyanide binding by HPII catalases*

The assay conditions are as described in the legend of Figure 30. The absorbance changes were plotted against cyanide concentrations for wavelength pairs 420-406 nm (■) and 630-590 nm (●). A) HPII wild-type; B) HPII N201D; C) HPII N201Q. The data was fitted to determine the dissociation constants for cyanide. The equations used to fit data are shown in appendix D, table D-2.

Figure 31.

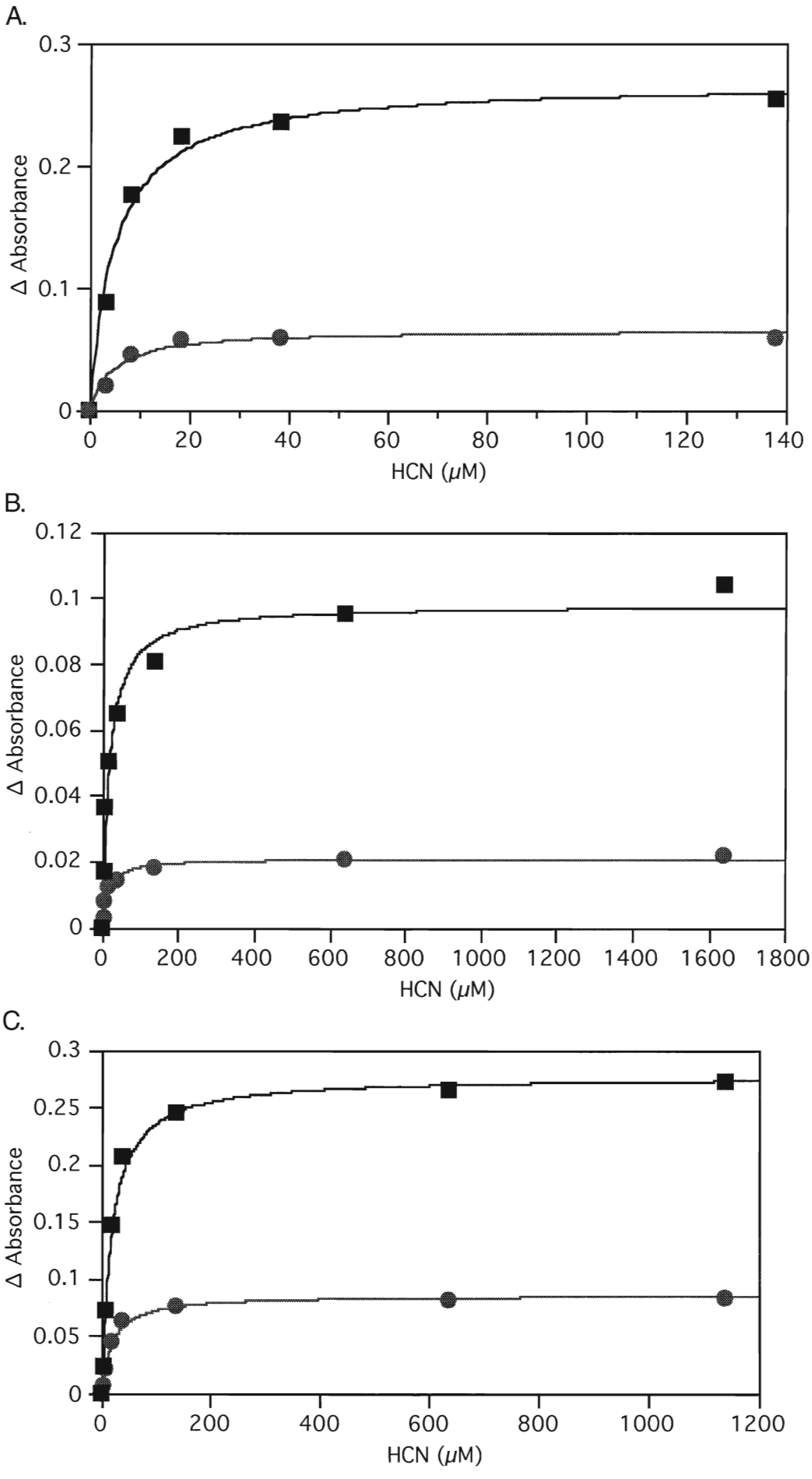
A.
0.3
0.2
0.1
0
Δ Absorbance
0
20
40
60
80
100
120
140
HCN (μM)
B.
0.12
0.1
0.08
0.06
0.04
0.02
0
Δ Absorbance
0
200
400
600
800
1000
1200
1400
1600
1800
HCN (μM)
C.
0.3
0.25
0.2
0.15
0.1
0.05
0
Δ Absorbance
0
200
400
600
800
1000
1200
HCN (μM)

*Rate of formate binding to Beef liver catalase*

The rate of formate complex formation with beef liver catalase was monitored at 380, 417, 612 and 647 nm. Typical traces of complex formation are shown in Figure 32A. The reaction rates at 380-417nm and 647-612 nm were plotted as a function of formate concentration (Figure 33B) to give second-order rate and dissociation constants of 160 $M^{-1}s^{-1}$ and 18 mM respectively. Table 7 summarizes catalase affinities for formate.

*Compound II reduction by formate*

Formate prevents the formation of compound II by keeping a low steady state concentration of compound I (cf. Figure 15 and 16) Formate also accelerates the reduction of compound II. Compound II was formed by incubating the beef liver enzyme with peracetate and ferrocyanide. The assay was performed at pH 5.8 which is favorable to the formation of compound II. Representative traces of compound II reduction upon the addition of formate are shown in Figure 34A. The rates were plotted as a function of formate concentration and fitted to equation 13 (Figure 34B). The dissociation constant for compound II/formate complex at pH 5.8 is 6 mM. The maximum rate of compound II decay in the presence of formate was estimated to be 0.06 $s^{-1}$ with a spontaneous decay rate of 0.0005 $s^{-1}$. Table 8 summarizes the catalase reactions with formate.

**Table 8. Summary of catalase rate and equilibria constants with formate.**

Rate and equilibria constants of formate binding at pH 7.4 from Figure 33B & C. Data for rate of comp I reduction by formate and spontaneous reduction of comp I from Figures 15 & 16 at pH 7.4, data for compound II reactions from Figure 34A & B at pH 5.8.

| Catalase Species | pH 7.4 | | | pH 5.8 |
|---|---|---|---|---|
| | reaction rate | $k_{min}$* ($s^{-1}$) | $K_d$ (mM) | $K_d$ (mM) |
| Ferric | 160 $M^{-1}s^{-1}$ | | 23 | 0.53 |
| Comp I ($H_2O_2$) | 237 $M^{-1}s^{-1}$ | 0.1 | | |
| Comp I (pera) | 161 $M^{-1}s^{-1}$ | 0.007 | | |
| Comp II (perac&FeCN) | 0.06 $s^{-1}$¥ | 0.0005 | | 6.0** |

*$k_{min}$=rate of peroxide compound reduction by endogenous donor.

**The affinity of compound II for formate is reduced due to interaction with the endogenous donor.

¥This is a maximal rate (s-1) as compound II does not oxidize formate directly.

Figure 32. *Summary plots of formate and cyanide dissociation constants.*

The dissociation constants for cyanide by HPII catalases and their formate complexes were plotted against formate concentration. These Dixon-type plots were used to determine the formate dissociation constants of the mutant enzymes.
(Data for the wild-type and N201Q enzymes at pH 5.8 are presented in appendix C, curve fitting in appendix D).

Figure 32.

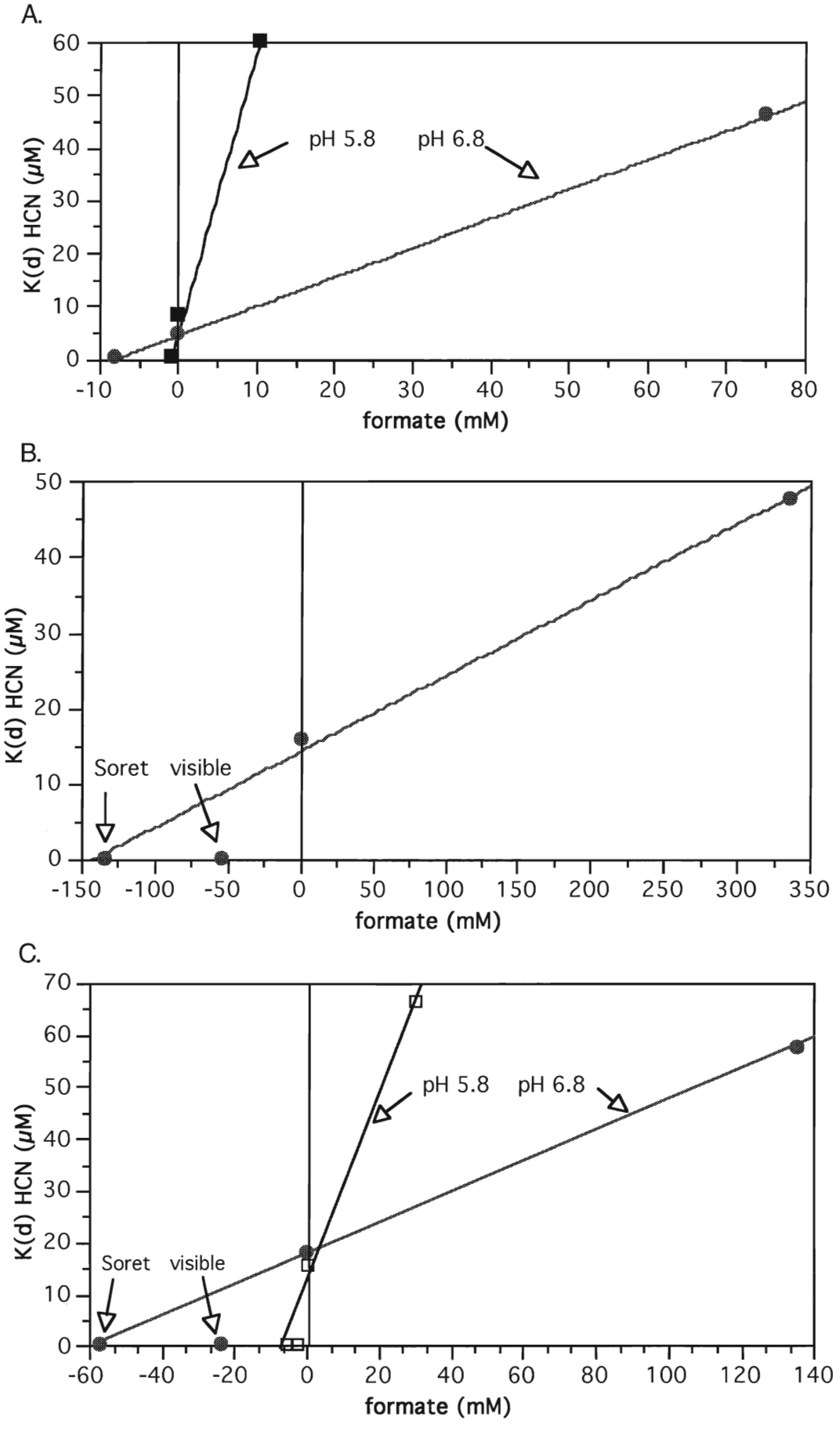
A.
K(d) HCN (μM)
formate (mM)
pH 5.8
pH 6.8
B.
K(d) HCN (μM)
formate (mM)
Soret
visible
C.
K(d) HCN (μM)
formate (mM)
pH 5.8
pH 6.8
Soret
visible

Figure 33. *The kinetics of formate binding by beef liver catalase*

The rate of formate binding to 3 μM catalase was monitored on the stopped-flow spectrophotometer at pH 7.4 in 50 mM potassium phosphate buffer at 30°C. A) The reaction of formate binding was monitored at 380 (*a*), 647 (*b*), 612 (*c*) and 417nm (*d*) for formate concentrations ranging from 5-125 mM; B) the reaction rate at 380-417 nm (Soret, ■) and 647-612 nm (visible, ●) were plotted against formate concentration. C) Formate was added to 18 μM BLC in a step-wise fashion with concentrations ranging from 2.7-53.4 mM. The experiment was performed on the DU-7. The absorbance change at 612-645 nm were plotted against formate concentration.

Figure 33.

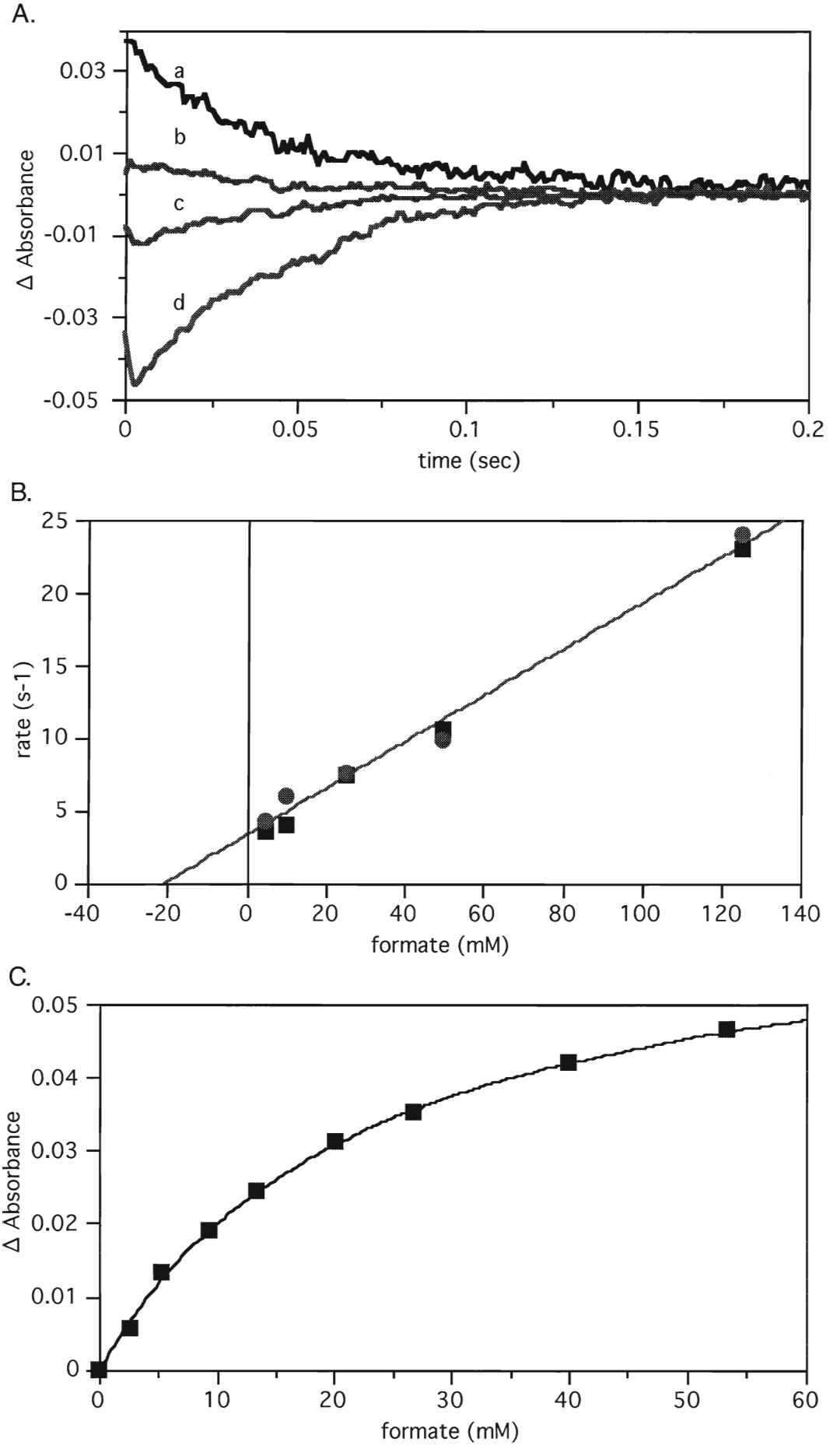
A.
0.03
0.01
-0.01
-0.03
-0.05
Δ Absorbance
a
b
c
d
0
0.05
0.1
0.15
0.2
time (sec)
B.
25
20
15
10
5
0
rate (s-1)
-40
-20
0
20
40
60
80
100
120
140
formate (mM)
C.
0.05
0.04
0.03
0.02
0.01
0
Δ Absorbance
0
10
20
30
40
50
60
formate (mM)

Figure 34. *Formate reduction of compound II.*

A) The rates of compound II decay in the presence of increasing amounts of formate (0.4-13.3 mM) were monitored on the DW-2 spectrophotometer at 435-405 nm. Compound II was generated by the addition of 400 μM peracetate and 33 μM ferrocyanide to 11 μM beef liver enzyme at pH 5.8 in 100 mM potassium phosphate buffer at 30°C. B) The reaction rates were plotted against formate concentration.

Figure 34.

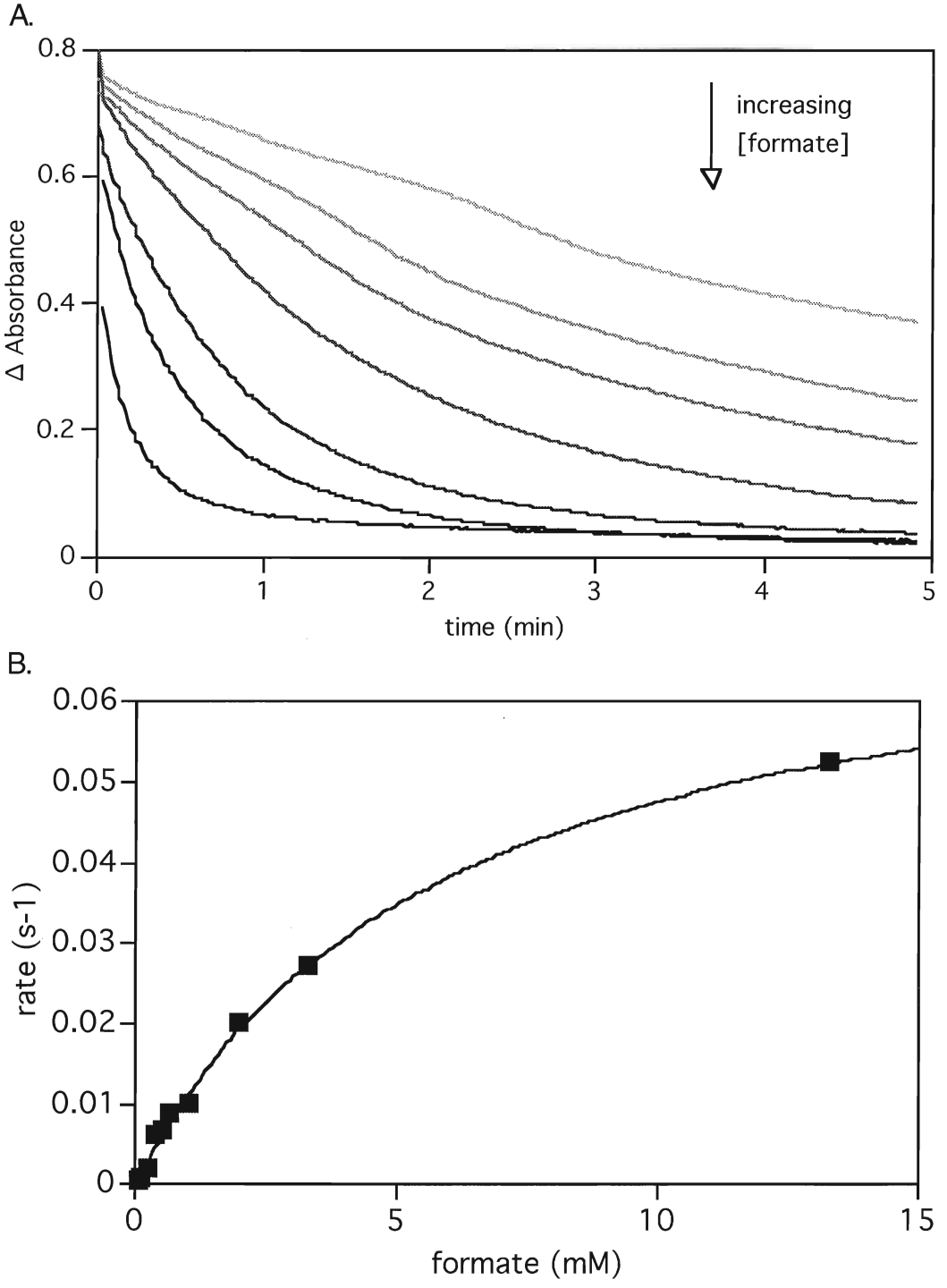
A.
0.8
0.6
0.4
0.2
0
Δ Absorbance
increasing
[formate]
0
1
2
3
4
5
time (min)
B.
0.06
0.05
0.04
0.03
0.02
0.01
0
rate (s-1)
0
5
10
15
formate (mM)

## Structural comparisons

Structural analysis of four catalase enzymes was performed. The channel and active sites for the beef liver, *Micrococcus*, *Penicillium* and HPII enzymes show 80-90% homology (Figures 35 A, B, C and D). The active site channel for all four enzymes is lined mainly with hydrophobic residues. Their heme group is located some 20-30Å from the surface of the protein. All four enzymes contain the distal residues histidine (blue) and asparagine (red) at similar orientations within the active site. The residues are also at similar distances from the heme iron, histidine 4-5 Å and asparagine 5.5-6 Å. These distal residues are important for the binding and stabilization of substrate at the active site. The proximal ligand is tyrosine for all four proteins. Both beef liver and *Micrococcus* catalases contain protoheme (Figures 35A and B) and contain an alanine residue ~ 2Å below pyrrole ring III. The analogous residue for HPII and *Penicillium* catalase is serine, also located ~ 2Å below pyrrole ring III (Figure C and D). This serine residue may assist in the hydroxylation of ring III to produce heme d. HPII and *Penicillium* enzymes originally associate with protoheme as the prosthetic group which is converted to heme d during the catalytic reaction. The details of the heme modification are still unknown. A summary of proximal and distal residues for the four enzymes are shown in table 9.

The channel stereochemistry of the four enzymes is compared in Figures 36 and 37. The beef liver enzyme is the most accessible to solvent. The channel of the *Micrococcus* enzyme is obstructed by a stretch of protein backbone shown in pink in Figure 36B. This protein moiety is located one third of the way from the channel entrance. Interestingly, the activity of the *Micrococcus* enzyme is nearly twice that of the beef liver. The channels of *penicillium* (37A) and HPII (37B) catalases are also obstructed by a stretch of protein backbone. Both the *Penicillium* and HPII enzymes contain residues which may block the channel entrance, gln308 (yellow), trp304 (green) and phe529 (orange) in HPII and gln243 (yellow), trp239 (green) and his464 (orange) in *Penicillium*. The HPII enzyme has 10-15% the activity of the beef liver protein. A summary of the structural information concerning the active site channel is shown in table 10 and 11.

**Table 9. Comparison of heme pocket residues**

Distal residue histidine is located ≈4.8 Å from the heme iron for all enzymes. The distal residue asparagine is located ≈6 Å from the heme iron for all enzymes. A tyrosine residue occupies the 5$^{th}$ coordination site for typical catalases. The residue proximal to the 3$^{rd}$ pyrrole ring for all four enzymes is indicated below at distances ≤2.4 Å from porphyrin.

| Catalase | distal residues | | proximal residues | |
|---|---|---|---|---|
| | His | Asn | Tyr | 3$^{rd}$ pyrrole |
| BLC | 74 | 147 | 357 | ala 356 |
| MLC | 57 | 129 | 399 | ala 338 |
| PVC | 63 | 136 | 350 | ser 349 |
| HPII | 128 | 201 | 415 | ser 414 |

**Table 10. Comparison of residues found at the entrance of the heme channel**

*The entrance of the heme channel for the heme d enzymes is partially occluded by large residues. The residues are listed below as well as analogous residues for the protoheme enzymes.

| Catalase | Heme Channel | | |
|---|---|---|---|
| BLC | Gly 464 | Val 246 | Ala 250 |
| MLC | Gly 448 | Asn 228 | Thr 232 |
| PVC | His 464* | Trp 239* | Glu 243* |
| HPII | Phe 529* | Trp 304* | Gln 308* |

**Table 11. Protein backbone obstruction of the channel**

The protein backbone moieties which obstruct solvent access are located ≈17Å from the heme iron in the active site channel.

| Catalase | Blocking Backbone Sections |
|---|---|
| MLC | Val 491, Gly 490, Pro 489, Ile 488, Gly 487 |
| PVC | Ala 167, Ala 168, Val 169 |
| HPII | Gly 232, Gln 233, Ser 234 |

Figure 35. *Active site residues*

The heme environment for A) beef liver, B) *Micrococcus lysodektus* , C) *Penicillium vitale* and D) *Escherichia coli* HPII catalases. The distal histidines and asparagines are colored in blue and red respectively. Most of the hydrophobic residues which line the channel are conserved. The protoheme enzymes (A&B) contain an alanine residue on the distal side of the heme directly below pyrrole ring d. The analogous residues for both of heme d enzymes (C&D) is a serine residue. This slight modification in the heme pocket environment of the heme d enzymes is thought to assist in the conversion of protoheme to heme d (Murshudov *et al.* 1996). Structural coordinates (in pdb format) courtesy of PL and GM (see acknowledgments).

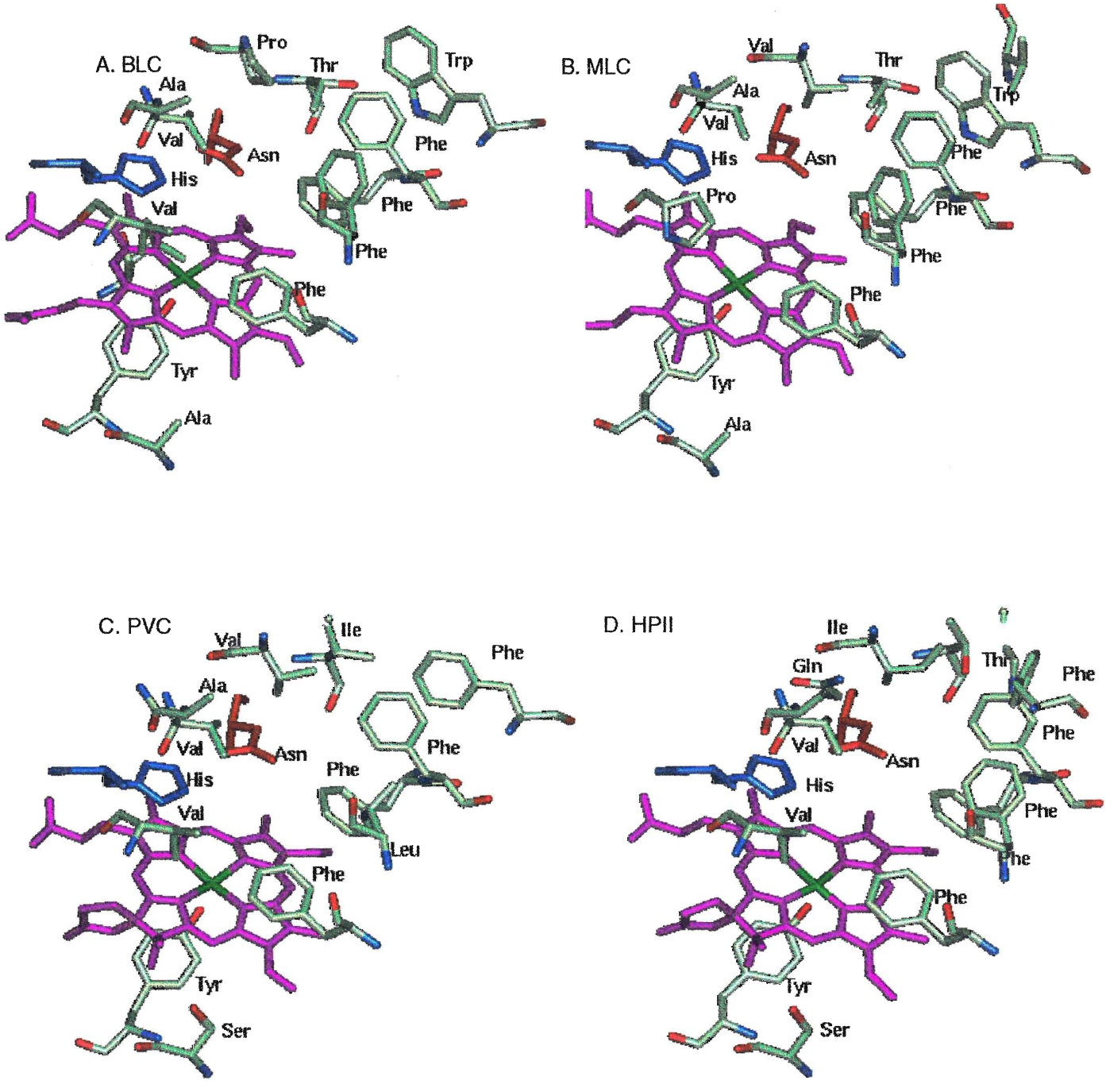
A. BLC
Pro
Thr
Trp
Ala
Val
Asn
Phe
His
Phe
Val
Phe
Phe
Tyr
Ala
B. MLC
Val
Thr
Ala
Trp
Val
Asn
His
Phe
Pro
Phe
Phe
Phe
Tyr
Ala
C. PVC
Val
Ile
Phe
Ala
Val
Asn
Phe
His
Phe
Val
Leu
Phe
Tyr
Ser
D. HPII
Ile
Gln
Thr
Phe
Phe
Val
Asn
His
Phe
Val
Phe
Phe
Tyr
Ser

Figure 36. *The heme pocket configurations of protoheme catalases*

The channel stereochemistry of (A) beef liver & B) *M. lysodeikticus* enzymes. Distal histidines are colored blue, distal asparagines are in red. Proximal tyrosines are not shown. The active site channel for MLC is partially occluded by a short stretch of backbone compared to BLC (shown in pink). Structural coordinates as in Figure 35.

A. BLC

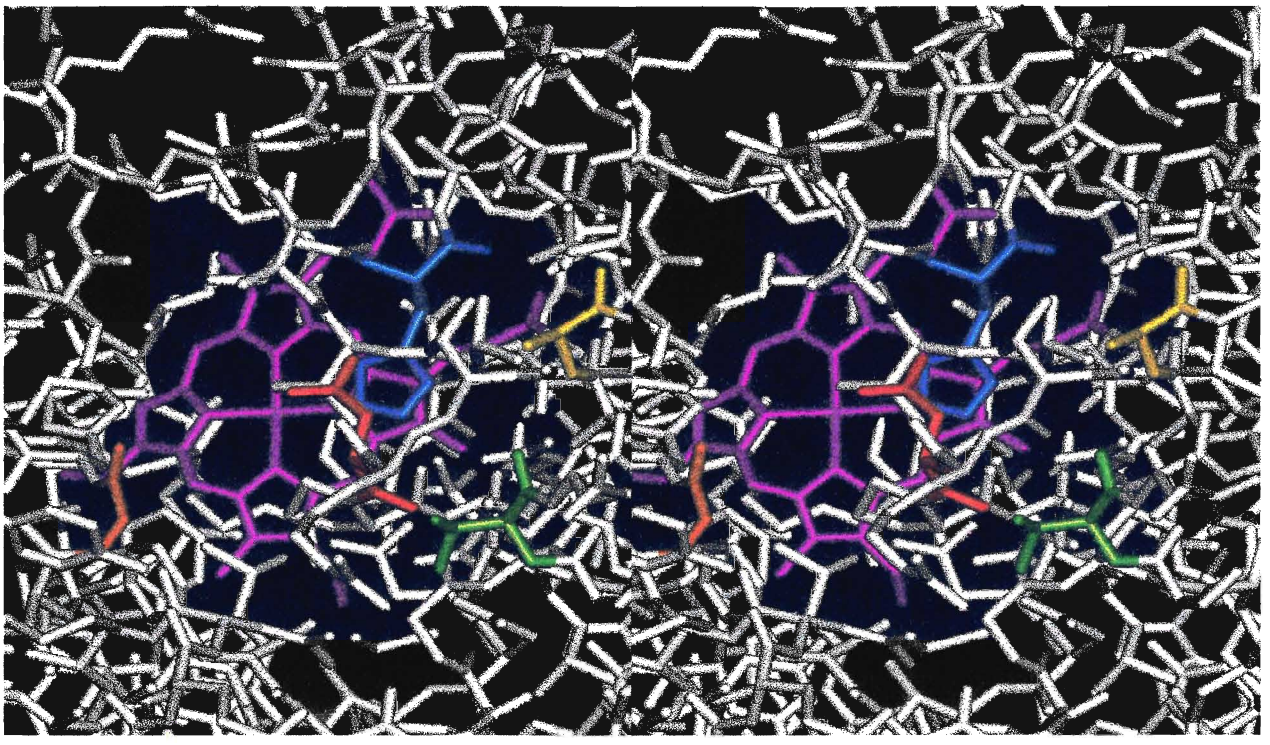

B. MLC

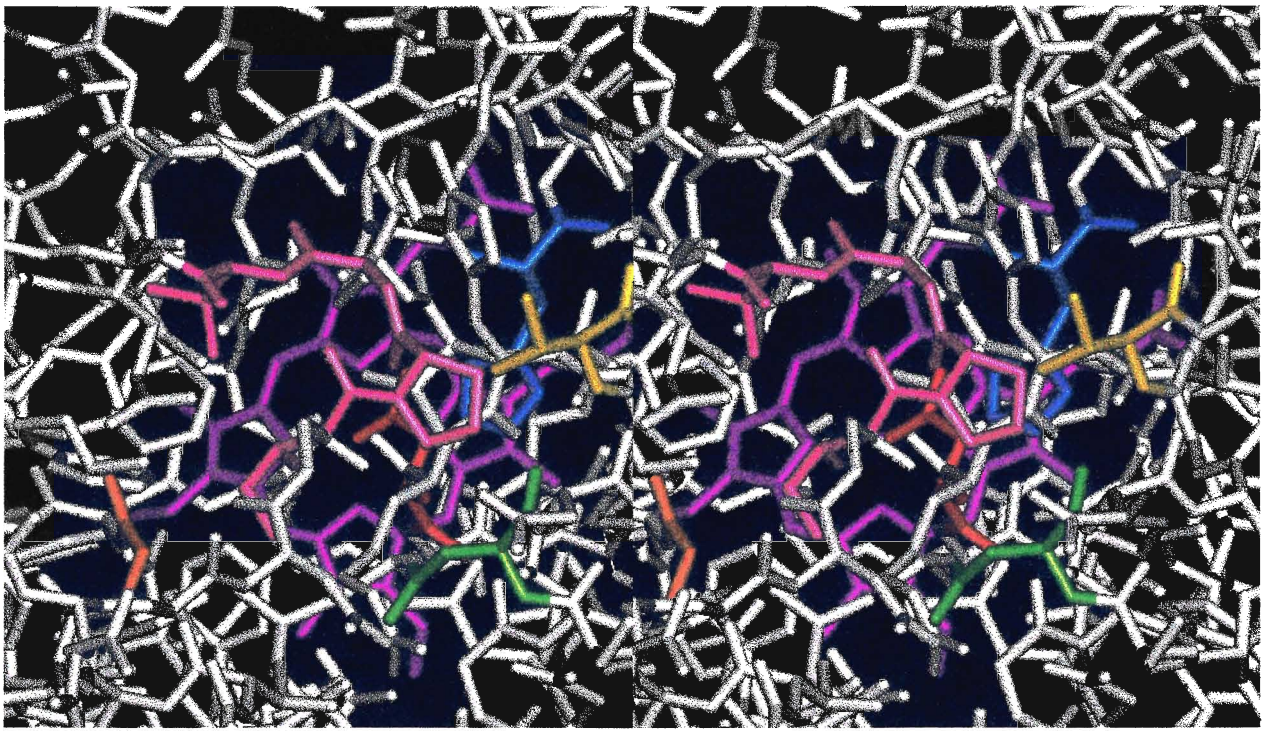

Figure 37. *The heme pocket configurations of heme$_d$ catalases*

The channel stereochemistry of A) *P. vitale* and B) *E. coli* HPII enzymes. Distal histidines are colored blue, distal asparagines are in red. Proximal tyrosines are not shown. The active site channel for PVC and HPII enzymes are partially occluded by a short stretch of backbone (shown in pink). PVC and HPII channels are further occluded by aromatic residues at the entrance of the channel (green and orange residues). Structural coordinates as in Figure 35.

. PVC

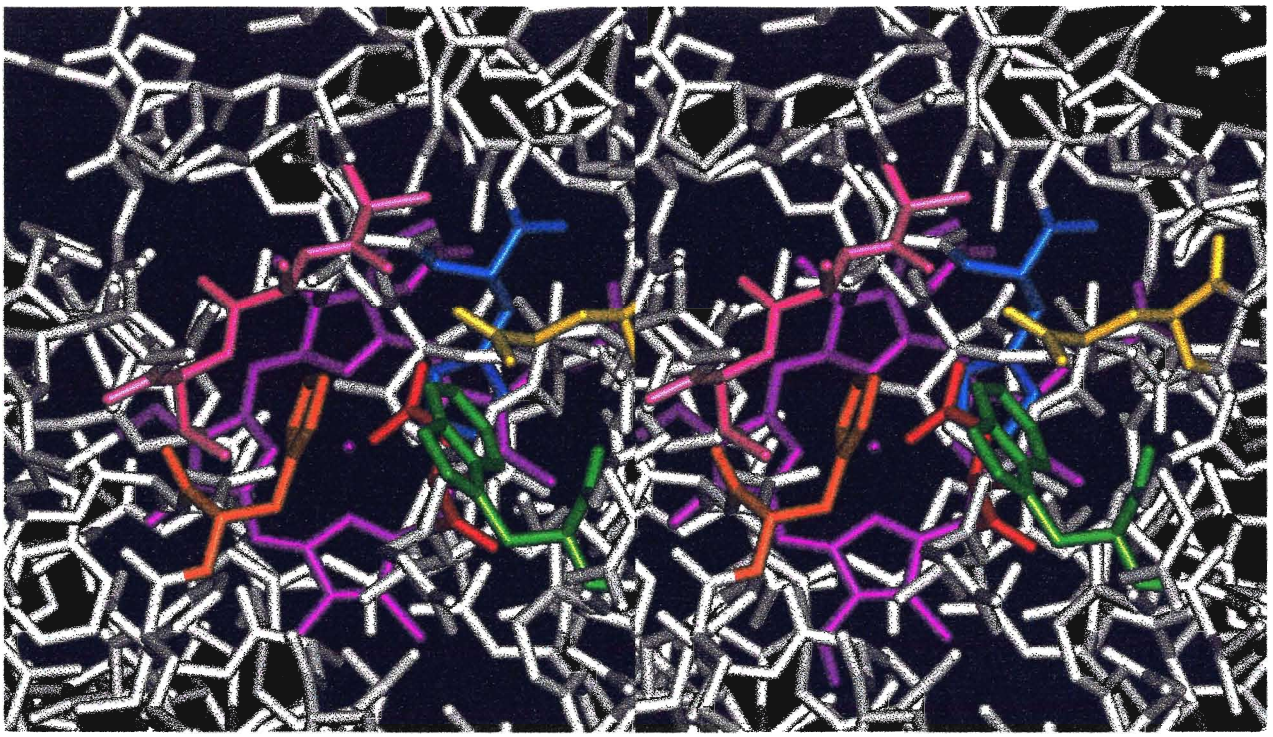

. HPII

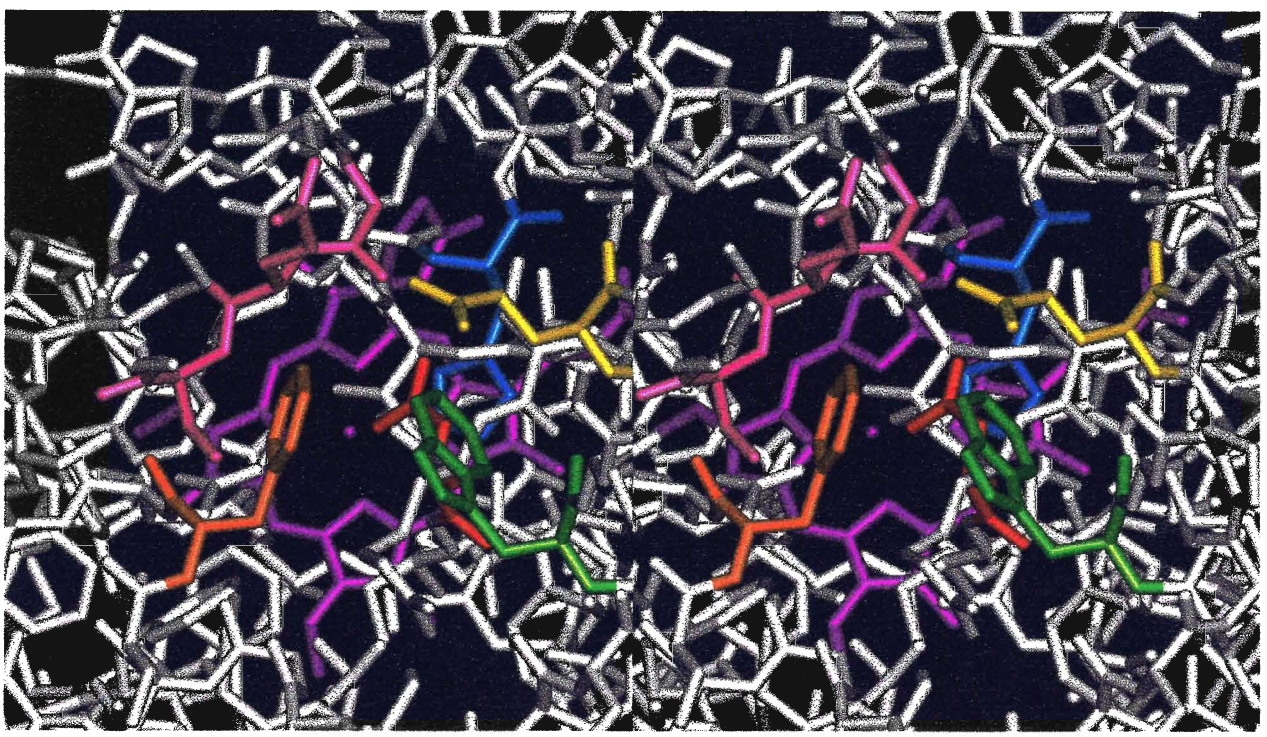

## Discussion

*pH effects*

This work confirmed the classical finding that affinities of formate and fluoride for catalases increase as the pH is lowered; and I have extended this observation to include the reactions of E. coli enzyme HPII. In contrast, the Kd values for cyanide interaction with catalase, whether from beef liver or E. coli, varied only slightly between pH 5.8 and 6.8.

*Low-spin ligand binding by catalases with different heme pocket environments*

Cyanide is a low-spin ligand which inhibits both prokaryotic and eukaryotic catalases. Protoheme, heme d and mutant enzymes have similar affinities for cyanide (Figure 38). However, cyanide has a much lower affinity for the peroxide intermediates than for the ferric enzyme (Nicholls 1961) and the heme d enzymes bind cyanide much more slowly than beef liver. These findings suggests that catalase affinity for cyanide is governed by the oxidation state of the heme iron and not by the heme pocket environment.

Resonance Raman investigation of cyanide ligated beef liver and *A. niger* catalases provides evidence that cyanide can bind with

two geometries, one a linear and the other a bent conformer. The observed heterogeneity can be attributed to H-bonding to two alternative distal residues (Al-Mustafa et al. 1995). Hydrogen bonding to the distal histidine gives rise to a linear conformer with stretching and bending frequencies at 434 and 413 cm-1. The bent conformer gives stretching and bending frequencies at 445 and 456 cm-1. The percentage of bent conformer is proportional to the percentage deprotonation of the distal histidine which becomes pronounced above pH 8. Cyanide ligation with two conformers has also been reported for horse radish peroxidase (Al-Mustafa and Kincaid 1994, Han et al. 1989).

*High-spin ligand binding by catalases with different heme pocket environments*

Fluoride binding

Fluoride binding to catalases with different heme pocket environments was explored. HPII (wild type) has a ten-fold higher affinity for fluoride than does beef liver enzyme (Figure 38). The heme d environment may provide a more polar environment favorable to the binding of fluoride. Plots of fluoride binding to the ferric forms of the bacterial catalases all show biphasic characteristics in the Soret region. Absorbance changes in the visible spectra upon binding fluoride show a single sigmoidal curve. Mutation of asparagine to glutamine decreases the affinity

of HPII for fluoride probably due to steric effects. The negative environment provided by the mutation of asparagine to aspartic acid further decreases the high-spin ligand binding affinity, with an equilibrium constant of the N201D/fluoride complex similar to that of the mammalian enzyme.

Formate binding

The structure of formic acid, in contrast to the structure of hydrofluoric acid, more closely resembles the structure of hydrogen peroxide. The affinity of the HPII wild-type enzyme for formate is less than that of the mammalian enzyme. The occlusion of the heme channel by bulky side chains may contribute to this lower formate affinity of the E coli enzyme. This may be compared with the ten-fold reduction of HPII activity compared to that of beef liver enzyme. As seen with fluoride, the glutamine and aspartic acid HPII mutants also demonstrate a decrease in their affinity for formate. The affinity of the N201D enzyme for formate is only 3% that of BLC. Equilibrium experiments performed with the bacterial mutants N201D and N201Q yielded different dissociation constants in the Soret and visible regions. The equilibrium constants in the visible region were approximately one third of those estimated from absorbance changes in the Soret region suggesting that formate is more dependent on hydrogen bonding interactions with asparagine than is fluoride.

Catalase complexes with high-spin ligands, like those with cyanide, may have two binding geometries which cannot be differentiated through absorption spectroscopy. The putative 'secondary binding conformation' appears to be spectroscopically silent with protoheme catalases and involves a 'bent ligand conformer' which is stabilized by hydrogen bonding to the distal residue asparagine (Al-Mustafa *et al.* 1995). The bent ligand conformer may no longer be spectroscopically silent with the HPII enzymes due to partial saturation of the pyrrole ring d affecting the $\pi$–$\pi^*$ transitions. The primary and secondary ligand conformers may then be resolvable in the Soret but not the visible region, as shown experimentally.

*Ligand competition*

Cyanide induced spectral changes of the catalase/formate complex support the idea that formate and cyanide are competing for a common binding site at the heme. The more cyanide present, the higher the apparent $K_d$ for formate (cf. figure 32). Mutation of the distal asparagine residue does not affect the catalase affinity for cyanide. However it does affect the enzyme affinity for high-spin ligands. The affinity for formate is more sensitive to mutation of the distal asparagine than is that of fluoride (see Figure 38) suggesting that the stabilization of formate at the active site is more dependent on the distal asparagine residue.

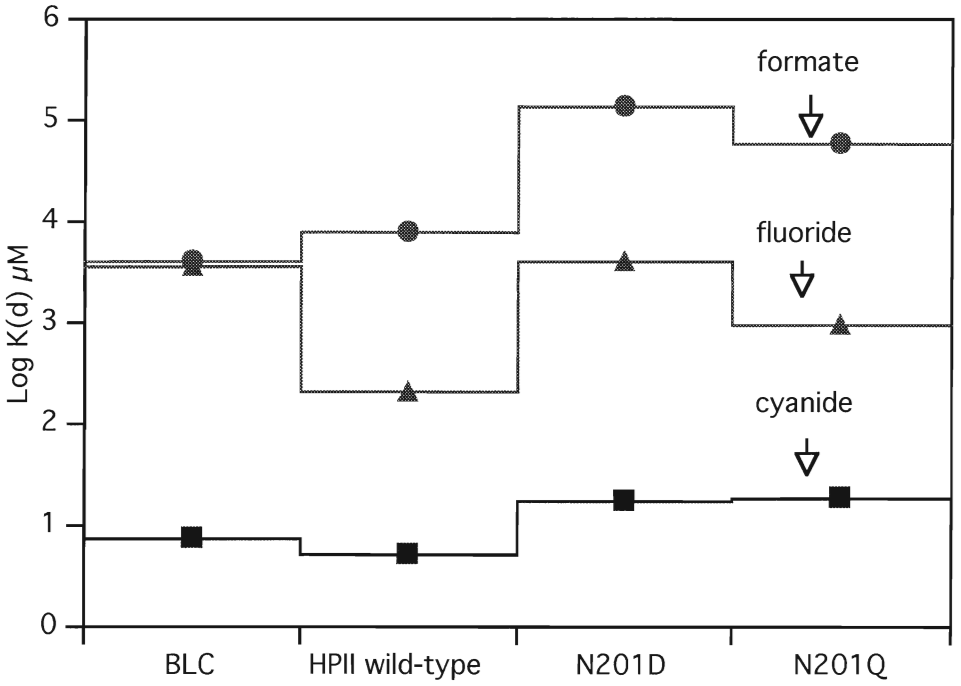


**Figure 38. Summary of catalase equilibrium constants.**

Cyanide data at pH 6.8 is presented in table D-2, formate at pH 6.8 from table 6 and fluoride data at pH 5.0 is from table 4.

The dissociation constants of catalase complexes with cyanide, fluoride and formate are presented in Figure 38. All catalases show similar affinities for the high-spin ligand cyanide, though the bacterial enzymes bind cyanide approximately 1000 times more slowly. Amino acids distal to the heme govern high-spin ligand complex formation as shown as shown for the reduced affinity the mutant enzymes have for fluoride and formate. Both fluoride and formate binding are more sensitive to changes of the electrostatic environment than to steric modifications of the active site.

*High-spin ligand binding by catalase peroxide compounds*

Fluoride binding

It is shown here that ferric catalase, compound I and compound II all have the same affinity for fluoride, in agreement with the observations of Nicholls (1961) on the horse liver enzyme. Though fluoride is thermodynamically incapable of directly reducing compound I or II, it accelerates the rate of the endogenous 1-electron reductions of the compound I and compound II approximately ten and 100-fold respectively (cf. Nicholls, 1961). Similar affinities of the various oxidation states of catalase for fluoride suggest that fluoride binding is governed by the heme pocket environment and stabilized by distal residues. Because of their closeness to the heme iron, and their importance in the stabilization of substrate at the active site, the distal residues involved are probably his-74 and asn-147.

The spontaneous accumulation of compound II, accelerated by ligand anions, leads to inactivation of the enzyme. Bound NADPH may play a protective role in preventing the accumulation of compound II and associated enzyme inactivation (Kirkman *et al.* 1987, Hillar et al., 1994). The electron tunneling pathway from NADPH to the porphyrin ring has been the topic of much debate. Almarsson and co-workers (1993) have

proposed an electron tunneling path from NADPH through the protein to the heme porphyrin using the x-ray geometry of BLC and probable functional groups which could play the role required. They suggest that an electron will jump from NADPH to pro150 and transfer to thr149. An electron will jump from thr-149 to the distal residue asn147. The electron will then jump to the vinyl substituent of pyrole ring c.

If the binding of fluoride tightens the bonding network and increases the order of interactions upon forming a complex, then the binding of HF will assist in shortening of the pathway of electron tunneling, thereby increasing the rate of compound I and II reduction. This pro-thr-asn region is conserved in NADPH binding catalases which have been sequenced (cf. appendix A). and the spatial organization of this region for BLC, MLC and PMC enzymes are the same.

Formate binding

Not only does formate act as a high-spin ligand for the ferric enzyme, it also can act as both a two electron donor to compound I as well as a catalyst for the decomposition of compound II. In contrast to reported values by Nicholls 1961, compound II showed 10X lower affinity for formate than did catalase in the ferric state. Compound II does not directly oxidize formate as does compound I. The limiting step for formate association with and

subsequent reduction of compound II must involve interaction with the endogenous donor.

*Comparisons with cytochrome c peroxidase*

Thermodynamic investigation of cyanide and fluoride binding to cytochrome c peroxidase (CcP) by DeLauder and coworkers (1994) indicate that the binding enthalpy is significantly more positive for HCN (-48.6+-1.8 at pH 5.0) than for HF (-67.0+-1.9 at pH 5.0). They propose that the more negative values for fluoride reflect a stronger interaction between the distal residue arg-48 and fluoride in the HF-CcP complex. Crystallographic studies by Edwards and Poulos (1990) which compared the crystal structures of CcP complexes with cyanide and with fluoride demonstrated that the distal residue arg-48 moves towards the bound fluoride to form a strong interaction as contrasted with the movement of this side chain away from bound HCN. This suggests that there is a tight binding network and stronger, more ordered interactions in the HF-CcP complex than with the HCN-CcP complex . By analogy, the asn-147 residue of beef liver catalase may also form tight binding and strong more ordered interactions in the HF/catalase complex which may assist the electron tunneling pathway in the endogenous donor reaction.

## Conclusions

1. High-spin ligand binding and site-directed mutagenesis can be used to probe active sites in beef liver (protoheme) and *E. coli* HPII (heme d) catalases.

2. The conjugated porphyrin ring of heme d HPII is more saturated than the protoheme of beef liver catalase. This saturation of the porphyrin ring may lead to different energies between the $t_2g$ and eg d-orbitals of the high-spin heme iron, leading to high-spin ligand affinities of HPII being different from those of the beef liver enzyme.

3. HPII has a higher affinity for fluoride than does beef liver catalase. The heme d pocket may provide a more polar environment favorable to fluoride binding.

4. Formic acid, unlike fluoride, structurally resembles hydrogen peroxide. HPII wild-type and mutants have lower affinities for HCOOH than the mammalian enzyme. The occlusion of the heme channel by bulky side chains may contribute to a lower activity and formate affinity of the *E. coli* enzymes.

5. Beef liver catalase and its peroxide compounds I and II have similar affinities for fluoride. Fluoride cannot directly reduce compound I or II, but accelerates the endogenous 1-electron reduction rates of the compounds approximately 10- and 100-fold

respectively. Similar affinities of the various oxidation states of the beef liver enzyme for fluoride suggest that fluoride binding is determined by residues in the heme pocket rather than the redox state of the heme iron.

6. Formate, a high-spin ligand for ferric beef liver catalase, is a 2-electron donor to compound I and a catalyst for compound II decomposition. The rates of formate association with and subsequent reduction of compounds I and II are also controlled by heme pocket residues rather than by the oxidation state of the heme iron.

## Literature Cited

Almarsson, O. & Bruice, T. C., (1993) Journal of the American Chemical Society, **115**, 2125-2138.

Al-Mustafa J. & Kincaid JR (1994) Biochemistry **33**, 2191-2197,

Al-Mustafu, J., Sykora, M. & Kincaid, J. R., (1995) Resonance raman investigation of cyanide ligated beef liver and Aspergillus niger catalases. The Journal of Biological Chemistry. **270**, 18, pp. 10449-10460.

Albers, H. Z., (1933) Zeitschrift fur Physiologisches Chemie. **218**, p. 113.

Andersson, L. A., Johnson, A. K., Simms, M. D. & Willingham, T. R., (1995) Comparative analysis of catalases: Spectral evidence against heme-bound water for the solution enzymes. Federation of European Microbiological Societies Microbiology Letters, **370**, pp. 97-100.

Beers, R. F. & Sizer, I. W., (1952) A spectroscopic method for measuring the breakdown of hydrogen peroxide by catalase. Journal of Biological Chemistry. **195**, pp 133-140.

Bengal, R., Momemteau, M. & Meunier, B., (1989) Why an oxygen and not a nitrogen atom as proximal ligand in catalase? Hydrogen peroxide dismutation catalyzed by synthetic iron and manganese porphyrins. New Journal of Chemistry, **13**, 12, pp. 853-862.

Bonnichsen, R. K., Chance, B. & Theorell, H., (1947) Catalase activity. Acta Chemica Scandinavica **1**, pp. 685-709.

Boveris, A., Oshino, N. & Chance, B., (1972) The cellular production of hydrogen peroxide Biochemical Journal **128**, 617-630.

Bravo, J., Verdaquer, N., Tormo, J., Betzel, C., Switala, J., Loewen, P. C. & Fita, I., (1995) Crystal structure of catalase HPII from *Escherichia coli* Structure. **3**, 491-502.

Brill, A. S. & Williams, R. J. P., (1961) Primary compounds of catalase and peroxidase, Biochemical Journal, **78**, pp 253-262.

Brill, A. S. (1966) In: Biological oxidation. edited by M Florkin and E. H. Stotz., New York, Elsevier vol **14**, pp. 447-479.

Cerutti, P. A. (1985) Science. **227**, pp. 375-381.

Chance, B., (1947a) Review of Scientific instrumentation, **68**, 601.

Chance, B., (1947b) An intermediate compound in the catalase-hydrogen peroxide reaction. Acta Chemica Scandinavica **1,** pp 236-267.

Chance, B., (1948) The enzyme-substrate compounds of catalase and peroxides, Nature (London) **161**, pp. 914-917.

Chance, B., (1949a) The primary and secondary compounds of catalase and methyl or ethyl hydrogen peroxide I. Spectra. The Journal of Biological Chemistry. **179,** 1311-1329

Chance, B., (1949b) The primary and secondary compounds of catalase and methyl or ethyl hydrogen peroxide II. Kinetics and activity. The Journal of Biological Chemistry. **179,** 3, pp. 1341-1369.

Chance, B. & Herbert, D., (1950) The enzyme-substrate compounds of bacterial catalase and peroxides. The Journal of Biological Chemistry. **4**, 46, pp. 402-414.

Chance, B., (1950a) On the reaction of catalase peroxides with acceptors. The Journal of Biological Chemistry, **182**, 2, pp. 649-658.

Chance, B., (1950b) The reactions of catalase in the presence of the notatin system. Biochemical Journal, **46**, pp. 387-402.

Chance, B., Greenstein, D. S., Higgins, J. & Yang, C. C., (1952a) The mechanism of catalase action. II. Electric analog computer studies. Archives of Biochemistry and Biophysics. **37**, 2, pp 321-339.

Chance, B., Greenstein, D. S., Higgins, J. & Yang, C. C., (1952b) The mechanism of catalase action. I. Steady-state analysis. Archives of Biochemistry and Biophysics. **37**, 2, pp 301-321.

Chance, B., (1952a) The spectra of the enzyme-substrate complexes of catalase and peroxidase. Archives of Biochemistry and Biophysics, **41**, pp 404-415

Chance, B.,(1952b) The effect of pH upon the equilibria of catalase compounds. The Journal of Biological Chemistry. **194,** 2, pp 483-496.

Chance, B., Sies, H. & Boveris, A., (1979) Physiological Review. **59**, pp. 527-605.

Chance, B., Powers, L., Ching, Y., Poulos, T., Schonbaum, G. R., Yamazaki, I. & Paul, K. G., (1984) X-ray absorption studies of intermediates in peroxidase activity. Archives of Biochemistry and Biophysics, **235**, pp. 596-611.

Chiu, J. T. Loewen, P. C., Switala, J., Gennis, R. B. & Timkovich, R., (1989) Proposed structure for the prosthetic group of the catalase HPII from *Escherichia coli*. **111**, pp. 7046-7050.

Claiborne, A. & Fridovich, I., (1979) Purification of the o-dianisidine peroxidase from *Escherichia coli* B. Physicochemical characterization and analysis of its dual catalatic and peroxidatic activities. Journal of Biological Chemistry, **254**, pp. 4245-4252.

Conner, H. D., Gao, G., Lemasters, J. J., Mason, R. P. & Thurman, R. G., (1992) Free radicals are involves in graft failure following orthotopic liver transplantation : an EPR spin trapping study. Transplantation, **54**, pp 199-204.

Coryell, C. D., Stitt, F. & Pauling, L., (1937) The magnetic properties and structure of ferrihemoglobin (methemoglobin) and some of its compounds, Journal of the American Chemical society, **59**, 633-642.

Darley-Usmar, V. M., Mason, R. P., Chamulitrat, W., Hogg, N. & Kalyanaraman, B., (1995) Lipid peroxidation and cardiovascular disease. Immunopharmacology of free radical species. pp 23-27.

Dawson, J. H., Bracete, A. M., Huff, A. M, Kadkhodayan, S., Zeitler, C. M., Sono, M., Chang, C. K. & Loewen, P. C., (1991) Federation of European Microbiological Societies Microbiology Letters, **295,** 1,2,3, pp. 123-126.

de Duve, C., (1965) The separation and characterization of subcellular particles. Harvey Lectures **ser 59**, pp. 49-87.

del Rio, L. A., Sandalio, L. M., Palma, J. M., Bueno, P. & Corpas, F. J., (1992) Metabolism of oxygen radicals in peroxisomes and cellular implications. Free Radical Biology and Medicine. **13**, pp. 557-580.

De Lauder, S. F., Mauro, J. M., Poulos, T. L., Williams, J. C. & Schwarz, F. P., (1994) Thermodynamics of hydrogen cyanide and Hydrogen fluoride binding to cytochrome *c* peroxidase and its Asn-82->Asp mutant. Biochemical Journal, **302**, 437-442.

Deisseroth, A. & Dounce, A. L., (1970) Catalase: Physical and chemical properties, mechanism of catalysis, and physiological role. Physiological Reviews. **50**, 3, pp. 319-375.

Deutsch, H. F. & Ehrenberg, A., (1952) The magnetic properties of crystalline horse erythrocyte catalase and some of its derivatives. Acta Chemica Scandinavica, **6**, 1522-1527.

Dolphin, D., Forman, A., Borg, D. C., Fajer, J. & Felton. R. H., (1971) Compounds I of catalase and horse radish peroxidase: π-cation radicals. Proceedings of the National Academy of Sciences. &, 3, pp. 614-618.

Eaton, J. W., Boraas, M. & Etkin, N. L., (1972) Catalase activity and red cell metabolism. In: (N. Taylor ed.) Advances in experimental Medicine and Biology. **28**, pp. 68-72.

Edwards, S. L. & Poulos, T. L., (1990) Ligand binding and structural perturbations in cytochrome c peroxidase. A crystallographic study. Journal of Biological Chemistry, **265**, 2588-2595.

Fita, I. & Rossman, M. G., (1985a) The NADPH binding site on beef liver catalase. Proceedings of the National Academy of Science, USA. **82**, pp. 1604-1608.

Fita, I. & Rossman, M. G., (1985b) The active center of catalase. Journal of Molecular Biology. **185**, pp. 21-37.

Fita, I, Silva, A. M., Murthy, M. R. N. & Rossmann, M. G., (1986) The refined structure of beef liver catalase at 2.5 Angstroms resolution. Acta Crystallographica. Sect. B , **42**, p. 497.

Furuta, S., Hayashi, H., Hijikata, M., Miyazawa, S., Osumi, T. & Hashimoto, T., (1986) Complete nucleotide sequence of cDNA and deduced amino acid sequence of rat liver catalase. Proceedings of the National Academy of Science USA, **83**, pp. 313-317.

George, P., (1953) Biochemical Journal, **55**, p. 220.

Gouet, P., Jouve, H. M. & Dideburg, O., (1995) Crystal structure of *Proteus mirabilis* PR catalase with and without bound NADPH. Journal of Molecular Biology. **249**, pp. 933-954.

Greenwald, R. A., (1990) Superoxide dismutase and catalase as therapeutic agents for human diseases. Free Radical Biology and Medicine. **8**, pp. 201-209.

Han, S., Madden, J. F., Siegen, I. M. & Spiro, T. G. (1989) Biochemistry **28,** 5477-5485.

Hansson, M. &von Wachenfeldt, C., (1993) Heme b (protoheme IX) is a precursor of heme a and heme d in *Bacillus subtilis*. Federation of European Microbiological Societies Microbiology Letters, **107,** 121-126.

Hartree, E. F., (1946) Magnetic properties of haematin derivatives. Annual reports of the Chemical Society **43**, pp287-296

Hartree, E. F., (1947) Biochemistry: Magnetic properties of haematin derivatives. Annual Reports of the Chemical Society for 1946, Vol **43**, pp287-296.

Heimberger, A. & Eisenstark, A., (1988) Compartmentalization of catalases in *Escherichia coli.* Biochemical and Biophysical Research Communication, **154**, 392-397.

Hillar, A., Nicholls, P., Switala, J. & Loewen, P. C., (1994) NADPH binding and control of catalase compound II formation: comparison of bovine, yeast, and *Escherichia coli* enzymes. Biochemical Journal. **300**, pp. 531-539.

Hildebrand, D. P., Burk, D. L., Maurus, R., Ferrer, J. C., Brayer, G. D. & Mauk, A. G., (1995) The proximal ligand variant his93tyr of horse heart myoglobin. Biochemical Journal, **34**, pp. 1997-2005.

Hodgson, E. K. & Fridovich, I., (1975) Biochemistry, **14**, 5294-5299.

Holland, H. D., (1984) Oxygen in the Precambrian atmosphere: Evidence from terrestrial Environment In: *The chemical evolution of the atmosphere and oceans*, Princeton University Press, Princeton New Jersey, pp 277-440.

Igual, J. C., Gonzalez-Bosch, Dopazo, J. & Perez-Ortin, J. E., (1992) Phylogenetic analysis of the thiolase family. Implications for the evolutionary origin of peroxisomes. Journal of Molecular Evolution. **35,** pp. 147-155.

Jacob, G. S. & Orme-Johnson, W. H. (1979) Catalase of *Neurospora crassa*. 1. Induction, purification and physical properties. American Chemical Society. **18,** 14, 2967-2975.

Jones, P. & Middlemiss, D. N., (1972) Formation of compound I by the reaction of catalase with peroxoacetic acid. Biochemical Journal. **130**, pp 411-415.

Jones, P. & Willet, P. (1995) Docking small-molecule ligands into active sites. Current Opinion in Biotechnology. **6,** pp. 652-656.

Jouve, H. M., Beaumont, F., Leger, I., Foray, J. & Pelmont, J., (1989) Tightly bound NADPH in *Proteus mirablis* PR catalase. Biochemistry and Cell Biology. **221**, pp. 1075-1077.

Keilin, D. & Hartree, E. F., (1935) Proceedings of the Royal Society, **B117**, pp. 1-15.

Keilin, D. & Hartree, E. F., (1936a) Proceedings of the Royal Society, **B119**, 141.

Keilin, D. & Hartree, E. F., (1936b) On some properties of catalase haematin. Proceedings of the Royal Society. **B121**, pp. 173-191.

Keilin, D. & Hartree, E. F., (1951) Purification of horse-radish peroxidase and comparison of its properties with those of catalase and methaemoglobin. Biochemical Journal, **49**, pp. 88.

Keilin, G. & Hartree, E. F., (1955) Catalase, peroxidase and metmyoglobin as catalysts of coupled peroxidatic reactions. Biochemical Journal. **60**, pp. 310-325.

Keilin, D. & Nicholls, P., (1958) Reactions of catalase with hydrogen peroxide and hydrogen donors. Biochimica et Biophysica Acta, **29,** 302-307.

Kirkman, H. N. & Gaetani, G. F., (1984) Catalase: A tetrameric enzyme with four tightly bound molecules of NADPH. Proceedings of the National Academy of Sciences USA. **81**, pp. 4343-4348.

Kirkman, H. N., Galiano, S. & Gaetani, G. F., (1987) The function of catalase-bound NADPH. Journal of Biological Chemistry. **262**, 2, pp. 660-666.

Kono, Y. & Fridovich, I., (1982) Superoxide radical inhibits catalase. The Journal of Biological Chemistry, **257**, 10, pp. 5751-5754.)

Kragler, F., Langender, A., Raupachova, J., Binder, M. & Hartig, A., (1993) Two independent peroxisomal targeting signals in catalase A of *Saccharomyces cerevisiae*. The Journal of Cell Biology. **120**, 3, pp. 665-673.

Lardinois, O. M. (1995) Reactions of bovine liver catalase with superoxide radicals and hydrogen peroxide. Free Radical Research, **22**, 3, pp. 251-274.

Linde, D. R. (1990a) CRC Handbook of Chemistry and Physics. 71st edition, CRC Press, Boca Raton, p. 8-37.

Linde, D. R. (1990b) CRC Handbook of Chemistry and Physics. 71st edition, CRC Press, Boca Raton, p. 8-36.

Loew, O., (1901) U. S. Department of Agricultural Reports No. **68**, p. 47.

Loewen, P. C., Switala, J. & Triggs-Baine, B. L., (1985) Catalases HPI and HPII in *Eschericia coli* are induced independently. Archives of Biochemistry and Biophysics. **243**, 1, pp. 144-149.

Loewen, P. C. & Switala, J., (1986) Purification and characterization of catalase HPII from *Escherichia coli* K12. Biochemical Cell Biology, **64,** pp. 638-646.

Loewen, P. C., Switala, J., von Ossowski, I., Hillar, A., Christie, A., Tattrie, B. & Nicholls. P., (1993) Catalase HPII of *Escherichia coli* catalyzes the conversion of protoheme to cis-heme d. Biochemistry, **32**, pp. 10159-10164.

Luft, R., (1994) Proceedings of the National Academy of Science. **91**, 8731-8738.

Lybrand, T. P. (1995) Ligand-protein docking and rational drug design. Current Opinion in Structural Biology. **4,** pp. 224-228.

Maeda, Y. & Morita, Y., (1968) In: *Structure and function of cytochromes,* (K. Okunuki, M. D. Kamen, I. Sekuzu eds.) University of Tokyo Press, p. 523.

Maj, M., (1994) B. Sc. Hons Thesis.

Maj, M., Nicholls, P., Obinger, C., Hillar, A. & Loewen, P., (1996) Reaction of *E coli* catalase HPII with cyanide as ligand and as inhibitor, BBA, in preparation.

McCormick, J.P., Fischer, J. R., Pachlatki, J. P. & Eisenstark, A. A. (1976) Characterization of a cell-lethal product from the photooxidation of tryptophan: hydrogen peroxide. Science **191**: 468-469.

Melik-Adamyan, W. R., Baryin, V. V., Vagin, A. A., Borisov, V. V., Vainshtein, B. K., Fita, I., Murthy, M. R. N. & Rossman, M. G., (1986) Comparison of beef liver and *Penicillium vitale* catalases. Journal of Molecular Biology, **188**, pp. 63-72.

Murthy, M. R. N., Reid T. J., Sicignano, A., Tanaka, N. & Rossmann, M. G, (1981) Structure of beef liver catalase. Journal of Molecular Biology, **152**, p. 465.

Murshudov, G. N., Grebenko, A. I., Barynin, V., Dauter, Z., Wilson, K. S., Vainshtein, B. K., Melik-Adamyan, W., Bravo, J., Ferran, J. M. Ferrer, J. C., Switala, J., Loewen, P. C. & Fita, I., (1996) Structure of the heme d of *Penicillium vitale* and *Escherichia coli* catalases. Journal of Biological Chemistry. 271, **15**, pp. 8863-8868.

Murshudov, G. N., Melik-Adamyan, W. R., Grebenko, A. I., Barynin, V. V., Vagin, A. A., Vainshtein, B. K., Dauter, Z. & Wilson, K. S., (1992) Three-dimensional structure of catalase from *Micrococcus lysodeikticus* at 1.5 A resolution. Federation of European Biochemical Societies. **312**, 2, 3, pp. 127-131.

Nicholls, P., (1961) The action of anions on catalase peroxide compounds. Biochemical Journal, **81**, 635-374.

Nicholls, P. & Schonbaum, G. R., (1963) Catalases. In: (Lardy et al, eds.) *The Enzymes*, vol. 2, pp. 147-222. Academic Press, New York.

Nicholls, P., (1965) Activity of catalase in the red cell, Biochimica et Biophysica Acta, **99**, pp. 286-297.

Olson, L. P. & Bruice, T. C., (1995) Electron tunneling and *ab Initio* calculations related to the one-electron oxidation of NAD(P)H bound to catalase, Biochemistry, **34**, 7335-7347.

Oshino, N., Chance, B. & Sies, H., (1973) The properties of the secondary catalase-peroxide complex (compound II) in the hemoglobin-free perfused rat liver. Archives of Biochemistry and Biophysics, **159,** pp. 704-711.

Plaine, H.L. (1955) The effect of oxygen and of hydrogen peroxide on the action of a specific gene and on tumor induction in *Drosophila melanogaster*. Genetics **40**: 268-280.

Reid, T. J., Murthy, M. R. N., Sicignano, A., Tanaka, N., Musick, W. D. L. & Rossman, M. G., (1981) Structure and heme environment of beef liver catalase at 2.5 Å resolution. Proceedings of the National Academy of Science, USA. 28, **8**, pp. 4767-4771.

Robert, A., Loock, B., Momenteau, M. & Meunier, B., (1991) Catalase modeling with metalloporphyrin complexes having an oxygen ligand in a proximal position. Comparison with complexes containing a proximal nitrogen. Inorganic Chemistry. **30**, pp. 706-711.

Rocha, E. R. & Smith, C. J., (1995) Biochemical and genetic analysis of a catalase from the anaerobic bacterium *Bacteroides fragilis*. Journal of Bacteriology. 177, **11**, pp. 3111-3119.

Sanders, B. C., Holmes-Siedle, A. G. & Stark, B. P., (1964) Peroxidase. Washington, D. C.: Butterworths, pp 114-119.)

Shakhnovich, E. I. (1996) Modeling protein folding: the beauty and power of simplicity. Folding & Design. **1**, R00-R00.

Sharma, K. D., Andersson, L. A. & Loehr, T. M., (1989) Comparative spectral analysis of mammalian, fungal, and bacterial catalases. The Journal of Biological Chemistry. **264,** 22, pp. 12772-12779.

Shimizu, N., Kobayashi, K. & Hayashi, K., (1984) The reaction of superoxide radical with catalase. Mechanism of the inhibition of catalase by superoxide radical. The Journal of Biological Chemistry. **259**, pp. 4414-4418.

Sies, H., Bucher,T., Oshino, N. & Chance, B., (1973) Heme occupancy of catalase in hemoglobin-free perfused rat liver and of Isolated rat liver catalase Archives of biochemistry and biophysics **154**, 106-116.

Sies, H., (1993) Strategies of antioxidant defense. European Journal of Biochemistry. **215**, pp. 213-219.

Schonbaum, G. R. & Chance, B. (1976) Catalase. In: (Boyer, P. D. ed.) *The Enzymes*, vol. XIII pt. C, third edition. pp. 363-408. Academic Press, London.

Simon, R.H., C.H. Scoggin, & D. Patterson. (1981). Hydrogen peroxide causes the fatal injury to human fibroblasts exposed to oxygen radicals. Journal of Biological Chemistry. **256**: 7181-7186.

Sohol, R. S., Agarwal, S. & Orr, W. C. (1995) Simultaneous overexpression of copper and zinc-containing superoxide dismutase and catalase retards age-related oxidative damage and increases metabolic potential in *Drosophila melanogaster*. Journal of Biological Chemistry. **270**, 26, p. 15671.

Stern, K. G. (1936) On the mechanism of enzyme action. A study of the decomposition of monoethyl hydrogen peroxide by catalase and of an intermediate enzyme-substrate compound. Journal of Biological Chemistry **114**, pp 473-494.

Stoll, V. S., Kimber, M. S. & Pai, E. F. (1996) Insights into substrate binding by D-2-ketoacid dehydrogenases from the structure of *Lactobacillus pentosus* D-lactate dehydrogenase. Structure. **4,** 437-447.

Sumner, J. B. & Dounce, A. L. (1937) Crystalline catalase. Journal of Biological Chemistry **121**, pp. 417-424.

Szelgi, G., Herold, A., Negut, E., Bucurenge, N., Mazilu, E., Arion, R., Dejiga, D., Turganu, L., Golea, C., Sima, I., Alexianu, D., Chirila, M., Tansanu, I. & Strat, A., (1986) Clinical efficacy of a new anti inflammatory drug with free radicals scavenging properties: superoxide dismutase and catalase of human origin. Arch. Roum. Path. Exp. Microbiol. **45**, pp. 299-310.

Theorell, H. & Agner, K., (1943) Magnetic and other properties of horse liver catalase and derivatives. Arkiv For Kemi Mineralogi Geologi, **16A,** PP. 1-14.

Theorell, H., & Ehrenberg, A., (1952) Magnetic properties of some peroxide compounds of myoglobin, peroxidase and catalase, Archives of Biochemistry and Biophysics, **41**, pp443-461.

Timkovich, R. & Bondoc, L. L., (1990) Diversity in the structure of the hemes, Advances in Biophysical Chemistry. **1,** pp. 203-247.

Tolbert, N. E. & Essner, E., (1981) Microbodies: peroxisomes and glyoxysomes. Journal of Cell Biology. **91**, pp. 271s-283s.

Toyokuni, S., Okamoto, K., Yodoi, J., & Hiai, H. (1995) Persistent oxidative stress in cancer. Federation of European Microbiological Societies Microbiology Letters. **358**, 1-3.

Tullis, T. D., (1987) Chemical 'snapshots' of DNA: using the hydroxyl radical to study the structure of DNA and DNA-protein complexes. Trends in Biochemical Sciences. **12**, 8, pp. 297-300.

Vainshtein, R. K., Melick-Adamyan, W. R., Baryin, V. V., Vagin, A. A. & Rossmann, M. G. (1986) Three-dimensional structure of catalase from *Penicillium vitale* at 2.0 Å resolution. Journal of Molecular Biology. **188**, pp. 49-61.

Varva, M. K., Timkovich, R., Yap, F. & Gennis, R. B., (1986) Spectroscopic studies on heme d in the visible and infrared. Archives of Biochemistry and Biophysics. **250**, pp. 461-468.

Veizer, J., (1983) Geological evolution of the Archean-early Proterozoic earth, In: Earths earliest biosphere, (ed. J. William Schopf) Princeton University Press, Princeton New Jersey, pp 240-259.

von Ossowski, I., Mulvey, M. R., Leco, P. A., Borys, A. & Loewen, P. C., (1991) Nucleotide sequence of *Escherichia coli* katE, which encodes catalase HPII. Journal of Bacteriology. **173**, 2, pp. 514-520.

von Ossowski, I., Hausner, G. & Loewen, P. C., (1993) Molecular evolutionary analysis based on the amino acid sequence of catalase. Journal of Molecular Evolution, **37**: 71-76.

Walker, J. C. G., Klein, C., Schidlowski, M., Schopf, J. W., Stevenson, D. J., & Walter, M. R., (1983) Environmental evolution of the Archean-early Proterozoic earth, In: Earths earliest

biosphere. Princeton University Press, Princeton New Jersey, pp 260-268.

Zamoky, M., Herzog, C., Nykyri, L. M. & Koller, F., (1995) Site directed mutagenesis of the lower parts of the major substrate channel of yeast catalase A leads to highly increased peroxidatic activity. Federation of European Microbiological Societies Microbiology Letters, **367**, pp. 241-245.

Zeile, K., Hellstrom, H., (1930) Zeitschrift fur Physiologisches Chemie. **192**, p. 171.

Zigler, J.S., Jr., Jernigan, H.M., Garland, D. & Reddy, V.N. (1985) The effects of "oxygen radicals" generated in the medium on lenses in organ culture: inhibition of damage by chelated iron. Archives of Biochemistry and Biophysics **241**, pp. 163-172.

# Appendix A - Sequence alignment of 30 catalases

## Table A-1. Aligned sequences of 30 catalases.

```
                    10        20        30        40        50        60        70        80        90
                     .         .         .       *.        h.         .         .         .         .
PORYSA     TTTTNAGAPV WNDNEALTVG PRGPILLEDY HLIEKVAHFA RERIPERVVH,ARGASAKGFF ECTHDVTDIT CADFLRSPGA QTPVIVRFST
PPEA       FWTTNSGAPV WNNNSSLTVG SRGPILLEDY HLVEKLAQFD RERIPERVVH ARGASAKGFF EVTHDISHLT CADFLRAPGV QTPVIVRFST
PPHAAU     FWTTNSGAPV WNNNNSLTVG TRGPILLEDY HLVEKLANFD RERIPERVVH ARGASAKGFF EVTHDVSHLT CADFLRAPGV QTPVIVRFST
PSOYBN     FWTTNSGAPI WNNNSSLTVG SRGPILLEDY HLVEKLANFD RERIPERVVH ARGASAKGFF EVTHDISHLT CADFLRAPGV QTPLIVRFST
PGOSH1     ---------- -NNNSSLTVG PRGQYLLEDY HLVEKLANFD RERIPERVVH ARGASAKGFF DVTHDISHLT CADFLRAPGV QTPVIVRFST
PLYCES     ---------- -NNVSSLTVG PRGPVLLEDY YLIEKLATFD REKIPERVVH ARGASAKGFF EVTHDISHLT CADFLRAPGA QTPVICRFST
PMAIZ1     ---------- -NNNSALTVG QRGPILLEDY HLIEKLAQFD RERIPERVVH ARGASAKGFF EVTHDVSHLT CADFLRAPGV QTPVIVRFST
PGOSH2     ---------- -NNNSSLTVG ARGPILLEDY HLVEKLANFD RERIPERVVH ARGASAKGFF EVTHDISQLT CADFLRAPGV QTPLIVRFST
PMAIZ2     ---------- -NNDSSLTVG ARGPILLEDY H-CEKLANFD RERIPERVVH ARGASAKGFF EVTHDITHLT CADFLRAPGV QTPVIVRFST
PMAIZ3     ---------- -NDNEALTVG PRGPILLEDY HLIEKVAHFD RERIPERVVH ARGASAKGFF ESTHDVTSLT CADFLRAPGV RTPVIVRFSQ
PARATH     ---------- -NNNSSMTVG PRGLILLEDY HLVEKLANFD RERIPERVVH ARGASAKGFF EVTHDISNLT CADFLRAPGV QTPVIVRFST
ABOVIN     ---------- -DKLNSLTVG PRGPLLVQDV VFTDEMAHFD RERIPERVVH AKGAGAFGYF EVTHDITRYS KAKVFEHIGK RTPIAVRFST
ADROME     ---------- -IKDASQTVG PRGPILLQDV NFLDEMSHFD RERIPERVVH AKGAGAFGYF EVTHDITQYC AAKIFDKVKK RTPLAVRFST
AHUMAN     VLTTGAGNPV GDKLNVITVG PRGPLLVQDV VFTDEMAHFD RERIPERVVH AKGAGAFGYF EVTHDITKYS KAKVFEHIGK KTPIAVRFST
ARAT       VLTTGGGNPI GDKLNIMTAG PRGPLLVQDV VFTDEMAHFD RERIPERVVH AKGAGAFGYF EVTHDITRYS KAKVFEHIGK RTPIAVRFST
AMOUSE     VLTTGGGNPI GDKLNIMTAG SRGPLLVQDV VFTDEMAHFD RERIPERVVH AKGAGAFGYF EVTHDITRYS KAKVFEHIGK RTPIAVRFST
FHANPO     ---------- -DSTGYKYAP PIGPLLLQDF KLIDTLSHFD RERIPERVVH AKGAGAYGVF EVTDDITDVC SAKFLDTVGK KTRIFTRFST
FCANTR     ---------- -EPFATQRVG QHGPLLLQDF NLIDSLAHFD RERIPERVVH AKGSGAYGVF EVTDDITDVC AAKFLDTVGK KTRIFTRFST
FPENJA     ---------- -ESESSLTDG DAGALLLQDI SEWDEVFRFD RLEAVERAAH AAAAAAFGAF VARGDWTASA AA-AFQAAGK QIAFMAAFST
FYEASA     VVTNSTGNPI NEPFVTQRIG EHGPLLLQDY NLIDSLAHFN RENIPQRNPH AHGSGAFGYF EVTDDITDIC GSAMFSKIGK RTKCLTRFST
FYEAST     ---------- -HPYASQYSR PDGPILLQDF HLLENIASFD RERVPERVVH AKGGGCRLEF ELTDSLSDIT YAAPYQNVGY KCPGLVRFST
BVBACS     KLTTSWGAPV GDNQNSMTAG SRGPTLIQDV HLLEKLAHFN RERVPERVVH AKGAGAHGYF EVTNDVTKYT KAAFLSEVGK RTPLFIRFST
BBACFI     KLTTNQGLKV SEDEFSLKAG ERGPTLMEDF HFREKMTHFD HERIPERIVH ARGFAAHGEF QVYDSMKEFT KAKFLQDPSV KTPVFVRFST
BPROMI     KLTTAAGAPV VDNNNVITAG PRGPMLLQDV WFLEKLAHFD REVIPERRMH AKGSGAFGTF TVTHDITKYT RAKIFSEVGK KTEMFARFST
BSTRVE     ---------- -DNQNSETAG VGGPVLVQDQ LLLEKLAHFN RERIPERVVH ARGAGAYGTF TLTRDVSRWT RAAFLSEVGK RTETFLRFST
BLACSK     QLTTNEGQPW ADNQHSQTAA NAAPSLIQDY QLLEKLAHFN RERIPERVVH AKGAGRKGYF KVTKDMSAYT KAAVFSGVGK KTPLITRFSQ
BLISSE     NLTTNQGVPI GDNQNSMTAG LKGPTLLEDY VLIEKLAHFD RERVPERVVH ARGAGAHGKF VTKKSMKKYT KAQFLQEEGT ETEVFARFST
BMICLU     ---------- -SDRESLTVG SEGPIVLHDV HLLETHQHFD RMNIPERRPH AKGSGAFGVF EVTEDVSSYT KA-LVFEPGV ETEVLLRFST
BECOLI     ALTTNQGVRI ADDQNSLRAG SRGPTLLEDF ILREKITHFD HERIPERIVH ARGSAAHGYF QPYKSLSDIT KADFLSDPNK ITPVFVRFST

                   100       110       120       130       140       150       160       170       180
                     .         .         .       À.         .         .         .         .         .
PIPOBA     VIHERGSPET IRDPRGFAVK MYTRGGNWDL VGNNFPVFFI RDGTQ----- ---------- -------LDY LSHLPESLNT FAWFYDDVGI
PORYSA     VIHERGSQET IRDPRGFAVK FYTREGNWDL LGNNFPVFFI RDGIK----- ---------- -------FDF LSHHPESLHT FFFLFDDVGI
PPEA       VIHERGSPET LRDPRGFAVK FYTREGNYDL VGNNFPVFFV HDGMN----- ---------- -------LDF FYNFPESLHM FSFLFDDVGV
PPHAAU     VIHERGSPET LRDPRGFAVK FYTREGNFDL VGNNLPVFFV RDGMK----- ---------- -------LDF FSHFPESLHM FSFLFDDLGV
PSOYBN     VIHERGSPET LRDPRGFAVK FYTREGNFDL VGNNFPVFFV RDGLK----- ---------- -------LDF FSHHPESLHM FSFLFDDVGI
PGOSH1     VIHERGSPET LRDPRGFAVK FYTREGNFDL VGNNFPVFFI RDGMK----- ---------- -------LDF FSHHPESLHM FTFLFDDLGV
PLYCES     VVHERGSPES IRDIRGFAVK FYTREGNFDL VGNNVPVFFN RDAKS----- ---------- -------LDF FSFLPESLHT FAFFYDDVCL
PMAIZ1     VVHERGSPET LRDPRGFAVK FYTREGNFDL VGNNMPVFFI RDGMKFPDMV HAFKPNPKTN LQENWRIVDF FSHHPESLHM FTFLFDDVGI
PGOSH2     VIHERGSPET LRDPRGFAVK FYTREGNFDL VGNNFPVFFI RDGMK----- ---------- -------LDF FSHHPESLHM FTFLFDDIGV
PMAIZ2     VIHERGSPET LRDPRGFAVK FYTREGNWDL VGNNFPVFFI RDGIK----- ---------- -------LDF FSHHPESLHM FSFLFDDVGI
PMAIZ3     VIPEPGSGRT IRDARGFAVK FYTREGNWDL LGNNFPVFFI RDGIK----- ---------- -------FDF LSHLPESLHT FFFLFDHVGV
PARATH     VIHARGSPET LRDPRGFAVK FYTREGNFDL VGNNFPVFFI RDGMK----- ---------- -------LDF FSHHPESLNM FTFLFDDIGI
ABOVIN     VAGESGSADT VRDPRGFAVK FYTEDGNWDL VGNNTPIFFI RDALL----- ---------- -------WDF WSLRPESLHQ VSFLFSDRGI
ADROME     VGGESGSADT ARDPRGFAVK FYTEDGVWDL VGNNTPVFFI RDPIL----- ---------- -------WDF LTLRPESAHQ VCILFSDRGT
AHUMAN     VAGESGSADT VRDPRGFAVK FYTEDGNWDL VGNNTPIFFI RDPIL----- ---------- -------WDF WSLRPESLHQ VSFLFSDRGI
ARAT       VAGESGSADT VRDPRGFAVK FYTEDGNWDL VGNNTPIFFI RDAML----- ---------- -------WDF WSLCPESLHQ VTFLFSDRGI
AMOUSE     VAGESGSADT VRDPRGFAVK FYTEDGNWDL VGNNTPIFFI RDAIL----- ---------- -------WDF WSLRPESLHQ VSFLFSDRGI
FHANPO     VGGEKGSADT ARDPRGFATK FYTEDGNLDL VYNNTPIFFI RDPIK----- ---------- -------WDY LTANDESLHQ VMYLFSNRGT
FCANTR     VGGELGSADT ARDPRGFATK FYTEEGNLDL VYNNTPVFFI RDPSK----- ---------- -------WDY LTTNEESVHQ VMVLFSDRGT
FPENJA     VAGAKGSA-T VRDADAFAAK FASAAALQEL VGNNSPISFF IFDLL----- ---------- -------ESL FVRLPSLHQV SFFALAGFAA
FYEASA     VGGDKGSADT VRDPRGFATK FYTEEGNLDW VYNNTPVFFI RDPSK----- ---------- ---------- ---NQVAIHQ VMILFSDRGT
FYEAST     VGGESGTPDT ARDPRGVSFK FYTEWGNHDW VFNNTPVFFL RDAIK----- ---------- -------WDY LTLNPESIHQ ITYMFGDRGT
BVBACS     VAGELGSADT VRDPRGFAVK FYTEEGNYDI VGNNTPVFFI RDAIK----- ---------- -------WDF WSLSPESLHQ VTILMSDRGI
BBACFI     VAGSKGSAET VRDARGFATK FYTEEGNYDL VGNNIPVFFI QDAIK----- ---------- -------WDF IANNQESAHM VMWAMSDRSI
BPROMI     VAGERGAADA ERDIRGFALK FYTEEGNWDM VGNNTPVFYL RDPLKFPDLN HIVKRDPRTN MRNMAYKWDF FSHLPESLHQ LTIDMSDRGL
BSTRVE     VAGSLGAADA VRDPRGWALK FYTEEGNYDL VGNNTPVFFI KDAIK----- ---------- -------WDF WGLSPESTHQ VTWLFGDRGI
BLACSK     VAGEAGYPDT YRDVRGFAVK FYTEEGNYDI VGNNTPVFFV NDPLK----- ---------- -------WDF WSLSPESVHQ VTILMSDRGI
BLISSE     VIHGQHSPET LRDPRGFSVK FYTEEGNYDF VGNNLPVFFI RDAIK----- ---------- -------WDF FSLTPEATTM ITYLFSDEGT
BMICLU     VAGENGSPDT WRDTRGFALR FYTSEGNYDL VGNNTPIFFL RDPMK----- ---------- -------WDF WTNNPESAHQ VTYLMGPRGL
BECOLI     VQGGAGSADT VRDIRGFATK FYTEEGIFDL VGNNTPIFFI QDAHK----- ---------- -------WDY VSLQPETLHN VMWAMSDRGI

                   190       200       210       220       230       240       250       260       270
                     .       *.        .         .         .         .         .         .         .
PIPOBA     PTDYRHMEGF GVHTFTMINK EGKANYVKFH WKPTCGVKCL LEEEAIRIGG ENHSHATQDL YESIAA-GNY PEWKLYIQVM DPDHEDR-FD
PORYSA     PTDYRHMDGF GVNTYTFVTR DAKARYVKFH WKPTCGVSCL MDDEATLVGG KNHSHATQDL YDSIAA-GNF PEWKLFVQVI DPEEEER-FD
PPEA       PQDYRHMDGF GVNTYTLINK AGKSVYVKFH WKPTCGVKCL LEEEAIQVGG SNHSHATKDL YDSIAA-GNY PEWKLYIQTI DPAHEDR-FE
PPHAAU     PQDYRHMDGF GVNTYTLINK AGKAVYVKFH WKTTSGVKCL LEEEAIKVGG ANHSHATQDL HDSIAA-GNY PEWKLFIQTI DPEHEDK-FD
PSOYBN     PQDYRHMDGF GVNTYTLINK AGKALYVKFH WKTTSGEKSL LDDEAIRVGG SNHSHATQDL YDSIAA-GNY PEWKLYIQTL DPENEDR-LD
PGOSH1     PQDYRHMEGS GVNTYTLINK AGKAHYVKFH WKPTCGVKCL LEDEAIKVGG ANHSHATQDL YDSIAA-GNY PEWKLFIQTI DPDHEDK-FD
PLYCES     PTDYRHMEGF GVHAYQLINK EGKAHYVKFH WKPTCGVKCM SEEEAIRVGG TNHSHATKDL YDSIAA-GNY PEWKLFIQTM DPEDVDK-FD
PMAIZ1     PLNYRHMEGF GVNTYSLINR DGKPHLVKFH WKPTCGVKCL LDNEAVTVGG TCHSHATKDL YDSIAA-GNY PEWKLYIQTI DLDHEDK-FD
PGOSH2     PQDYRHMDGS GVHTYTLINK AGKSHYVKFH WKPTCGVKSL LEDEAIRVGG ANHSHATQDL YDSIAA-GNY PEWKLFIQIM DPLHEDR-FD
PMAIZ2     PADYRHMDGS GVHTYTLVSR AGTVTYVKFH WRPTCGVRSL MDDEAVR-CG ANHSHATKDL TDAIAA-GNF PEWTLYIQTM DPEMEDRLDD
PMAIZ3     PSDYRHMEGF GVNTYTFVSA AGKAQYVKFH WKPTCGERSI LTDEEARVGG RNHSH-TQDL YDSIAAEGSF PEWTLYVQVM DPAQQEQ-YD
PARATH     PQDYRHMDGS GVNTYMLINK AGKAHYVKFH WKPTCGVKSL LEEDAIRLGG TNHSHATQDL YDSIAA-GNY PEWKLFIQII DPADEDK-FD
ABOVIN     PDGHRHMDGY GSHTFKLVNA DGEAVYCKFH YKTDQGIKNL SVEDAARLAH EDPDYGLRDL FNAIAT-GNY PSWTLYIQVM TFSEAEI-FP
ADROME     PDGYCHMNGY GSHTFKLINA KGEPIYAKFH FKTDQGIKNL DVKTADQLAS TDPDYSIRDL YNRIKT-CKF PSWTMYIQVM TYEQAKK-FK
AHUMAN     PDGHRHMNGY GSHTFKLVNA NGEAVYCKFH YKTDQGIKNL SVEDAARLSQ EDPDYGIRDL FNAIAT-GKY PSWTFYIQVM TFNQAET-FP
ARAT       PDGHRHMNGY GSHTFKLVNA NGEAVYCKFH YKTDQGIKNL PVEEAGRLAQ EDPDYGLRDL FNAIAS-GNY PSWTFYIQVM TFKEAET-FP
AMOUSE     PDGHRHMNGY GSHTFKLVNA DGEAVYCKFH YKTDQGIKNL PVGEAGRLAQ EDPDYGLRDL FNAIAN-GNY PSWTFYIQVM TFKEAET-FP
FHANPO     PASYRTMNGY SGHTYKWYNS KGEWVYVQVH FIANQGVHNL LDEEAGRLAG EDPDHSTRDL WEAIEK-GDY PSWECYIQTM TLEQSKK-LP
FCANTR     PASYREMNGY SGHTYKWSNN KGEWFYVQVH FISDQGIKTL TNEEAGSLAG SNPDYAQEDL FKNIAA-GNY PSWTCYIQTM TEAQAKE-AE
FPENJA     VAAHRHMNGY GSHTFKLVAK DGSVYCSKFW YKADQGQAAE VWKDAEEVAA EDVDYFRDLN FQAEAA-GRY PLWELASQVM TFSDFEI-DP
FYEASA     PANYRSMHGY SGHTYKWSNK NGDWHYVQVH IKTDQGIKNL TIEEATKIAG SNPDYCQQDL FEAIQN-GNY PSWTVYIQTM TERDAKK-LP
FYEAST     PASWASMNAY SGHSFIMVNK EGKDTYVQFH VLSDTGFETL TGDKAAELSG SHPDYNQAKL FTQLQN-GEK PKFNCYVQTM TPEQATK-FR
BVBACS     PATLRHMHGF GSHTFKWTNA EPEGVWIKYH FKTEQGVKNL DVNTAAKIAG ENPDYHTEDL FNAIEN-GDY PAWKLYVQIM PLEDANT-YR
BBACFI     PRSFRMMEGF GVHTFRFVNE EGKAHFVKFH WKPVLGIHSL VWDEAQKIAG KDPDFHRRDL WESIEN-GDY PEYELGVQLI SEEDEFN-FD
BPROMI     PLSYRFVHGF GSHTYSFINK DNERFWVKFH FRCQQGIKNL MDDEAEALVG KDRESSQRDL FEAIER-GDY PRWKLQIQIM PEKEAST-VP
BSTRVE     PASYRHMNGY GSHTYQWNNE AGEVFWVKYH FKTDQGIKNL TQDEANRLAG EDPDSHQRDL REAIER-GDF PTWTVQVQIM PAADAAG-YR
BLACSK     PASYRMMHGF GSHTFKWVNA QGEQFWVIFH FKTNQGIHNL SNELADELAG KDTDYLQNDL FDAIET-GDY PSWTVAVQLV LMKMAEL-SP
BLISSE     PASYREIRGS SVHAFKWINE EGKTVYVKLR WVPKAGIVNL STDQAAQIQA KEFNHASRDL YEAIEN-GDY PEWDLYVQVL DPKDLDN-YD
BMICLU     PRTWREMDGY GSHTYLWVNA EGAKHWVKYH FISQEGVHNL SNDEATQIAG ENADFHRQDL FEVIAK-GVF PKWNLYIQAI PYSQGKT-YR
BECOLI     PRSYRTMEGF GIHTFRLINA EGKATFVRFH WKPLAGKASL VWDEAQKLTG RDPDFHRREL WEAIEA-GDF PEYELGFQLI PEEDEFK-FD
```

```
                280        290        300        310        320        330        340        350        360
                 *  .       .          *.         .          .          * .     §†    .          .          .
PIPOBA     FDPLDDTTKIW PEELIPLQPV GRMVLNKNID NFFAENEMLA MDP-AHIVPG IYFSDDKMLQ ARVFAYADTH RHRLG-PNYM LLPVNAP-K-
PORYSA     FDPLDDTKTW PEDEVPLRPV GRLVLNRNVD NFFNENEQLA FGP-GLVVPG IYYSDDKMLQ CRVFAYADTQ RYRLG-PNYL MLPVNAP-K-
PPEA       FDPLDVTKTW PEDIIPLQPV GRMVLNKNID NFFAENEQLA FCP-AIMLPG IYYSDDKMLQ TRVFSYADSQ RHRLG-PNYL QLPVNAP-K-
PPHAAU     FDPLDVTKTW PEDIIPLQPV GRLVLNKNID NFFAENEQLA FCP-AIIVPG VYYSDDKMLQ TRIFSYADSQ RHRLG-PNYL LLPANAP-K-
PSOYBN     FDPLDVTKTW PEDVLPLQPV GRMVLNKNID NFFAENEQLA FCP-AIIVPG VYYSDDKLLQ TRVFSYADTQ RHRLG-PNYL QLPANAP-K-
PGOSH1     FDPLDVTKTW PEDILPLQPV GRLVLNKNID NFFAENEQLA FCP-AIVVPG IYYSDDKLLQ TRIFSYSDTQ RHRLG-QTYL QLPANAP-K-
PLYCES     FDPLDVTKTW PEDLLPLIPV GRLVLNRNID NFFAENEQLA FNP-GHIVPG IYYSEDKLLQ TRIFAYADTQ RHRIG-PNYM QLPVNAP-K-
PMAIZ1     FDPLDVTKTW PEDIIPLQPV GRMVLNKNVD NFFAENEQIA FCP-AISVPA IHYSDDKLLQ TRIFSYADTQ RHRLG-PNYL MLPVNAP-K-
PGOSH2     FDPLDVTKTW PEDIFPLQPM GRMVLNKNID NFFAENEQLA FCP-SLIVPG IYYSDDKLLQ TRIFSYSDTQ RHRLG-PNYL QLPANAP-K-
PMAIZ2     LDPLDVTKTW PEDTFPLQPV GRLVLNRNID NFFAENEQLA FCP-GLIVPG IYYSDDKLLQ TRIFSYSDTQ RHRLG-PNYL LLPANAP-K-
PMAIZ3     FDPLDDTKTW PEDLLPLRPV GRLVLDRNVD NFLNENEQLA FGP-GLVVPG IYYSDDKMLQ CRVFAYADTQ RYRLG-PNYL MLPVNAP-R-
PARATH     FDPLDVTKTW PEDILPLQPV GRMVLNKNID NFFAENEQLA FCP-AIIVPG IHYSDDKLLQ TRVFSYADTQ RHRLG-PNYL QLPVNAP-K-
ABOVIN     FNPFDLTKVW PHGDYPLIPV GKLVLNRNPV NYFAEVEQLA FDP-SNMPPG IEPSPDKMLQ GRLFAYPDTH RHRLG-PNYL QIPVNCPYR-
ADROME     YNPFDVTKVW SQKEYPLIPV GKMVLDRNPK NYFAEVEQIA FSP-AHLVPG VEPSPDKMLH GRLFSYSDTH RHRLG-PNYL QIPVNCPYK-
AHUMAN     FNPFDLTKVW PHKDYPLIPV GKLVLNRNPV NYFAEVEQIA FDP-SNMPPG IEASPDKMLQ GRLFAYPDTH RHRLG-PNYL HIPVNCPYR-
ARAT       FNPFDLTKVW PHKDYPLIPV GKLVLNRNPA NYFAEVEQMA FDP-SNMPPG IEPSPDKMLQ GRLFAYPDTH RHRLG-PNYL QIPVNCPYR-
AMOUSE     FNPFDLTKVW PHKDYPLIPV GKLVLNKNPV NYFAEVEQMA FDP-SNMPPG IEPSPDKMLQ GRLFAYPDTH RHRLG-PNYL QIPVNCPYR-
FHANPO     FSVFDLTKVW PHKDFPLRHF GRFTLNENPK NYYAETEQIA FSP-SHTVPG MEPSNDPVLQ SRLFSYPDTH RHRLG-PNYH QIPVNCPLKS
FCANTR     FSVFDLTKVW PHGKYPMRRF GKFTLNENPK NYFAEVEQAA FSP-AHTVPH MEPSADPVLQ SRLFSYADTH RHRLG-TNYT QIPVNCPVTG
FPENJA     FNENIPTKVV PRESVPLIVD AELLLNRNPL NMFAEVEQVF MDV-AAASKG ADEVEDPLIQ -RQFAYIDTH LSEL--TASY GIPVCRPYAT
FYEASA     FSVFDLTKVW PQGQFPLRRV GKIVLNENPL NFFAQVEQAA FAP-STTVPY QEASADPVLQ ARLFSYADAH RYRLG-PNFH QIPVNCPYAS
FYEAST     YSVNDLTKIW PHKEFPLRKF GTITLTENVD NYFQEIEQVA FSPTNTCIPG IKPSNDSVLQ ARLFSYPDTQ RHRLGA-NYQ QLPVNRP
BVBACS     FDPFDVTKVW SQKDYPLIEV GRMVLDRNPE NYFAEVEQAT FSP-GTLVPG IDVSPDKMLQ GRLFAYHDAH RYRVGA-NHQ ALPINRA-RN
BBACFI     FDVLDPTKIW PEEEVPVKII GKMTLNRNVD NVFAETEQVA FHP-GHVVPG IDFTNDPLLQ GRLFSYTDTQ LIRLGGPNFH ELPINRP-VC
BPROMI     YNPFDLTKVW PHADYPLMDV GYFELNRNPD NYFSDVEQAA FSP-ANIVPG ISFSPDKMLQ GRLFSYGDAH RYRLGV-NHH QIPVNAP-KC
BSTRVE     FNPFDLTKVW PHEDYPPVEI GTLELNRNPE NIFAEVEQSI FSP-AHFVPG IGPSPDKMLQ GRLFAYGDAH RYRVG-INAD HLPVNRPHAT
BLACSK     KDIFDVTKVI SQKDYPLIEI GQMVLDENPT NNFEDIQELA FSP-ANLVPG IEASPDKLLQ GRLFGYKDAE RYRLGA-NYE QLPVNRP-KV
BLISSE     FNPLDATKDW FEDVFPYEHV GTMTLNRNPD NIFAETESVG FNP-GVLVPG MLPSEDRVLQ GRLFSYSDTQ RHRVG-PNYL QLPINSP-KT
BMICLU     FNPFDLTKTI SQANYPRIKV GVNTLNRNPK NFFAEIESAA FSP-SNTVPG IGLSPDRMLL GRAFAYHDAQ LYRVGA-HVN QLPVNSP-DD
BECOLI     FDLLDPTKLI PEELVPVQRV GKMVLNRNPD NFFAENEQAA FHP-GHIVPG LDFTNDPLLQ GRLFSYTDTQ ISRLGGPNFH EIPINRP-TC

                370        380        390        400        410        420        430        440        450
                 .          .          .          .          .          .          .          .          .
PIPOBA     CAHHNNSYDG YMNFVHRDEE VDYFPSKFDN TRNAERFPT- PLRIVTGQRD KCVIEKENNF KQPGDRYRSW APDRQDRFI
PORYSA     CAHHNNHYDG AMNFMHRDEE VDYYPSRHAP LRHAPPT-PI TPRPVVGRRQ KATIHKQNDF KQPGERYRSW APDRQERFI
PPEA       WSHHNNHHEG FMNAIHRDEE VNYFPSRHDT VRHAERV-PI PTTHLSARRE KCNIPKQNHF KQAGERYRTW APDRQERFL
PPHAAU     SAHHNNHHEG FMNFIHRDEE VNYFPSRYDP VRHAEKF-PI PPAVFSGRRE KIAIEKENNF KQAGERFRSW APDRQDRFI
PSOYBN     CAHHNNHHDG FMNFMHRDEE VNYFPSRYDP VRHAEKV-PV PPRILGGKRE KCMIEKENNF KQPGERYRSW PSDRQERFV
PGOSH1     CAHHNNHHEG FMNFMHRDEE INY-FPSRYD PVRHAEMFPI PPAVCTGRRE KCIIEKENNF KQPGERYRSW AADRQERFI
PLYCES     CGHHNNHRDG AMNMTHRDEE VDY-LPSRFD PCRPAEQYPI PSCVLNGRRT NCVIPKENNF KQAGERYRSW EPDRQDRYI
PMAIZ1     CAHHNNHHDG FMNFMHRDEE VNY-FPSRFD PARHAEKVPI PPRVLTRCRE KCIIQKENNF KQAGERYRSF DPARQDRFI
PGOSH2     CAHHNNHHEG FMNFMHRDEE VNY-FPSRYD PVRHAEKHPI PSTVLSGKRE KCIIGKENNF KQPGERYRSF SADRQERFI
PMAIZ2     CAHHNNHYDG SMNFMHRHEE VDYFPSRYDA VRNAPRY-PI PTAHIAGRRE KTVISKENNF KQPGERYRAM DPARQERFI
PMAIZ3     CGTHNNHYDG AMNLMHRDEE VDY---HARR CGRAAPT-PL PPRPVAGRRE KATIRKPNDF KQPGERYRSW DADRQDRFV
PARATH     CAHHNNHHEG FMNFMHRDEE VNY-FPSRYD QVRHAEKYPT PPAVCSGKRE RCIIEKENNF KEPGERYRTF TPERQERFI
ABOVIN     ARVANYQRDG PMCMMDNQGG APNYYPNSFS APEHQPSALE HRTHFSGDVQ RFNSANDDNV TQVRTFYLKV LNEEQRKRLC ENIAGHLKDA
ADROME     VKIENFQRDG AMNVTDNQDG APNYFPNSFN GPQECP---- ---------- -------DNF GQVTDFWVHV LDKCAKKRLV QNIAGHLSNA
AHUMAN     ARVA-YQRDG PMCMQDNQGG APNYYPNSFG APEQQPSALE HSIQYSGEVR RFNTANDDNV TQVRAFYVNV LNEEQRKRLC ENIAGHLKDA
ARAT       ARVANYQRDG PMCMHDNQGG APNYYPNSFS APEQQG---- ---------- -------DNV TQVRTFYTKV LNEEERKRLC ENIANHLKDA
AMOUSE     ARVANYQRDG PMCMHDNQGG APNYYPNSFS APEQQRSALE HSVQCAVDVK RFNSANEDNV TQVRTFYTKV LNEEERKRLC ENIAGHLKDA
FHANPO     GSFNPINRDG PMCVDGNLGG TP
FCANTR     AVFNPHMRDG AMNVNGNLGN HP
FPENJA     -VLN
FYEASA     KFFNPAIRDG PMNVNGNFGS EP
FYEAST
BVBACS     KV-NNYQRDG QMRFDDNGGG SVYYEPNSFG GPKESPEDKQ AAYPVQGIA DSVSYDHYDHY TQAGDLYRLM SEDERTRLVE NIVNAMKPVE
BBACFI     KV-NN-QRDG YGRQTINKGQ V-SY
BPROMI     PFHN-YHRDG AMRVDGNSGN GITYEPNS-G GVFQEQPDFK EPPLSIEGA ADHWNHREDED YFSQPRALYE LLSDDEHQRM FARIAGELSQ
BSTRVE     EARTH-SRDG FLYDGRHKGA K-NYEPNSFG GPVQTDRPL- --------- ----------D DFTQAGDLYR LMSEDEKGRL IDNLSGFIAK
BLACSK     PVHNY-ERDG AMAQNQATGV --NYE----- ---------- --------- ----------D YYSAAGKLYR LLSADEQTRL IENIRMNLGQ
BLISSE     PVDNN-QRDG QMPFKQQTS- SINYEPNSYD TEPKENPA-- --------- ----------PN NFGHAKEVWK RYSDAERAAL VKNIVDDWEG
BMICLU     ATHN-YAFEG EMWEDHTGNR S-TYVPNSDG NSWSNEVGPT --------- ----------N NFGEAGTLTR EVFSNEERNN FVQTVAGALK
BECOLI     PYHNF-QRDG -MHRMGIDTN PANY
```

À = distal asparagine, h = distal histidine, † = proximal tyrosine, § = serine of HPII and PVC
* = residues which may contribute to the orientation of the heme

## Comparison and Alignment of Sequences

The sequences of 30 catalases were imported from PIR and Swissprot data banks. Preliminary multiple sequence alignment was performed through the ECOCYC data base. The aligned sequences were imported into MacClade™ version 3.04 software for manual adjustment. For phylogenetic analysis, the variable carboxy terminus was not considered.

## Catalase Sequence Legend

PIPOBA = IPOMOEA BATATAS (SWEET POTATO) (BATATE) EUKARYOTA; PLANTA; EMBRYOPHYTA; ANGIOSPERMAE; DICOTYLEDONEAE;SOLANALES; CONVOLVULACEAE.

PORYSA = ORYZA SATIVA (RICE) EUKARYOTA; PLANTA; EMBRYOPHYTA; ANGIOSPERMAE; MONOCOTYLEDONEAE; CYPERALES; GRAMINEAE.

PPEA = PISUM SATIVUM (GARDEN PEA) EUKARYOTA; PLANTA; EMBRYOPHYTA; ANGIOSPERMAE; DICOTYLEDONEAE; FABALES; FABACEAE.

PPHAAU = PHASEOLUS AUREUS (MUNG BEAN) (VIGNARADIATA) EUKARYOTA; PLANTA; EMBRYOPHYTA; ANGIOSPERMAE; DICOTYLEDONEAE; FABALES; FABACEAE.

PSOYBN = GLYCINE MAX (SOYBEAN) EUKARYOTA; PLANTA; EMBRYOPHYTA; ANGIOSPERMAE; DICOTYLEDONEAE; FABALES; FABACEAE.

PGOSH1 = GOSSYPIUM HIRSUTUM (UPLAND COTTON) EUKARYOTA; PLANTA; EMBRYOPHYTA; ANGIOSPERMAE; DICOTYLEDONEAE.

PLYCES = LYCOPERSICON ESCULENTUM (TOMATO) EUKARYOTA; PLANTA; EMBRYOPHYTA; ANGIOSPERMAE; DICOTYLEDONEAE; SOLANALES; SOLANACEAE.

PMAIZ1 = ZEA MAYS (MAIZE) EUKARYOTA; PLANTA; EMBRYOPHYTA; ANGIOSPERMAE; MONOCOTYLEDONEAE; CYPERALES; GRAMINEAE.

PGOSH2 = ISOZYME 2.

PMAIZ2 = ISOZYME 2.

PMAIZ3 = ISOZYME 3.

**PARATH** = ARABIDOPSIS THALIANA (MOUSE-EARCRESS) EUKARYOTA; PLANTA; EMBRYOPHYTA; ANGIOSPERMAE; DICOTYLEDONEAE; CAPPARALES; CRUCIFERAE.

**ABOVIN** = BOS TAURUS (BOVINE) EUKARYOTA; METAZOA; CHORDATA; VERTEBRATA; TETRAPODA; MAMMALIA; EUTHERIA; ARTIODACTYLA. NADPH.

**ADROME** = DROSOPHILA MELANOGASTER (FRUITFLY).

**AHUMAN** = HOMO SAPIENS (HUMAN) EUKARYOTA; METAZOA; CHORDATA; VERTEBRATA; TETRAPODA; MAMMALIA; NADPH.

**ARAT** = RATTUS NORVEGICUS (RAT) EUKARYOTA; METAZOA; CHORDATA; VERTEBRATA; TETRAPODA; MAMMALIA; EUTHERIA; RODENTIA. NADPH.

**AMOUSE** = MUS MUSCULUS (MOUSE) EUKARYOTA; METAZOA; CHORDATA; VERTEBRATA; TETRAPODA; MAMMALIA; EUTHERIA; RODENTIA. NADPH.

**FHANPO** = HANSENULA POLYMORPHA (YEAST) EUKARYOTA; FUNGI; ASCOMYCOTINA; HEMIASCOMYCETES.

**FCANTR** = CANDIDA TROPICALIS (YEAST) EUKARYOTA; FUNGI; DEUTEROMYCOTINA (IMPERFECT FUNGI).

**FPENJA** = PENICILLIUM JANTHINELLUM (PENICILLIUM VITALE) EUKARYOTA; FUNGI; ASCOMYCOTINA; PLECTOMYCETES; EUROTIALES. FLAVODOXIN TYPE BINDING DOMAIN.

**FYEASA** = SACCHAROMYCES CEREVISIAE (BAKER'S YEAST) EUKARYOTA; FUNGI; ASCOMYCOTINA; HEMIASCOMYCETES. A FORM.

**FYEAST** = T FORM.

**BVBACS** = BACILLUS SUBTILIS PROKARYOTA; FIRMICUTES; ENDOSPORE-FORMING RODS AND COCCI; BACILLACEAE. CYTOPLASMIC (PROBABLE). GRAM POSITIVE.

**BBACFI** = BACILLUS FIRMUS PROKARYOTA; FIRMICUTES; ENDOSPORE-FORMING RODS AND COCCI; BACILLACEAE. GRAM NEGATIVE.

**BPROMI** = PROTEUS MIRABILIS.PROKARYOTA; GRACILICUTES; SCOTOBACTERIA; FACULTATIVELY ANAEROBIC RODS; ENTEROBACTERIACEAE. NADPH, CYTOPLASMIC. GRAM NEGATIVE.

**BSTRVE** = STREPTOMYCES VIOLACEUS PROKARYOTA; FIRMICUTES; ACTINOMYCETALES; STREPTOMYCETACEAE. GRAM POSITIVE.

**BLACSK** = LACTOBACILLUS SAKE PROKARYOTA; FIRMICUTES; REGULAR ASPOROGENOUS ROD PROKARYOTA; FIRMICUTES; REGULAR ASPOROGENOUS ROD; LACTOBACILLACEAE. CYTOPLASMIC (PROBABLE). GRAM POSITIVE.

**BLISSE** = LISTERIA SEELIGERI PROKARYOTA; FIRMICUTES; REGULAR ASPOROGENOUS ROD; UNCERTAIN.CYTOPLASMIC (PROBABLE). GRAM POSITIVE.

**BMICLU** = MICROCOCCUS LUTEUS (MICROCOCCUS LYSODEIKTICUS) PROKARYOTA; FIRMICUTES; COCCI; MICROCOCCACEAE. NADPH. GRAM POSITIVE.

**BECOLI** = HPII ESCHERICHIA COLI PROKARYOTA; GRACILICUTES; SCOTOBACTERIA; FACULTATIVELY ANAEROBIC RODS; ENTEROBACTERIACEAE. CYTOPLASMIC (PROBABLE). FLAVODOXIN TYPE BINDING DOMAIN. GRAM NEGATIVE.

## Appendix B

## Phylogenetic Analysis

From the set of 30 aligned sequences 100 bootstrap replicates were obtained for a 50% majority-rule consensus tree with heuristic search in the program PAUP™ version 3.1.1 (Smithsinian Institution 1993) at CLBRR Agriculture Canada. The tree construction with the corresponding distance matrix was unrooted. The bootstrap sampling was over non-excluded and non-ignored characters only and one tree was held at each step during stepwise addition. Tree-bisection reconnection branch swapping was also in effect.

### Results

The bootstrap consensus tree (figure B-1) had a length of 2074. Random trees of the sequences gave lengths between 4000 and 5000, suggesting that the results of the bootstrapped consensus tree is significant. 100% of the bootstrap replicates show a clear divergence pattern for plants and a minimum of 90% divergence for bacteria. 88% of the bootstrap replicates show a divergence between animals and fungi with *Penicillium vitale* being the only exception.

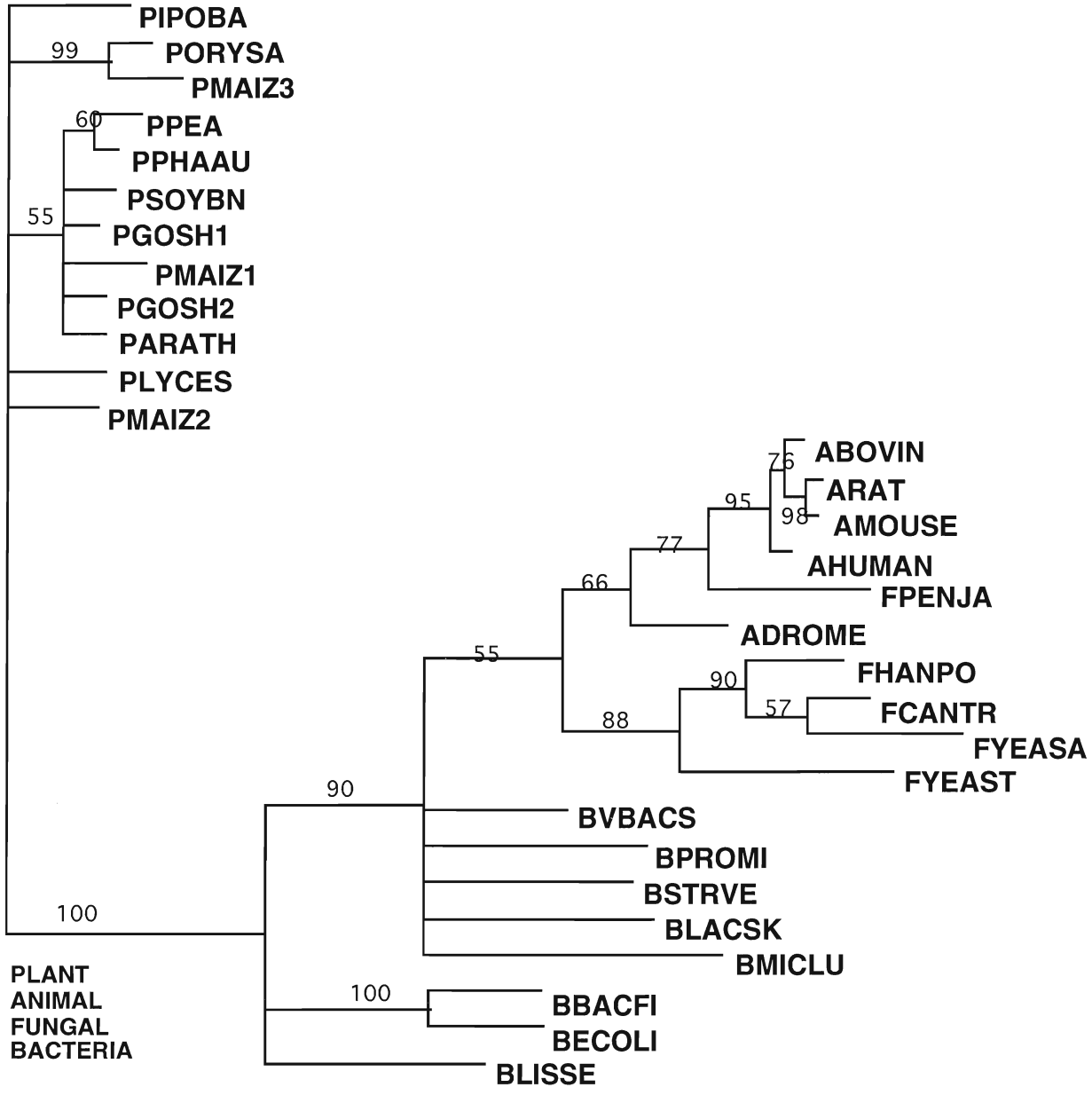


**Figure B-1. Phylogenetic analysis of 30 catalase sequences.**
Unrooted phylogenetic tree based on the amino acid sequences as constructed by 50% consensus of 100 bootstrap replicates with a heuristic search method. The numbers represent the level of confidence for the major branches which have been determined by bootstrap analysis.

Figure C-1. *Formate binding of HPII catalases at pH 5.8*

Experiments were performed on the DU-7 spectrophotometer at pH 5.8 in 100 mM potassium phosphate buffer at 23°C. Increasing amounts of formate were added in a step-wise fashion. The change in absorbance at wavelength pairs 420-400 nm (■) and 580-600 nm (●) were plotted against formate concentrations up to 30 mM for A) 5μM HPII wild-type and B) 7μM N201Q enzymes. C) 7μM BLC. The changes in absorbance at wavelength pairs 418-380 nm (■) and 612-648 nm (●) were plotted against formate concentrations up to 3.5 mM. The data was fitted to determine dissociation constants for catalase/formate complexes. Equations are shown in appendix D, table D-1.

## APPENDIX C - Formate binding data at pH 5.8

Figure C-1

A.

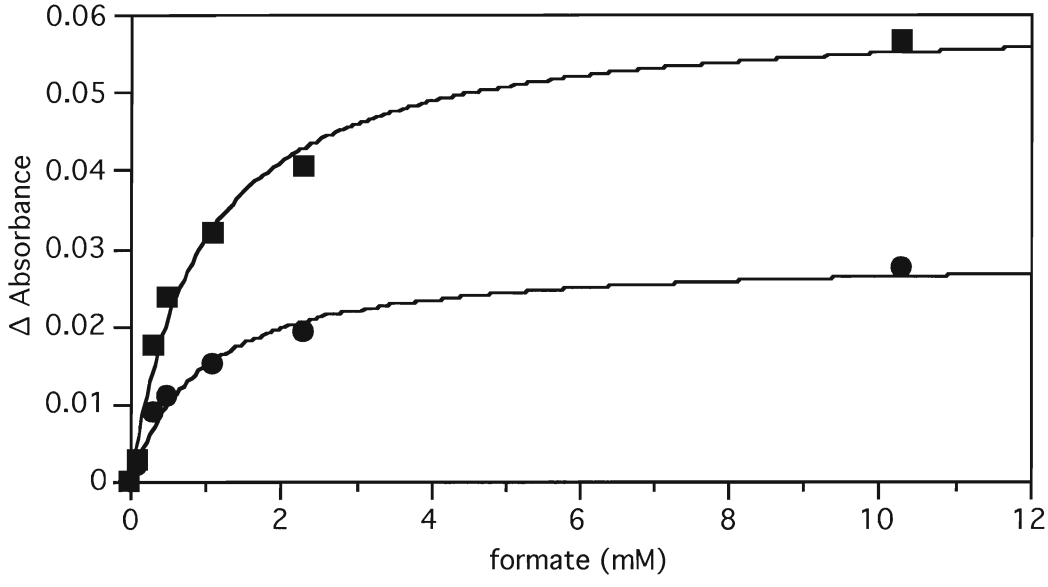


B.

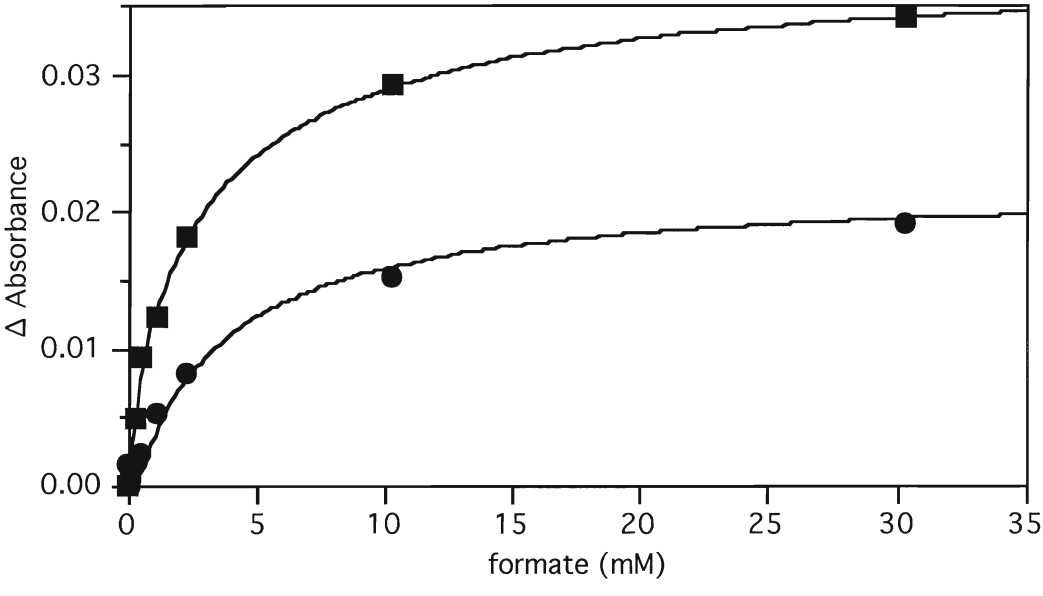


C.

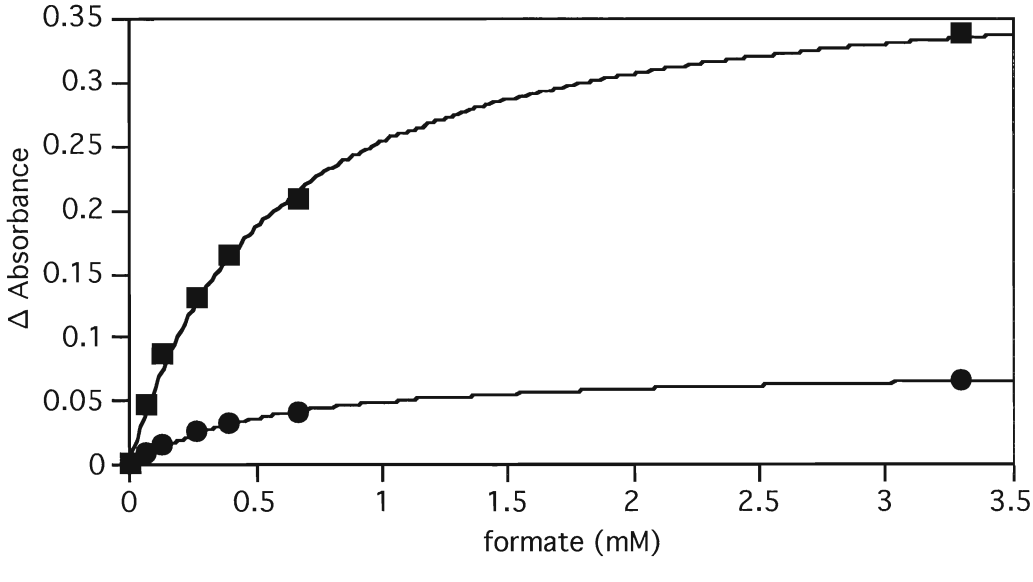

Figure C-2

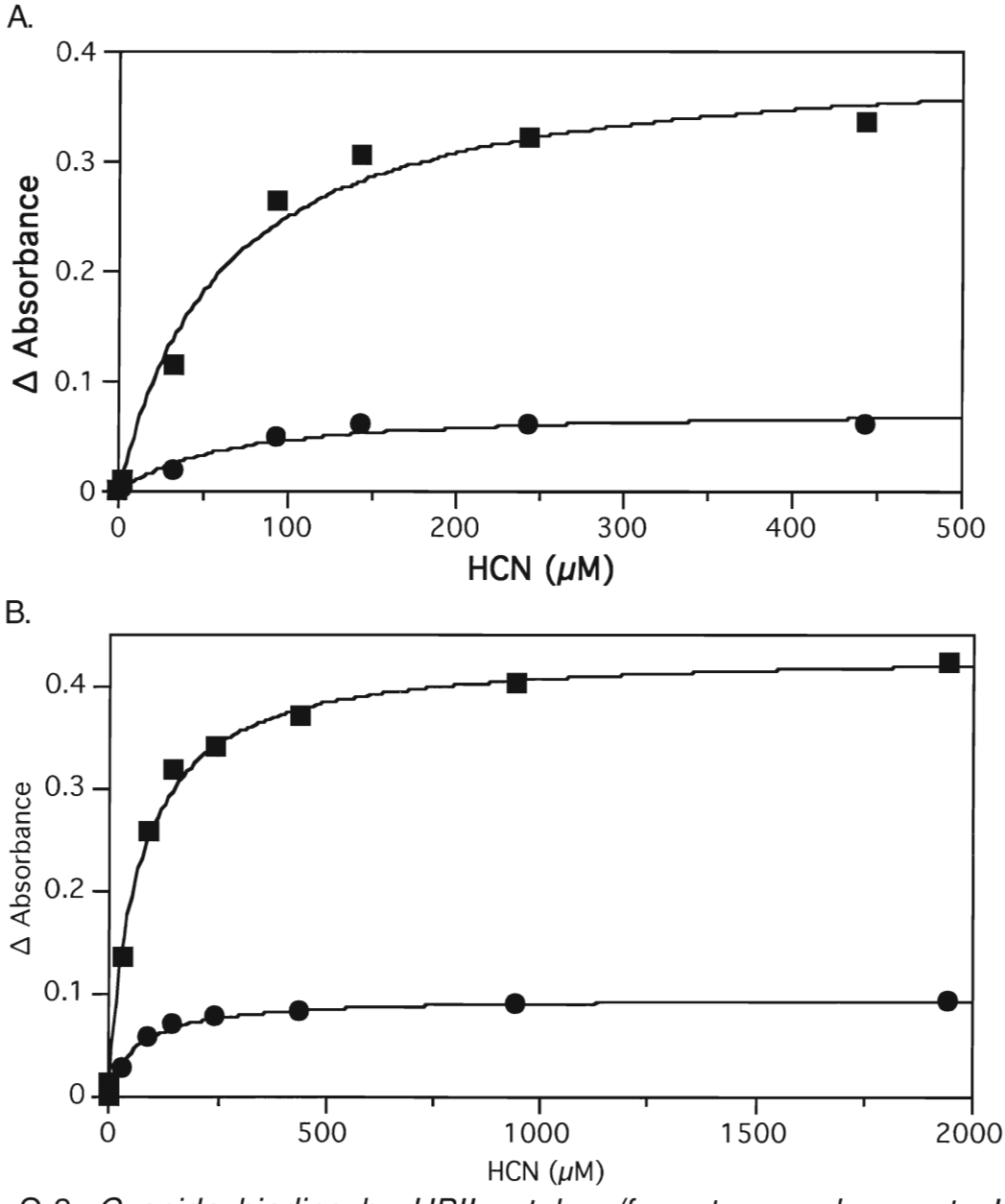


Figure C-2. *Cyanide binding by HPII catalase/formate complexes at pH 5.8*

Experiments were performed on the DU-7 spectrophotometer at pH 5.8 in 100 mM potassium phosphate buffer at 23°C. Increasing amounts of cyanide were added in a step-wise fashion to catalase/formate complexes. The change in absorbance at wavelength pairs 430-400 nm (■) and 630-580 nm (●) were plotted against cyanide concentrations up to 2 mM for A) 5μM HPII wild-type and B) 7μM N201Q enzymes. The data was fitted to determine competative dissociation constants for catalase/formate complexes with cyanide Equations are shown in appendix D, table D-2.

Figure C-3

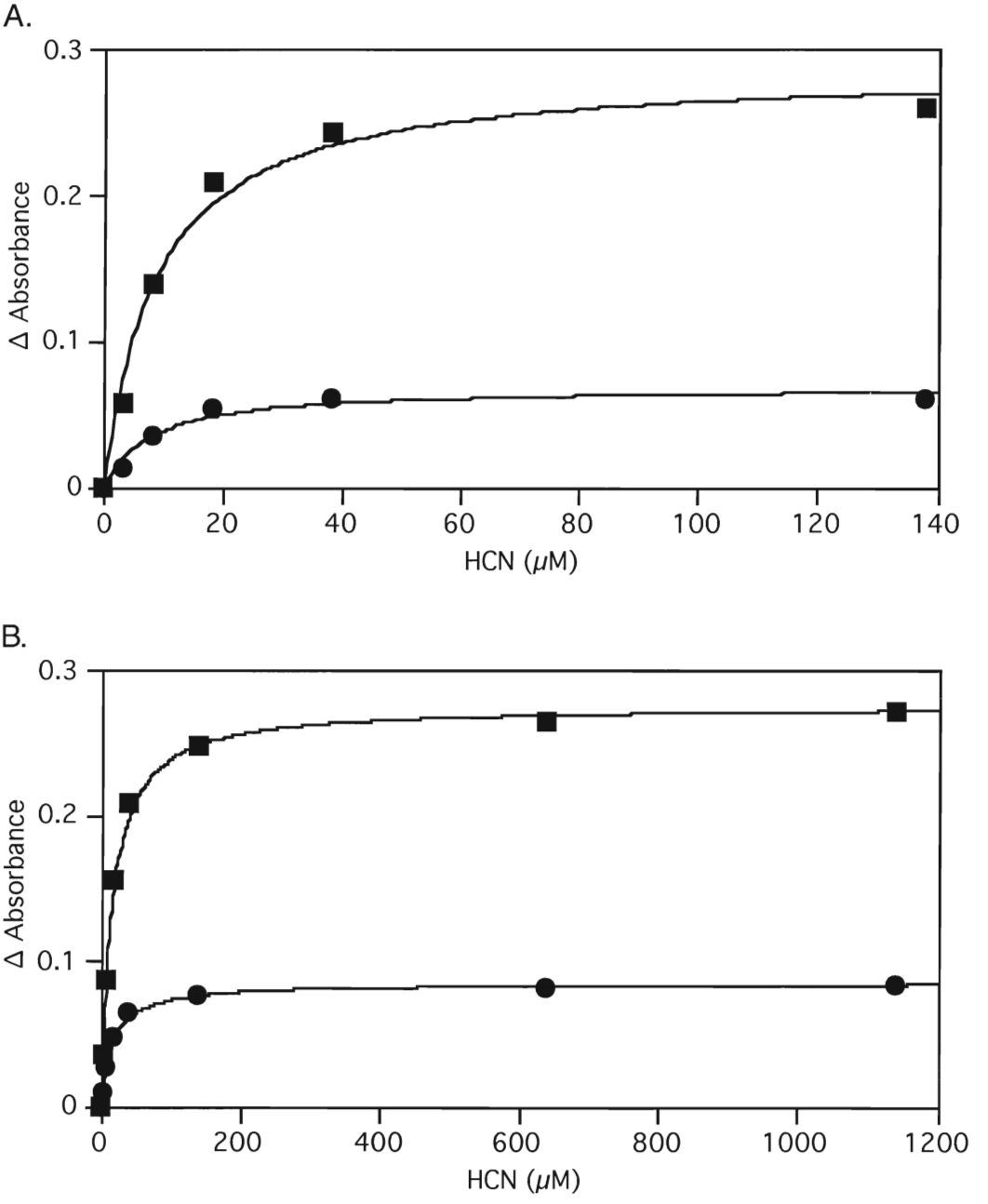


Figure C-3. *Cyanide binding of HPII catalases at pH 5.8*

Experiments were performed on the DU-7 spectrophotometer at pH 5.8 in 100 mM potassium phosphate buffer at 23°C. Increasing amounts of cyanide were added in a step-wise fashion. The change in absorbance at wavelength pairs 420-406 nm (■) and 630-590 nm (●) were plotted against cyanide concentrations up to 1.2 mM for A) 5μM HPII wild-type and B) 7μM N201Q enzymes. The data was fitted to determine dissociation constants for catalase/cyanide complexes. Equations are shown in appendix D, table D-2.

## APPENDIX D - Equations

Table D-1. Curve fitting equations and data for secondary plots of formate and fluoride binding to ferric catalases presented in results section.

| Catalase | sigmoidal curve fitting for data which plots Δ Absorbance vs log fluoride | curve fitting for data which plots Δ Absorbance vs formate | |
|---|---|---|---|
| | | pH 5.8 | pH 6.8 |
| **Beef liver** Soret region | y=Exp(2.303*(x-0.67))/(1+Exp(2.303*(x-0.67)))<br>R^2 = 0.99<br>**445-399nm** | y=0.39*x/(0.55+x)+0.22;<br>R^2 =0.99<br>**418-380nm** | y=0.11x/(3.9+x)<br>R^2 =0.99<br>**418-380nm** |
| visible region | y=Exp(2.303*(x-0.52))/(1+Exp(2.303*(x-0.52)))+-0.061<br>R^2 = 0.99<br>**596-636nm** | y=0.076*x/(0.52+x)+0.057;<br>R^2 = 0.99<br>**612-648nm** | y=0.024*x/(3.8+x)<br>R^2 = 0.99<br>**612-648nm** |
| **HPII Wild-type** soret region | - | Y=0.060*X/(0.91+X);<br>R^2 = 0.99<br>**420-400 nm** | Y=0.062*X/(7.7+X);<br>R^2 = 0.99<br>**420-400nm** |
| visible region | Y=Exp(2.303*(x-2.43))/(1+Exp(2.303*(x-2.43)));<br>R^2 = 0.99<br>**670-710nm** | Y=0.029*X/(0.92+X);<br>R^2 = 0.99<br>**580-600nm** | Y=0.033*X/(8.4+X);<br>R^2 = 0.99<br>**580-600 nm** |
| **N201D** soret region | - | - | Y=0.0032*X/(1.1+X)+0.019*X/(133.9+X);<br>R^2 = 0.99<br>**420-400nm** |
| visible region | Y=Exp(2.303*(x-3.59))/(1+Exp(2.303*(x-3.59)));<br>R^2 = 0.99<br>**670-710nm** | - | Y=0.0002*X/(1+X)+0.0027*X/(56.6+X);<br>R^2 = 0.96 **580-600 nm** |
| **N201Q** soret region | - | Y=0.017*X/(0.80+X)+0.02*X/(5.68+X);<br>R^2 = 0.99<br>**420-400 nm** | Y=0.0089*X/(1.1+X)+0.035*X/(57.2+X);<br>R^2 = 0.99<br>**420-400nm** |
| visible region | Y=Exp(2.303*(x-3.03))/(1+Exp(2.303*(x-3.03)))+0.030;<br>R^2 = 0.99 NQ<br>**670-710nm** | Y=-0.004*X/(0.27+X)+0.024*X/(3.45+X)+0.0015;<br>R^2 = 0.99<br>**580-600nm** | Y=-0.0085*X/(2+X)+0.025*X/(13.5+X)+0.001<br>R^2 = 0.99<br>**580-600nm** |

Table D-2. Curve fitting equations and data for secondary plots of cyanide and competative cyanide binding to ferric HPII catalases presented in results section.

| **HPII catalase** | Data fits: cyanide back titration | | Data fits: cyanide control | |
|---|---|---|---|---|
| | pH 5.8 | pH 6.8 | pH 5.8 | pH 6.8 |
| **Wild-Type** Soret region | Y=0.40*X/(59+X); R^2 = 0.99 **430-400nm** | Y=0.40*X/(45.8+X) R^2 = 0.99 **430-400nm** | Y=0.29*X/(8.43+X) R^2 = 0.99 **420-406 nm** | Y=0.27*X/(4.78+X) R^2 = 0.99 **420-406nm** |
| visible region | Y=0.08*X/(61+X)R ^2 = 0.97 **630-580nm** | Y=0.08*X/(46.2+X) R^2 = 0.97 **630-580nm** | Y=0.069*X/(7.7+X) R^2 = 0.97 **630-590 nm** | Y=0.07*X/(4.32+X) R^2 = 0.97 **630-590nm** |
| **N201D** Soret region | - | Y=0.14*X/(49.6+X) R^2 = 0.99 **430-400nm** | - | Y=0.098*X/(17+X) R^2 = 0.99 **420-406 nm** |
| visible region | - | Y=0.02*X/(45.6+X) R^2 = 0.99 **630-580nm** | - | Y=0.02*X/(14+X); R^2 = 0.99 **630-590nm** |
| **N201Q** Soret region | Y=0.43*X/(65+X); R^2 = 0.99 **430-400nm** | Y=0.37*X/(56.7+X) R^2 = 0.99 **430-400nm** | Y=0.28*X/(15.1+X) R^2 = 0.99 **420-406 nm** | Y=0.28*X/(17.6+X) R^2 = 9.91 **420-406 nm** |
| visible region | Y=0.1*X/(67+X); R^2 = 0.99 **630-580nm** | Y=0.08*X/(57.8+X) R^2 = 0.99 **630-580nm** | Y=0.09*X/(15.6+X) R^2 = 0.99 **630-590nm** | Y=0.09*X/(18.3+X) R^2 = 0.99 **630-590nm** |

## Derivation of equation 14.

1. $$K_d = \frac{[F][Y]}{[1-Y]}$$

2. $$K_d * \left(\frac{1-Y}{Y}\right) = F$$

3. $$\log K_d + \log\left(\frac{1-Y}{Y}\right) = \log F$$

4. $$\log\left(\frac{1-Y}{Y}\right) = \log F - \log K_d$$

5. $$1 - Y = \frac{\exp(2.303 * ((\log F - \log K_d)))}{1 + \exp(2.303 * (\log F - \log K_d))}$$

where Y=the fraction of free enzyme, 1-Y = fraction of fluoride complex = the absorbance of the fluoride complex, F is the concentration of fluoride and $K_d$ is the dissociation constant.